

**PKC ϵ and Cardioprotection:
An exploration of Putative mechanisms**

Submitted by Joy McCarthy BSc

Student Number : RCHJOY002

**for the degree of Doctor of Philosophy
(Medicine)**

**University of Cape Town Medical School
June 2006**

Supervisors

Dr M Faadiel Essop PhD
(Hatter Heart Research Institute, UCT)

Professor LH Opie PhD DSc DPhil
(Hatter Heart Research Institute, UCT)

The copyright of this thesis vests in the author. No quotation from it or information derived from it is to be published without full acknowledgement of the source. The thesis is to be used for private study or non-commercial research purposes only.

Published by the University of Cape Town (UCT) in terms of the non-exclusive license granted to UCT by the author.

Acknowledgements

It is with great pleasure that I acknowledge the support and encouragement of the following people without whom this thesis would not have been possible.

- Firstly, Dr Michael Sack who believed in me sufficiently to encourage my aspirations towards a higher degree.
- Secondly, I would like to thank Professor Lionel Opie, a motivation and inspiration to all who pass through his laboratory. His unflagging enthusiasm for heart research, incredible memory and incisive criticisms, especially now as an Emeritus Professor, is admired and valued. His help with the final preparation of this thesis was really appreciated.
- Thirdly, Professor Ralph Kirsch – a truly amazing human being. He encouraged me by really appreciating my contribution to the Heart Research Unit over years spent in the department and by motivating me to upgrade from Masters to PhD.
- I would also like to thank my supervisor, Dr Faadiel Essop, for his support and encouragement. Things were not always easy (like when you went to Houston !), but we worked together and achieved in the end.
- Dr Sandrine Lecour, for her calm and sensible scientific advice, as well as for stepping into the breach when things were hectic.
- Adri Winckler, an oasis of calm and fount of knowledge in the maze of officialdom. Your encouragement and advice is sincerely appreciated.

- Dr Mohammed Jaffer of the University's Electron Microscopy Unit, who introduced me to the mysteries of the electron microscope with much patience, and also processed all the photos for me.
- Professor Dhiren Govender of the Dept of Lab Medicine (Anat Path), who gave permission for Danie Rademeyer to process/prepare the tissue samples for electron microscopy.
- Dr Sumaya Sharma, from Prof Heinrich Taegtmeyer's lab , for the quantitative RT-PCR data
- To my fellow researchers: all the many who have passed through the laboratory in the 30 years I have been here. Most have contributed to this achievement directly or by inspiration. I thank you all, but in particular the following:
 - Sylvia Dennis: PA of note! Thank you for the innumerable orders, queries, End Note and conference arrangements. All this plus the quiet lunches at Lady B helped smooth the way and soothe the nerves.
 - Victor "Victorious" Claasen, for always being so helpful and obliging, especially with regard to the references and library. May you always remain "happy and glorious" and as helpful as you are.
 - Noel Markgraaff and the Animal Unit staff, for tirelessly and patiently breeding and supplying animals required for this study on demand.

- Nuashaad Suleman, for competently performing the isolated mouse heart perfusions required for this thesis
- Pat van der Walt and Beauty Kom, our “cleaning fairies”, who supplied clean coats and glassware, sterile tips by the thousands and a clean and neat environment to work in.
- The students who drove me crazy, but stimulated my intellect with their incessant questioning: Anna Chan, Makhosi Zungu, Tasneem Adam, Naushaad Suleman.
- Lydia Lacerda, for help with the FACS machine. Shared the same (thesis) troubles, and so often my sounding board.
- Helen Barrett, my breath of sanity (or was it insanity?) in the midst of all the angst

Finally, thank you to my family, all of whom firmly believed I was capable of achieving this, even when I hesitated.

In particular, I would like to thank my husband Justin, for his unfailing encouragement and emotional support in all my aspirations throughout the years.

I would like to thank my son Jonathan, for his unfailing interest in my scientific blurb and his sustained encouragement.

Also my daughter Kathryn, who endured much, particularly this year, while continually had my nose in various papers and at the computer most nights till midnight!

Summary

Introduction

Preconditioning is a cardioprotective process initiated by short bursts of a trigger phenomenon like ischemia or hypoxia interspersed with reperfusion or normoxic episodes. The result is the activation of powerful protective pathways in the cell, conferring resistance to a subsequent more severe ischemic or hypoxic insult. Protein kinase C epsilon (PKC ϵ), an isoform member of a serine-threonine family of kinases involved in numerous protective signaling pathways in the cell, is directly involved in the preconditioning response in numerous species.[1]-[2] PKC ϵ translocates to the mitochondrion and the nucleus in response to the preconditioning stimulus

[3, 4] Furthermore, PKC ϵ expression and activity levels increase simultaneously, arguing for its cardioprotective role.[5] The preconditioning response is abolished when PKC ϵ activation is blocked using a specific inhibitor.[6] Together these data underscore the importance of PKC ϵ in the heart in response to oxygen lack.

Recent studies have investigated the underlying regulatory mechanisms that may explain the cardioprotective role of PKC ϵ . Sub-proteome analysis has identified interactions between activated PKC ϵ and various mitochondrial proteins, which orchestrate mitochondrial homeostasis, including proteins governing mitochondrial oxidative phosphorylation, electron transfer, ion transport and control of mitochondrial permeability transition (MPT).[7] MPT disruption is regarded as a key step in the initiation of an apoptotic cascade. However, brief pore opening may be beneficial in triggering the generation of small amounts of protective reactive oxygen species (ROS)[3] and restoring calcium homeostasis.[8]

PKC ϵ also interacts with adenine nucleotide translocases (ANTs), inner mitochondrial membrane proteins essential for ATP production and an integral component of the permeability transition pore.[3] An augmented capacity to generate ATP would fundamentally enhance resilience to ischemia.[9]

Aims and Objectives

In light of this, I hypothesized that modest activation of PKC ϵ promotes mitochondrial tolerance to an oxygen lack by maintenance of ATP production during such stress. Further, preservation of ATP generation and maintenance of intracellular homeostasis by prevention of MPT may be a functional target of PKC ϵ cardioprotective signaling. If the mice were protected against an acute oxygen lack, the same mechanisms might also protect against a more chronic stress, like hypobaric hypoxia

To explore this hypothesis, I utilised a mouse model currently available in our laboratory overexpressing an activated isoform of PKC ϵ in a cardiospecific manner.[7] It was necessary to first establish that the transgenic mouse was cardioprotected, before work on the hypothesis could commence.

Methods

- a. To establish that these mice expressed a cardioprotective phenotype, hearts from PKC ϵ overexpressing mice as well as wildtype littermates were subjected to global ischemia followed by reperfusion. Hearts were stained with triphenyltetrazolium chloride (TTC) and infarct size was compared, as an estimate of myocardial ischemia-reperfusion injury. Cardiac function and heart weight was compared at baseline to ensure that PKC ϵ overexpression had not adversely affected the PKC ϵ hearts.
- b. Mitochondria at baseline were isolated from PKC ϵ and wildtype mice to compare mitochondrial phenotype. Polarographic assays were performed at 25°C for the following endpoints:
 - Basal mitochondrial respiration
 - Membrane potential, measured with two specific and distinct potentiometric dyes, JC-1 and DiOC6
 - Rate of ATP synthesis, by luciferin-luciferase luminometry
 - Peptide levels of key mitochondrial regulatory proteins in wildtype and PKC ϵ mice were compared by SDS-PAGE analysis
- c. Additional mitochondria were subjected to an acute ADP-induced anoxic insult (45 minutes), then also to 45 minutes ADP-induced anoxia followed by 7 minutes reoxygenation. The same mitochondrial endpoints assayed in at baseline were repeated and PKC ϵ overexpressing hearts compared with wildtypes.
- d. PKC ϵ and wildtype mice were placed in a hypobaric hypoxic chamber for 7 or 14 days at 11% oxygen. Hearts were harvested from each group at both time points, together with appropriate normoxic control hearts and the following investigated:
 - Basal mitochondrial respiration
 - Cardiac function, utilizing retrogradely perfused hearts
 - Rate of ATP synthesis
 - Electron microscopy on LV muscle sections for mitochondrial biogenesis
 - Quantitative RT-PCR for genes thought to be implicated in the PKC ϵ cardioprotective program

Results

- a. The PKC ϵ hearts were protected at baseline, demonstrating a 40% reduction in infarct size in response to ischemia-reperfusion, compared to the wildtypes exposed to the same degree of oxygen lack ($p < 0.03$ vs WT). Cardiac function, as evaluated by developed tension, was identical in both groups and there was no evidence of hypertrophy on comparison of cardiac tissue wet weights with the wildtypes.
- b. Basal mitochondrial respiration was apparently no different, with similar rates of ADP-stimulated respiration and ADP phosphorylation. However, the mitochondria from PKC ϵ overexpressing mice were hyperpolarised compared to the wildtype. ($p < 0.0001$ and $p < 0.03$ with JC-1 and DiOC6 ,

respectively) Consonant with this finding, the rate of ATP synthesis was higher in the PKC ϵ mitochondria than in the wildtypes ($p < 0.0001$ at time zero), yet the ANT functional content was similar to the wildtypes. There was also no difference in the peptide levels of key mitochondrial proteins VDAC1, ANT, cytochrome c or UCP2.

- c. After an acute anoxic stress and after anoxia-reoxygenation, the PKC ϵ mitochondria recovered state 3 respiration better than the wildtype mitochondria ($p < 0.03$ for respiration and $p < 0.0001$ for membrane potential). Functional ANT content and rate of ATP synthesis was higher in the PKC ϵ overexpressing mice than in WT ($p < 0.0001$ and $p < 0.03$, respectively). Cytochrome c content in the wildtype mitochondria was diminished, compared to PKC ϵ mitochondrial ($p < 0.0002$).
- d. In response to hypobaric hypoxia, mitochondrial respiration and cardiac function appeared identical at both 7 and 14 days. In the wildtype hearts there was RV hypertrophy at both time points, but none detected in the PKC ϵ mice ($p < 0.001$ and $p < 0.005$ vs WT). On electron microscopic examination of hypoxic LV tissue at 7 and 14 days, the wildtype hearts exhibited marked mitochondrial biogenesis compared to the PKC ϵ overexpressing hearts. Rate of ATP synthesis was similar at 7 days but increased in the PKC ϵ hearts at 14 days. ($p < 0.03$ vs WT) PKC ϵ hearts appear to express a fetal gene pattern at baseline (\uparrow GLUT1 and MHC β), but switch to FAO when stressed (\uparrow PPAR α , CPT1, \downarrow UCP3). WT hearts follow the expected pattern – utilizing FA at baseline (\uparrow PPAR α , CPT1) and switching to glucose utilization when stressed (\uparrow GLUT1).

Conclusion

Hearts overexpressing a constitutively active form of PKC ϵ are protected at baseline and against an acute anoxic stress and reoxygenation injury by preservation of mitochondrial ATP production and maintenance of intracellular homeostasis by modulation of the mitochondrial permeability transition pore, a functional target in PKC ϵ cardioprotective signaling.

Furthermore, in response to hypobaric hypoxia, PKC ϵ modulates gene expression at the transcriptional level to regulate metabolic genes (GLUT1, PPAR α , CPT1, UCP3) and other genes (mitochondrial biogenesis, possibly via NRF-1 or PGC-1 α).

These findings support the hypothesis that modest activation of PKC ϵ promotes mitochondrial tolerance to acute and chronic oxygen lack by:

- Maintenance of cellular energetics
- Prevention of MPT and pore opening
- Gene regulation at the transcriptional level

Table of Contents

Declaration	i
Acknowledgements	ii
Summary	1
Table of Contents	4
Glossary of molecular Biology Terms	8
Abbreviations	11
List of Figures and Tables	13
Chapter 1: Introduction	17
A. BACKGROUND	18
1.1 Heart Disease: global and local burden	
B. DEFINITIONS	18
1.2 Ischemia	20
1.2.1 Ischemia and Infarction	20
1.2.2 Ischemic Damage	21
1.2.3 Reperfusion Injury	22
1.2.4 Ischemia/Reperfusion vs Hypoxia/reoxygenation	23
1.3 Preconditioning Stimuli	
1.3.1 Ischemic preconditioning	24
1.3.2 Pharmacological preconditioning	26
1.3.3 Remote preconditioning	26
1.3.4 Postconditioning	27
C PKC: PHYSIOLOGY AND BIOCHEMISTRY	
1.4 PKC family of proteins	27
1.5 PKC and the heart	29
1.6 PKC ϵ and ischemia/reperfusion	30
1.7 PKC and Ischemic preconditioning	31
1.8 PKC ϵ and cardioprotection	33
D MITOCHONDRIA: BACKGROUND AND OVERVIEW	38
E MITOCHONDRIAL ENERGY PRODUCTION	42

1.8.1	Tricarboxylic acid cycle (TCA cycle)	42
1.8.2	Cytosolic Reducing Equivalents	43
1.8.3	Fatty acid β -oxidation	45
1.8.4	Oxidative Phosphorylation	48
1.9	Perturbed mitochondrial energy production	55
1.10	Mitochondria control cell death	59
1.11	Hypothesis	69
Chapter 2: Materials and Methods		71
2.1	Animals	72
2.1.1	Ethics	72
2.1.2	PKC ϵ overexpressing transgenic mouse model	72
2.1.3	Genotyping of PKC ϵ transgenic mouse	74
2.1.3.1	DNA Extraction	74
2.1.3.2	Polymerase Chain Reaction	75
2.1.3.3	Agarose Gel Electrophoresis	77
2.2	Ischaemia/Reperfusion experiments: Infarct size	
2.2.1	Isolated mouse heart perfusion model	78
2.2.2	Cardiac Functional assessment	79
2.2.3	Infarct size determination	80
2.3	Mitochondrial Respiration Studies	
2.3.1	Mitochondrial isolation	81
2.3.2	Lowry protein determination	82
2.3.3	Determination of Mitochondrial respiration coupling	83
2.3.4	Determination of basal functional ANT content	84
2.3.5	Determination of basal mitochondrial proton leak	85
2.3.6	Determination of total inorganic phosphate	85
2.3.7	Rate of mitochondrial ATP synthesis	85
2.4	FACS analysis	86
2.5	Western Blot Analysis	87
2.5.1	Polyacrylamide Gel electrophoresis	88

Adaptation for	ANT1	89
	Cytochrome c	89
	UCP2	89
	VDAC1	89
2.6	Anoxia/reoxygenation experiments	91
2.6.1	Mitochondrial endpoints	92
2.6.2	Determination of functional ANT content in response to anoxia/reoxygenation	92
2.7	Hypobaric Hypoxia	93
2.7.1	Hypobaric hypoxic chamber	93
2.7.2	Real Time quantitative RT-PCR	94
2.7.3	Functional assessment	95
2.7.4	Mitochondrial respiration	95
2.7.5	Electron microscopy	96
2.7.6	Rate of ATP synthesis	96
2.8	Statistics	97
Chapter 3: Characterization of the protective phenotype of the PKCϵ cardiac-specific overexpressing mouse		
3.1	Introduction	99
3.2	Methods	101
3.2.1	Characterization of the protective phenotype	101
3.2.2	Mitochondrial functional phenotype	102
3.3	Statistics	104
3.4	Results	105
3.4.1	Characterization of the protective phenotype	105
3.4.2	Mitochondrial functional phenotype	108
3.4.3	Acute oxidative stress	113

3.5 Discussion	120
3.6 Conclusion	128
Chapter 4: A cardioprotective role for constitutively active PKCϵ	
 In response to hypobaric hypoxia	
4.1 Introduction	130
4.2 Materials and methods	
4.2.1 Transgenic mouse model	134
4.2.2 Mitochondrial Isolation	135
4.2.3 Characterization of mitochondrial function	135
4.2.4 Electron microscopy of left ventricular tissue	135
4.2.5 Heart perfusion studies	136
4.2.6 Assessment of hypertrophy	136
4.2.7 Quantitative RT-PCR	137
4.3 Statistics	137
4.4 Results	138
4.5 Discussion	150
 Chapter 5 : Conclusion	
5.1 Acute Oxygen lack	164
5.2 Chronic Oxygen lack	165
5.3 Proposed molecular mechanism for PKC ϵ	169
5.4 Future Directions	171
5.5 Possible Clinical Applications	172
5.6 Limitations of the study	174
5.7 Publications arising from this work	176
 References	 178

Glossary of Molecular Biology terms:

Adenylate Kinase: enzyme catalyzing the formation of ATP from two ADP molecules.

Anoxia: complete lack of oxygen in an environment

Apoptosis: programmed cell death. The process requires ATP and is initiated at the mitochondrion by a caspase cascade following membrane permeability transition (MPT) and cytochrome c release.

Cardioprotection: protection of the myocardium against injury.

Chaperone proteins: proteins involved in the sequestering and assembly of multi-protein complexes e.g. HSP 27.

Cristae: convoluted folds in the inner mitochondrial membrane that increase the surface area and bring molecules that interact into close proximity, as in the permeability transition pore.

Cyclophilin D: regulatory molecule of ANT in the mitochondrial matrix.

Cytochrome C: electron acceptor in the electron transport chain, located in the intermembrane space. Leakage into the cytosol triggers a caspase cascade, initiating apoptosis.

Electrochemical gradient: The transfer of electrons along the transfer chain is coupled to the generation of a proton gradient across the inner mitochondrial membrane, by the pumping of protons from the matrix to the outer edge of the inner mitochondrial membrane. The proton concentration is thus lower in the matrix, creating a "proton-motive force" that drives the synthesis of ATP at complex V. Protons are pumped back into the matrix at the conversion of this electron transfer potential to the phosphoryl transfer potential of ATP to facilitate the release of the ATP molecule.

Electron transfer: $\text{NADH}^+ + \text{H}^+$ and $\text{FAD}^+ + \text{H}^+$ each have a pair of high-energy electrons. When these electrons are transferred to oxygen, a large amount of free energy is liberated which can be utilised to generate ATP.

Energetic reserve: the energy reserve the heart has in the form of phosphocreatine, allowing it to cope with a sudden work jump.

Fas-ligand: A member of the TNF alpha superfamily, responsible for the balance of signals that confer cell death /cell survival.

Fatty acid oxidation: Stepwise enzymatic breakdown of activated acyl-fatty acids within the mitochondria, to yield ATP from acetyl CoA.

Functional proteomics: a study of the functional interactions of proteins occurring within the cell.

Genotyping: identifying a genetically engineered offspring from its wildtype littermate by isolation of genomic DNA and subsequent PCR

Glycolysis: A sequence of enzymatic reactions that converts glucose to pyruvate usually in response to a lack of oxygen. Generates cytosolic ATP to help maintain cellular energetics.

Heat shock proteins: (HSPs) proteins first noticed to be induced by heat shock in *E. coli*. Act as chaperone proteins in mammals, are protective and anti-apoptotic.

Homeostasis: maintenance of the cellular and ionic status quo

Hypoxia: abnormally reduced oxygen tension

Ion transport: ions are charged molecules. Biological membranes are also charged and the gradient across these membranes are vital to maintaining ion homeostasis. Transport of these across the cell membrane or mitochondrial membrane may be active (requiring energy, in the form of ATP) or passive (by diffusion).

Ischemia/ischaemia: poor blood flow (Greek, ischo – to hold back, haima - blood). Lack of blood (*in vivo*) or perfusate (*ex vivo*) to the myocardium due to an intervention or occlusion.

Isoform: proteins with slightly different molecular structures, but great homology and similar function.

Membrane permeability transition pore: In the mitochondria, at the points of contact of the double membrane. Generally accepted as being composed of VDAC1 (voltage dependent anion channel 1) spanning the outer mitochondrial membrane and ANT (adenine nucleotide translocator).

Membrane permeability transition: (MPT) Permeabilization of the inner mitochondrial membrane due a trigger event (ischemia/reperfusion or hypoxia/reoxygenation), leading to an influx of solutes into the mitochondrial matrix. This sequence may cause rupture of the outer mitochondrial membrane, release of cytochrome c and the initiation of the apoptotic cascade.

Oxidant stress: The adverse effect of reactive oxygen species.

Oxidative phosphorylation: the process in which ATP is formed as electrons are transferred from reducing equivalents $\text{NAD}^+\text{+H}^+$ and $\text{FADH}^+\text{+H}^+$ to oxygen, via a series of electron carriers located in the inner mitochondrial membrane.

PCr shuttle: Transfer of energy from phosphocreatine to ATP, utilizing creatine kinase to maintain the energy reserve during abrupt workload increase.

Post-ischemic: occurring after ischemia

Preconditioning: an intervention whereby short bursts of ischemia interspersed with episodes of reperfusion activate the cell's endogenous protective mechanisms, such that the tissue is protected against a subsequent more severe ischemic insult.

Pressure overload hypertrophy: a growth response initiated in the heart due to sustained increased afterload pressure, e.g aortic constriction, hypertension.

Reactive Oxygen Species: highly reactive oxygen groups containing unpaired electrons in their outer orbitals. They are important physiological and pathological signal molecules, often involved in pathways adverse to cell survival , but may protective functions at low concentrations.

Reperfusion: restoration of blood or perfusate flow to the tissue

Sub-proteome analysis: analysis of the functioning of active parts of individual proteins

Transgenic mouse: a mouse that has been genetically engineered to overexpress or underexpress a particular protein.

Abbreviations

ACC: Acetyl CoA carboxylase

Akt: Also called protein kinase B or PKB. Member of a protein kinase family that is part of the signal pathway that responds to growth signals, e.g. insulin

AMPK: 5'AMP-activated protein kinase. A master regulator of metabolism in response to altered energy requirements.

ANT 1/2: adenine nucleotide translocator or translocase. Two isoforms exist : 1 and 2. Situated on the inner mitochondrial membrane, along with its regulatory proteins (hexokinase 1 & II, cyclophilin D, Bad, Bax, Bcl-2, Bcl-xL). A component of the membrane permeability transition pore. Bax acts on ANT, as does reactive oxygen species, causing an inactivating conformational change, which is transmitted to VDAC, adjacent on the outer membrane. These changes result in permeabilization of the mitochondrial membrane, apoptosis and ensuing cell death.

ATP: Adenosine triphosphate. Composed of adenine, ribose and a triphosphate unit. Usually has a manganese or magnesium associated with it. Considered the universal currency of free energy in the cell, as hydrolysis of the pyrophosphate bonds yields large amounts of free energy.

Bad/Bax: Members of the Bcl-2 protein family that regulate cell death. Bax and Bad are proapoptotic.

Bcl-2: An antiapoptotic protein. Binds to VDAC to prevent membrane permeability transition (MPT).

CCCP: carbonyl cyanide 3-chlorophenylhydrazone. Dissipates membrane potential.

DISC: Death inducing signaling complex.

ERK1/2: A MAP kinase, activated in response to a growth stimulus. Also called p42/p44.

FACS machine: fluorescence activated cell sorting machine. Used for measuring mitochondrial membrane potential.

MCAD: malonyl CoA decarboxylase

mRNA: Messenger RNA, made in the nucleus during transcription of a gene.

NRF-1: Nuclear respiratory factor 1. Belongs to the NF-E2 family of transcription factor responsible for the regulation of many erythroid (red blood cell) genes.

PAGE: Poly acrylamide gel electrophoresis

PCr: phosphocreatine, also called creatine phosphate. Donates its phosphate group to ADP to maintain ATP stores via the PCr shuttle during acute workload increase.

PCR: Polymerase chain reaction, for amplifying DNA.

PGC1- α : PPAR-gamma coactivator 1-alpha. A transcription co-activating factor regulating transcription and repression of various genes in response to stressors.

PKC: Protein kinase C, a family of G-coupled serine-threonine kinases, having 11 isoforms and playing key regulatory roles in a variety of cell functions – cell growth, differentiation, gene expression, hormone expression, cardioprotection.

rRNA : ribosomal ribonucleic acid (RNA), constitutes nearly 60% of the mass of the ribosomes.

TNF- α : tumour necrosis factor alpha. A pleiotropic cytokine, hypothetically protective in low doses, adverse in high doses. Activates a host of signaling pathways.

TNFR: Tumour necrosis factor receptor

tRNA: transfer ribonucleic acid, act as carriers of specific amino acids during protein synthesis

VDAC1/2/3: Isoforms of voltage dependent anion channel. A component of the permeability transition pore, permeable to solutes up to 1500 kDa in size (non-specific). Act as mitochondrial binding sites for glycerol kinase, hexokinase and PKC ϵ .

List of Figures and Tables:

Chapter 1

Figure 1-1: Twenty leading causes of death (%), Western Cape 2000	19
Figure 1-2: Twenty single causes of death by gender in the total Western Cape population.	19
Figure 1-3: Experimental coronary artery occlusion	21
Figure 1-4: Ischemic preconditioning reduces the reperfusion damage	25
Figure 1-5: Hypothetical PKC Threshold for Ischemic preconditioning	32
Figure 1-6: Proposed signaling pathway involved in cardioprotection	36
Figure 1-7: PKC ϵ protective signaling pathways	37
Figure 1-8: Simplified schematic of a mitochondrion	40
Figure 1-9: Specific membrane transporters	41
Figure 1-10: Tricarboxylic Acid (TCA cycle)	42
Figure 1-11: Glycerol-3-phosphate shuttle	43
Figure 1-12: Malate aspartate shuttle	45
Figure 1-13: Fatty acid β -oxidation spiral	47
Figure 1-14: Oxidative Phosphorylation	49
Figure 1-15: Phosphocreatine shuttle	53
Table 1-1: Mitochondrial mutations and pathological manifestations (From Russell, 2005[10])	56
Figure 1-16: Mitochondrial Permeability Transition Pore (MPTP)	60
Figure 1-17: Regulation of the mitochondrial permeability transition pore (MPTP) in response to oxidant stress	61
Figure 1-18: Apoptosome formation	66
Figure 1-19: Schematic representation of hypothesis	70

Chapter 2

Figure 2-1(a and b): PKC ϵ expression levels in aPKC ϵ mice	73
Figure 2-2: Illustration of an isolated perfused mouse heart, subjected	78

to global ischemia by total occlusion of the aorta.	
Figure 2-3: Illustration of mouse heart perfusion model for cardiac function assessment	79
Figure 2-4: TTC staining for Infarct size estimation	80
Figure 2-5: Typical trace of mitochondria subjected to ADP- induced anoxia for 45 minutes, then reoxygenated.	91
Figure 2-6: Hypobaric hypoxic chamber, developed in-house	94

Chapter 3

Figure 3.1: Infarct size in response to ischemia.	105
Figure 3-2: Assessment of baseline cardiac function	106
Table 3-1: Working heart baseline cardiac function assessment	106
Figure 3-3(a) and (b): Comparison of PKC ϵ overexpressing baseline heart and bodyweights with WT	107
Table 3-2: Basal Mitochondrial Respiration	108
Figure 3-4: Baseline Mitochondrial membrane potential	109
Figure 3-5: Baseline functional adenine nucleotide translocator (ANT)	110
Content	
Figure 3-6: Baseline Inorganic phosphate (Pi) levels in isolated mitochondria	111
Figure 3-7: Baseline rate of ATP synthesis.	112
Figure 3-8: Baseline Western blot analysis of mitochondrial regulatory proteins	113
Figure 3-9: Mitochondrial respiration after excess ADP-induced anoxia / reoxygenation. (JC-1)	114
Figure 3-10: Mitochondrial membrane potential in response to excess ADP-induced anoxic stress (DiOC6)	115
Figure 3-11: Membrane potential after excess ADP-induced anoxia/reoxygenation	116

Figure 3-12: Functional ANT content after excess ADP-induced anoxic stress	117
Figure 3-13: ATP synthesis after ADP induced-anoxia / reoxygenation	118
Figure 3-14: Mitochondrial cytochrome c protein levels	119
Figure 3-15: Densitometric analysis of cytochrome c levels.	120

Chapter 4

Table 4-1: Hypoxic response mechanisms in the body	130
Figure 4-1a and b: Attenuated hypertrophic response in the RV of aPKC ϵ mice.	138 and 139
Figure 4-2a: Cardiac function after 7 days of hypobaric hypoxia	140
Figure 4-2b: Cardiac function after 14 days of hypobaric hypoxia	140
Figure 4-3a & 3b: Preserved mitochondrial respiration in response to 7 and 14 days of hypobaric hypoxia.	141
Figure 4-4a & 4b: ATP Synthesis in mitochondria isolated from RV in response to chronic hypobaric hypoxia	142
Figure 4-5a and b: Electron micrograph of longitudinal sections of normoxic left ventricle magnified 25000X	143
Figure 4-5c and d: Electron micrograph of longitudinal sections of 7 day hypoxic left ventricle, magnified 25000X	144
Figure 4-5e and f: Electron micrograph of longitudinal sections of 14 day hypoxic LV, magnified 25000X	144
Figure 4-6: mRNA expression of GLUT 1 in RV tissue	145
Figure 4-7: mRNA expression of MHC β in RV tissue	146
Figure 4-8: mRNA expression levels of UCP3 in RV tissue	147
Figure 4-9: mRNA expression for PPAR α in RV tissue	148
Figure 4-10: mRNA expression levels of mCPT1 in RV tissue	149
Figure 4-11: Proposed mechanism of PKC ϵ protection against hypoxia	150

Figure 4-12: PKC ϵ activates multiple pathways to exert its protective effects on the heart 162

Chapter 5

Figure 5-1: Proposed molecular mechanisms for PKC ϵ 169

University of Cape Town

Chapter 1

Introduction

University of Cape Town

A. BACKGROUND

1.1 Heart disease: global and local burden

A recent World Health Organization (WHO) report warns of the escalating global burden of cardiovascular diseases (CVD), projecting that it will become the major worldwide cause of death and disability by 2020.[11] In agreement, another report *A Race Against Time – the Challenge of Cardiovascular Disease in Developing Economies*, investigating the prevalence of CVD in South Africa, Brazil, India, Russia, Portugal and the USA, projects a marked increase for the incidence of CVD in developing countries by 2020/ 2040. [12] Moreover, despite the threat of HIV-AIDS, CVD forms the main proportion of deaths (35-44 years age range) in South Africa due to chronic disease, with 12% and 17.2% incidences for men and women, respectively. In agreement with this alarming trend, Professor Bradshaw of the South African Medical Research Council's Burden of Disease Unit recently reported that in the Western Cape (the southern most province of South Africa), ischemic heart disease is the leading cause of death in the total population in a single year (Fig. 1-1).[13] When these figures are broken down according to gender, ischemic heart disease is the major killer of females and the second leading cause of death in males in the Western Cape (Fig. 1-2).[13] These findings therefore underscore the growing global burden of CVD, with especially younger individuals residing in developing countries being most affected.

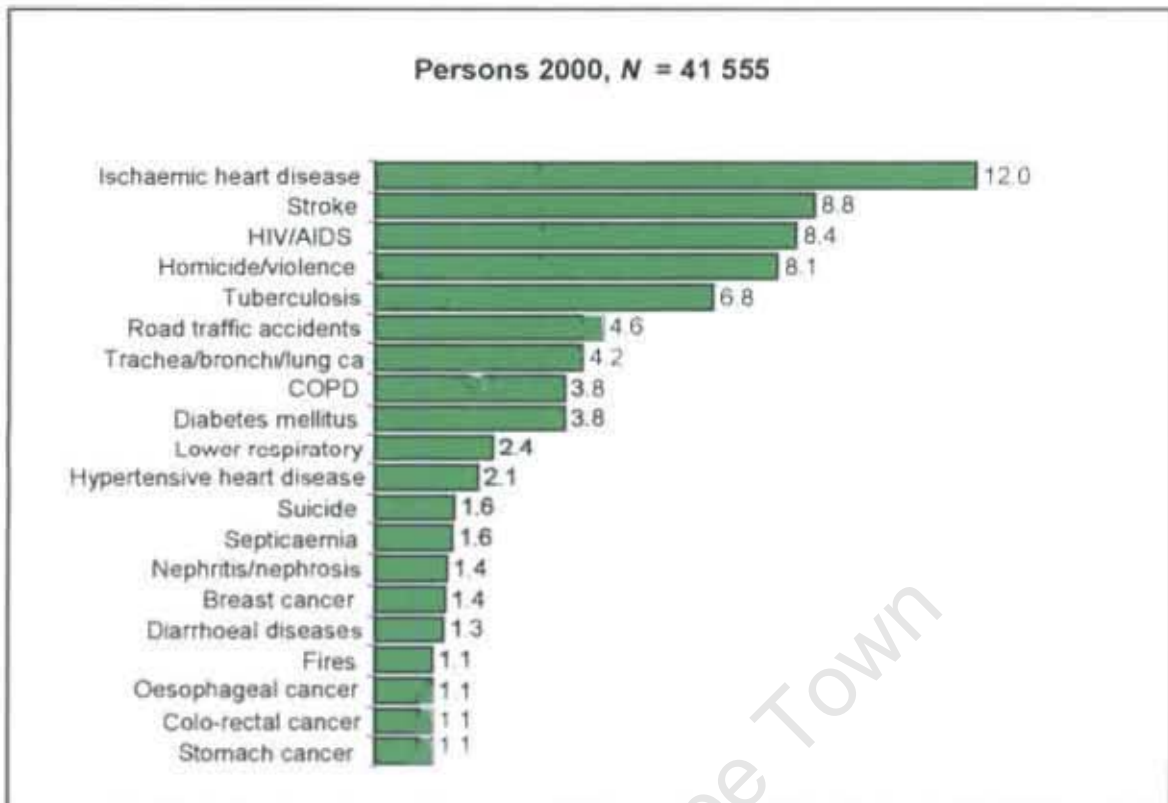


Figure 1-1. The twenty leading causes of death (%) in the Western Cape population [13]

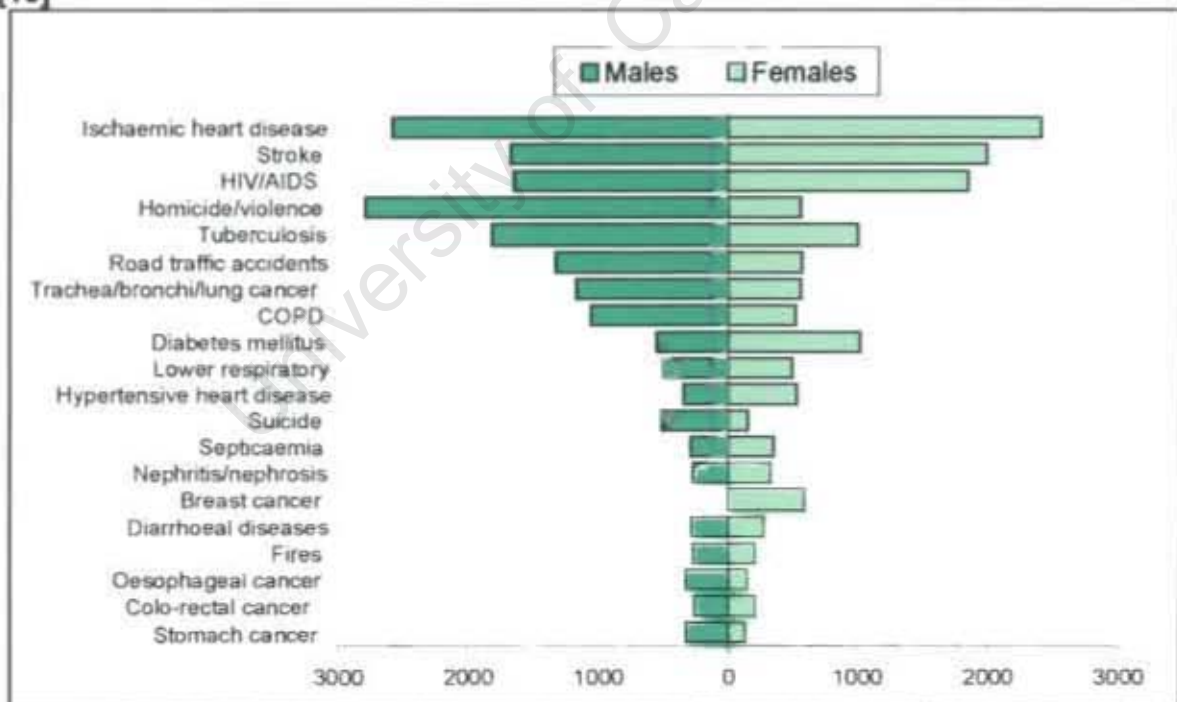


Figure 1-2. Twenty leading single causes of death by gender in the Western Cape region. [13] COPD – chronic obstructive pulmonary disease

The disease burden is being exacerbated by the influx of rural populations into the cities in search of employment. Once urbanized, rural people generally abandon their traditional lifestyle and diet, readily adopting the more sedentary Western lifestyle and diet i.e. one high in fat and refined carbohydrates. As a direct result their health profile is steadily changing, with an increase in obesity and type 2 diabetes, hence the increase in the risk of coronary artery disease, hypertension and heart failure.[14, 15]

The higher mortalities and morbidities associated with increased CVD rates will have serious socio-economic implications, including disruption of family units, greater health-care costs and diminished productivity. Therefore, with the projected increases for CVD rates in South Africa, this will place an enormous burden on the country's resources. In order to attenuate/reverse these disturbing projections, a concerted, ongoing intervention strategy is urgently required. Part of such a strategy includes investigation into basic mechanisms that may lead to protection of the heart ("cardioprotection") in response to various stresses for e.g. ischemic attacks, high blood pressure, etc.

B. DEFINITIONS:

1.2.1 Ischemia and infarction

Coronary artery disease in humans commonly causes thrombosis, resulting in occlusion of a coronary artery. When blood and oxygen supply to the myocardium is reduced by such an occlusion, the oxygen demand may exceed

the supply and myocardial ischemia occurs. If the occlusion is left untreated an acute myocardial infarction occurs, defined as an “area of coagulation necrosis in tissue due to local anemia resulting from an obstruction of circulation to the area”.[16]. In experimental animal models, infarction is usually created by coronary artery occlusion, often followed by reperfusion (Figure 1-3).

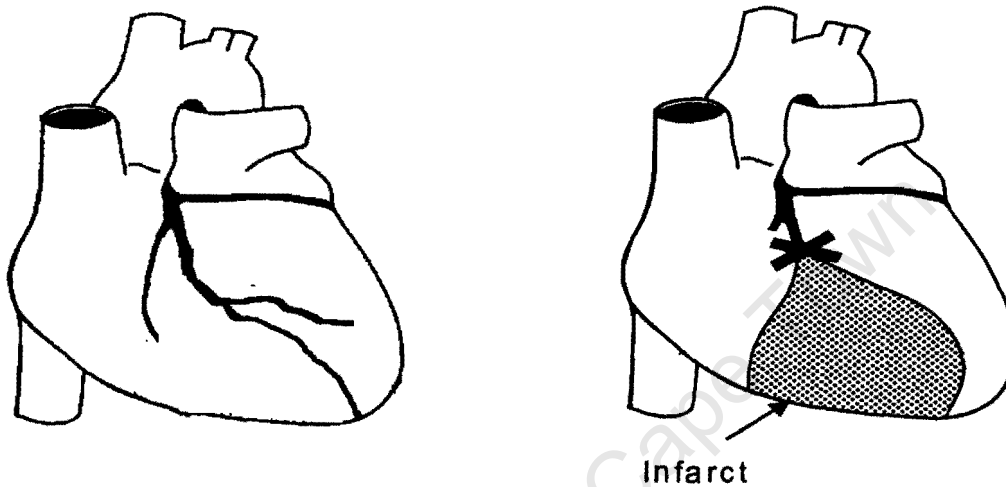


Figure 1-3. Prolonged experimental coronary artery occlusion (regional ischemia) results in some degree of permanent and irreversible damage – acute myocardial infarction. (With permission [9]).

Various drug therapies have been employed in an attempt to reduce infarct size (β blockers, calcium channel blockers and anti-inflammatory compounds),[17] but with limited success. The lack of successful intervention could possibly be attributed to incomplete understanding of the mechanisms of ischemic damage, which are not yet clearly defined.[18]

1.2.2 Ischemic damage

After an ischemic episode, the area of tissue immediately distal to the occlusion undergoes irreversible processes including mitochondrial collapse, rapid energy

depletion and ion pump failure.[19] Oxidative phosphorylation rates decrease and pre-existing intracellular ATP is utilized to maintain the ion pumps.[9] Contraction is downscaled and anaerobic energy production via glycolysis is upregulated, [9, 20] so for a short while the myocardium is able to maintain intracellular ATP levels. However, accumulation of ATP breakdown products (AMP, adenosine and P_i) activate diverse cytosolic cascades, increasing calcium (Ca^{2+}) entry into the cell with concomitant loss of intracellular K^+ . [19] In response to increased localized Ca^{2+} in the cytosol, proximal mitochondria rapidly take up Ca^{2+} to reduce the deleterious effects.[21] However, with continued Ca^{2+} influx, the mitochondria are not able to buffer the Ca^{2+} increase indefinitely. Whether programmed cell death (apoptosis) or necrotic/oncotic cell death ensues is dependent on the severity and duration of the ischemic episode.[22] Apoptosis is generally accepted as an energy requiring process. Thus, as ATP levels drop and the ion imbalance is aggravated, cells become edematous and necrotic or oncotic cell death ensues. Autophagy (literally meaning "self-eating") may also occur as a result of lysosomal activation. In addition, there is an inflammatory response to the release of proapoptotic factors during programmed cell death, including the generation of excess reactive oxygen species (ROS) and the triggering of inflammatory cytokines such as $TNF\alpha$.

1.2.3 Reperfusion injury

Jennings and Reimer[23] demonstrated that after a complete coronary occlusion, rapid restoration of blood flow (reperfusion) is essential to protect the ischemic

myocardium. This intervention reduces infarct size but does not totally eliminate infarction because reperfusion has deleterious effects: arrhythmias, enzyme leakage and/or intramyocardial hemorrhage.[24-27] Reperfusion injury was defined by Jennings as “cell death caused by reperfusion only, distinct from cell death caused by the preceding ischemia”. [28]

Initially, the damage in the ischemic area is reversible.[29] Salvage of the at-risk tissue depends on reversing or arresting the detrimental intracellular processes that would control the propagation of the infarct beyond the necrotic core.[19] Within an hour, the total infarct (irreversibly damaged cells) approximately equals the area still at risk.[29] Mitochondrial damage might be the critical feature of the irreversible cellular damage,[30] as mitochondria isolated from damaged cells exhibit reduced oxidative phosphorylation and are more fragile, containing granules thought to be composed of calcium, phosphate and magnesium. This supports the hypothesis that mitochondrial damage may be reflected by cellular damage and death.[30] Indicators of such damage are decreased high-energy phosphate stores, increased Ca^{2+} content and free radical generation.

1.2.4 Ischemia/reperfusion versus hypoxia/reoxygenation

Similarities in intracellular conditions exist during ischemia and hypoxia, but there are also several important differences. During ischemia, there is insufficient oxygen (hypoxia) due to reduced blood supply, but the hypoxia is localized to the infarcting area. There is also reduced washout of accumulated metabolites (H^+ and lactate). Upon reperfusion, the restored blood flow washes out metabolites

but elicits an inflammatory response by the presence of neutrophils and macrophages in the area. In experimental models of hypoxia the oxygen lack is generally systemic, not restricted to the heart only. Although there is also poor oxygen delivery and reduced oxidative phosphorylation, there is no accumulation of detrimental metabolites in the heart. In a study of reoxygenation of anoxic potassium-arrested reperfused hearts, Hearse et al.[31] reported a biphasic enzyme release (creatine kinase and glyceraldehyde-3-phosphate dehydrogenase) i.e. the first within 10-60 minutes of anoxia, and a larger second release at reoxygenation. This illustrates the similarities between “reoxygenation injury” and “reperfusion injury”. In addition, re-admission of oxygen to the reperfusion area could have a deleterious effect by creating a hyperoxic environment, favoring the formation of reactive oxygen species (ROS) and lipid peroxidation that permeabilizes cell and organelle membranes. Overall, the effects of reperfusion/reoxygenation damage include: decreased high energy phosphate stores, poor functional recovery, Ca^{2+} accumulation, enzyme leakage and the generation of free radicals, resulting in oxidative microvascular damage and cell death.[32] It follows that intervention at reperfusion or reoxygenation is necessary to minimize this reperfusion/ reoxygenation damage.

1.3 Preconditioning Stimuli

1.3.1 Ischemic Preconditioning

Several powerful endogenous protective mechanisms have been discovered in the heart, triggered by a variety of stimuli. Murry, working with Jennings, showed

in their seminal paper on the decrease of lethal injury with ischemia[27] that when a severe prolonged occlusion was preceded by four cycles of brief occlusion interspersed with brief cycles of reperfusion, there was a major reduction in the size of the ultimate infarct.[27] They termed this cardioprotective phenomenon ischemic preconditioning (IPC). This period of protection is the first window of preconditioning or classical preconditioning, conferring transient yet robust protection on the myocardium for up to 6 hours. Subsequent to this first window of protection, a second delayed period of protection occurs within 24 hrs of the initial stimulus and lasts for up to 72 hrs. This second window of preconditioning (SWOP) although less robust than classical preconditioning, persists for longer.[33] IPC therefore seemed to protect against injury at reperfusion, through an as yet undetermined mechanism (Figure 1-4).

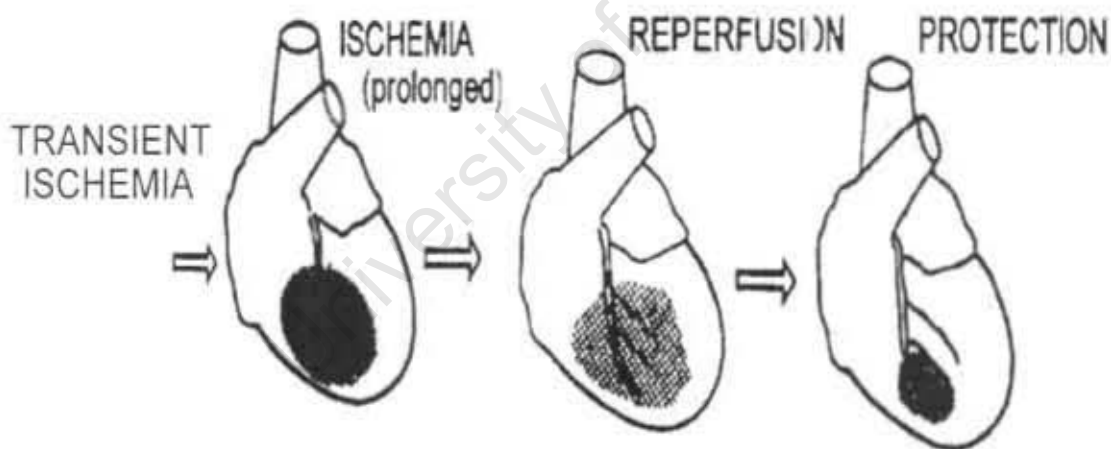


Figure 1-4. Ischemic preconditioning reduces the resultant reperfusion damage
When a severe prolonged occlusion is preceded by four cycles of brief occlusion interspersed with brief cycles of reperfusion, there is a major reduction in the size of the ultimate infarct. (With permission) [9].

1.3.2 Pharmacological preconditioning

IPC is not the only mechanism to reduce ischemia/reperfusion damage, as was shown by Downey and co-workers.[34] Rabbit hearts perfused with adenosine analogs showed a similar reduction in infarct size after ischemia/reperfusion. This was the first demonstration of an IPC-like protective mechanism in small animals mediated by “pharmacological preconditioning” without the ischemia/reperfusion pretreatment, yet conferring a reduction in infarct size. This was also the first indication of a possible messenger molecule to mediate the IPC effects.

1.3.3 Remote Preconditioning

During 1993 Przyklenk et al. showed that IPC performed in one region of the dog heart conferred protection on remote areas of the myocardium i.e. removed from the IPC site. They proposed that IPC must trigger the release of circulating substance(s), which act as triggers in the remote myocardium – phenomenon referred to as remote preconditioning. These findings were confirmed in 1996 by Verdouw et al,[35] who occluded and reperfused a mesenteric artery and initiated protection in the rat myocardium. Similarly, Wolfrum et al.[36] have further shown that remote preconditioning (occlusion of a mesenteric artery) in a rat model elevates myocardial PKC ϵ via a bradykinin-dependent mechanism. Protection of the myocardium by remote preconditioning could be abolished by the inhibition of PKC ϵ i.e. utilizing a PKC ϵ inhibitor (chelerythrine) or a bradykinin inhibitor (HOE 140), illustrating the involvement of PKC ϵ in this form of cardioprotection as well.

1.3.4 Post-conditioning

The powerful endogenous cellular protective mechanism of IPC protected against reperfusion injury at the laboratory bench, but still had limited application in the clinical situation. The most recent development in the field of IPC is post-conditioning.[37-39] Here, during the first minutes of reperfusion for acute myocardial infarction in humans, the myocardium is preconditioned by staged reperfusion utilizing an angioplasty balloon, as opposed to full abrupt opening of the occluded artery.[38, 40] The outcome of the ultimate reperfusion was reduced infarct size (damage was measured enzymatically).[37, 38] The molecular and signaling mechanisms of post-conditioning are proposed to be similar to that of IPC, viz. via activation of the PI3K/Akt pathway and downstream kinases like PKC.[39]

C. PKC: PHYSIOLOGY AND BIOCHEMISTRY

1.4 PKC family of proteins

Protein kinase C (PKC) is a family of serine/threonine kinases present in the cytosol, responsible for the transduction of a multitude of signals.[41] Members of the PKC family are single polypeptides, comprised of an N-terminal regulatory region (~ 20-40 kDa) and a C-terminal catalytic region (~ 45 kDa). The C1 domain contains a cysteine-rich motif that forms the diacylglycerol binding site. The C2 domain has a recognition site for acidic lipids and the C-3 and C-4 domains form the ATP-binding and substrate lobes of the kinase core. A hinge region that becomes proteolytically labile when the enzyme is membrane bound

separates the regulatory and catalytic halves of the molecule. The proteolytically generated kinase domain is the constitutively active site. [41]

The main function of PKC is to catalyze the transfer of the γ -terminal phosphate from ATP to the hydroxyl group of serine and/or threonine residues in various protein substrates, thereby regulating the activity of proteins involved in cellular growth and differentiation as well as immediate regulation of effector functions.[42-44] PKCs are activated in response to stresses like ischemia, anoxia and hypoxia and their actions may be protective or deleterious. When activated, PKCs translocate to the nucleus and the mitochondrion, but their mechanisms of action and signaling pathways are not clearly understood. One of the actions of the PKCs at the nucleus is thought to be the activation of transcription,[45] but they have been shown to phosphorylate and activate proteins directly, for e.g. troponin I and troponin T.[46] PKCs can act in parallel and in opposition, like PKC ϵ and PKC δ . Occasionally, as one isoform decreases, the others increase to compensate, while some isoforms directly antagonize one another.[47] Translocation of an isoform from the particulate to the membrane fraction does not alter the total PKC activity.[7]

There are 3 distinct subfamilies of protein kinase C[4]:

Classical (Ca^{2+} dependent, activated by diacylglycerol [48])	α, β, γ
Novel (Ca^{2+} independent, activated by DAG)	ϵ, η, θ
Atypical (activated by distinct lipids only)	ζ, λ, τ

One of the first steps in the activation of PKC is the binding of a signaling molecule to a G-protein linked receptor in the plasma membrane. In response the G-protein activates phospholipase C (PLC)[49] to cleave the cellular phospholipid phosphatidylinositol (PIP₂),[50] thereby generating diacylglycerol (DAG) and inositol triphosphate (IP₃). The latter couples receptor activation to mobilization of calcium stores, whereas DAG activates the novel and classical PKCs. PIP₂ cleavage by PLC is considered a crucial step for PKC activation as DAG acts as a hydrophobic factor, increasing the affinity of PKCs for the membranes, thereby facilitating the translocation of PKCs to the membranes compartments of the subcellular organelles.[41, 51]

1.5 PKC and the heart

The PKC isoform mediating cardioprotection in numerous species is PKC ϵ , a novel calcium-independent isoform. Adult rat hearts express mainly PKC ϵ and PKC δ ,[45] whereas in adult rabbit hearts 10 of the 13 isoforms have been identified with PKC α , β_1 , β_2 , and γ being the most abundant.[52] Canine hearts express mostly PKC ϵ and ζ , whereas human cardiac tissue expresses predominantly PKC δ , and to a lesser extent PKC ϵ , λ and τ .

The biological significance of this marked PKC isoform variance has not yet been clarified,[45] but PKC has been identified as a regulator of cardiac contractility[53] and its association with cardiac membranes has been shown to modulate ion channels, for e.g. decrease inward calcium transients.[54] Studies

have clearly demonstrated that PKCs can be involved in several important mechanisms underlying varied cellular effects and that PKCs may mediate responses to physiological or pathological stimuli, whilst also regulating transcription.[45]

1.6 PKC ϵ and ischemia/reperfusion

Ischemia/reperfusion results in energy substrate deprivation, cellular edema, Ca²⁺ overload, activation of autolytic enzymes disruption of membranes and mitochondrial abnormalities, all of which is likely to contribute to post-ischemic cardiac dysfunction. PKC was the first kinase examined in detail in the context of ischemia/reperfusion.[55] Translocation of the various isozymes was measured by protein kinase activity assays performed on the cytosol and membrane fractions of rat hearts subjected to ischemia or ischemia/reperfusion. Ischemia increased the activities of PKC ϵ , PKC α and PKC β in the membrane fraction and reperfusion did not alter the ischemic translocation pattern.[56] PKC ϵ , PKC α and PKC τ was also observed to translocate to the membrane fraction in a rat heart model of global ischemia, but again translocation was not altered by reperfusion.[57]

The contribution of multiple PKC isoforms to myocardial ischemic injury was demonstrated by the perfusion of isolated rat hearts with separate peptides that activated PKC ϵ (added prior to ischemia) and inhibited PKC δ (added during reperfusion). These hearts were protected from ischemia/reperfusion injury, as

demonstrated by increased cardiac functional recovery and decreased enzyme release and infarct size.[58]

1.7 PKC and ischemic preconditioning (IPC)

Despite almost 10 years of intensive study, the cellular mechanism of preconditioning protection remains obscure.[45] The role of PKC in preconditioning has been studied in numerous species both in vivo and in vitro, utilizing different experimental models and preconditioning protocols. During 1995, Downey et al.[59] explored signaling pathways in IPC, concluding that IPC existed in all species studied, including humans and speculated that IPC had possible clinical application. Ytrehus et al.[60] demonstrated a role for PKC in the mediation of cardioprotection during IPC and Liu[61] from the same group postulated that PKC translocation during the trigger episodes of IPC was responsible for the cardioprotection. Speechly-Dick[26] further demonstrated that inhibition of PKC by chelerythrine after an IPC stimulus, but before the index ischemia, abolished protection in an in vivo rat ischemia model. The research group of Marber et al. demonstrated that isolated perfused hearts of PKC ϵ -/- knock-out mice lost the reduction in infarct size observed with sibling heterozygous PKC ϵ +/- mice.[62] Subsequently, numerous signaling pathways have been identified that mediate cardioprotection for e.g. the PI3K/protein kinase B or Akt pathway, TNF α , adenosine, the MAP kinases (ERK1/2 and p38) and PKCs.

Hypothetically, there is a threshold level of PKC stimulation that must be reached for cardioprotection to occur.[63, 64] This threshold signal may be a composite of any of the triggers already implicated in IPC, because the effects may be additive in order to reach the PKC stimulation threshold and confer cardioprotection (Figure 1-5).

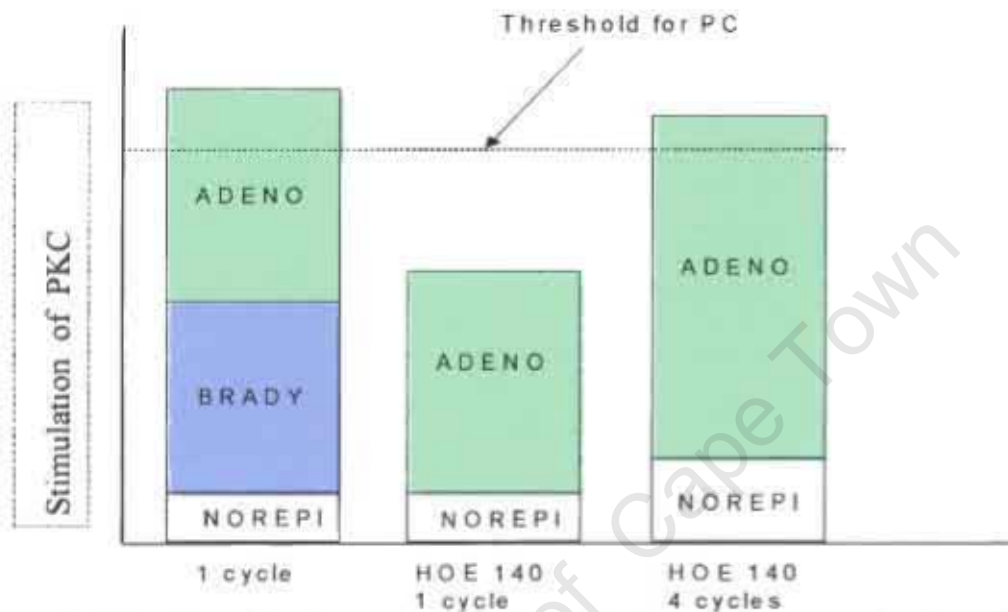


Figure 1-5. Hypothetical PKC threshold for ischemic preconditioning [63]

A hypothetical threshold of PKC stimulation must be reached for cardioprotection to ensue. One cycle of IPC releases multiple agonists, of which at least two (BRADY and ADENO) play major roles in triggering protection by having additive effects on PKC stimulation, such that the hypothetical threshold is exceeded. Where HOE 140 blocks bradykinin, additional PC cycles are required to stimulate other agonists sufficiently to attain the threshold required for IPC. BRADY-bradykinin, NOREPI-norepinephrine, ADENO-adenosine, HOE 140-bradykinin blocker

Focusing on PKC, adenosine and bradykinin receptors were proposed as putative mediators of these signals acting via activation of PKC.[52] Current research indicates that the major signaling pathways appear to converge at a common point, resulting in the activation of multiple protective kinases for e.g. Akt, PI3K and PKCs [65] It is proposed that there are downstream mediators which act at the mitochondrial level, inhibiting mitochondrial permeability

transition pore opening at reperfusion, thereby conferring cardioprotection by prevention of apoptosis. PKC ϵ is proposed to be an important mediator in this process.[66] It has been shown that inhibition of PKC ϵ abolishes the protection afforded by preconditioning.[7, 36, 67] Moreover, modest cardiac-specific overexpression of constitutively active PKC ϵ confers enhanced resistance to myocardial cell death following ischemia.[1, 7, 67, 68]

PKC activation and its role in IPC was further explored in conscious rabbits by Ping et al.[4] employing different ischemic preconditioning (IPC) protocols. Here, PKC ϵ and PKC ζ were activated and translocated to the particulate fraction during IPC, without affecting the total myocardial PKC activity. To examine the role of myocardial PKC ϵ in IPC, Ping et al.[47] investigated potential target proteins by performing a functional proteomics array on heart tissue isolated from PKC ϵ overexpressing mice.[69] Here they found that PKC ϵ is physically associated with at least 36 known proteins: structural proteins, signaling molecules, mitochondrial proteins (oxidative phosphorylation, pore proteins) and stress-responsive proteins.

1.8 PKC ϵ and cardioprotection

Cardioprotection induced by activation of PKC ϵ is coupled with recruitment and modulation of the PKC ϵ -associated proteins, for example cardiac alpha actin, myosin light chain, PI3K, Akt, p38 MAPK, ERK1/2, iNOS, eNOS, various heat

shock proteins and hypoxia inducible factor 1 alpha. In addition, Edmondson et al.[70] reported PKC ϵ complexes containing molecules known to be essential for metabolism and the regulation of protein synthesis, for e.g. glycolytic enzymes like enolase and glyceraldehydes dehydrogenase, citric acid cycle enzymes like isocitrate dehydrogenase and multiple mitochondrial enzymes involved in ATP production. This suggests that PKC ϵ performs specific functions in the mitochondria with regard to the regulation of cellular energy balance.

Further to this finding, numerous diverse cellular signaling modules have been implicated in PKC ϵ mediated tolerance to ischemia by the use of functional proteomics.[2, 3, 5, 70] Sub-proteome analysis has identified interactions between activated PKC ϵ and mitochondrial-enriched proteins controlling mitochondrial homeostasis, including those governing mitochondrial oxidative phosphorylation, electron transfer, ion transport and membrane permeability transition (MPT) control.[3, 70] Membrane permeability transition causes a reduction in mitochondrial oxidative phosphorylation resulting from a decline in the electrochemical gradient in the mitochondrial membrane, thereby activating the multiprotein complex constituting the membrane permeability transition pore (MPTP)[71-74] and committing the cell to programmed cell death by the release of proapoptotic factors like cytochrome c.

PKC ϵ has been shown by Baines et al.[3] to be associated with components of the permeability transition pore, a channel which spans the double mitochondrial membrane. This pore controls influx of solutes and charged molecules up to

1500 kDa via VDAC 1/2 (voltage dependent anion channel 1 or 2), yet maintaining the mitochondrial membrane potential and modulating energy production in response to extrinsic stimuli. The pore is generally accepted to be composed of VDAC 1 or 2 embedded in the outer mitochondrial membrane, ANT (adenine nucleotide translocator) in the inner mitochondrial membrane and various regulatory molecules.[75] PKC ϵ co-precipitates with VDAC1, subsequently inactivating it by phosphorylation *in vitro* and *in vivo*. [3] Stabilization of VDAC 1/2 by phosphorylation is suggested to fix its conformation, subsequently stabilizing the ANT conformation and thereby preventing membrane permeability transition.

The mechanism of engendering protection was postulated to involve three phases. Firstly, a trigger phase, during which a signal substance was released. Second, a signal transducing phase, where signal cascades are transduced and thirdly, an organ effector phase during which the mediator confers protection against apoptotic and necrotic cell death (Fig 1-6).[76] Due to the divided opinions and putative mechanisms put forward for animal and human models of ischemia/reperfusion injury at the time, it was proposed the simplest way to reduce reperfusion damage would be to minimize the ischemic time by reperfusion as soon as practicable and optimizing the metabolic status of the ischemic myocardium at the end of the ischemic period. (For review, see Opie, 1989[32])

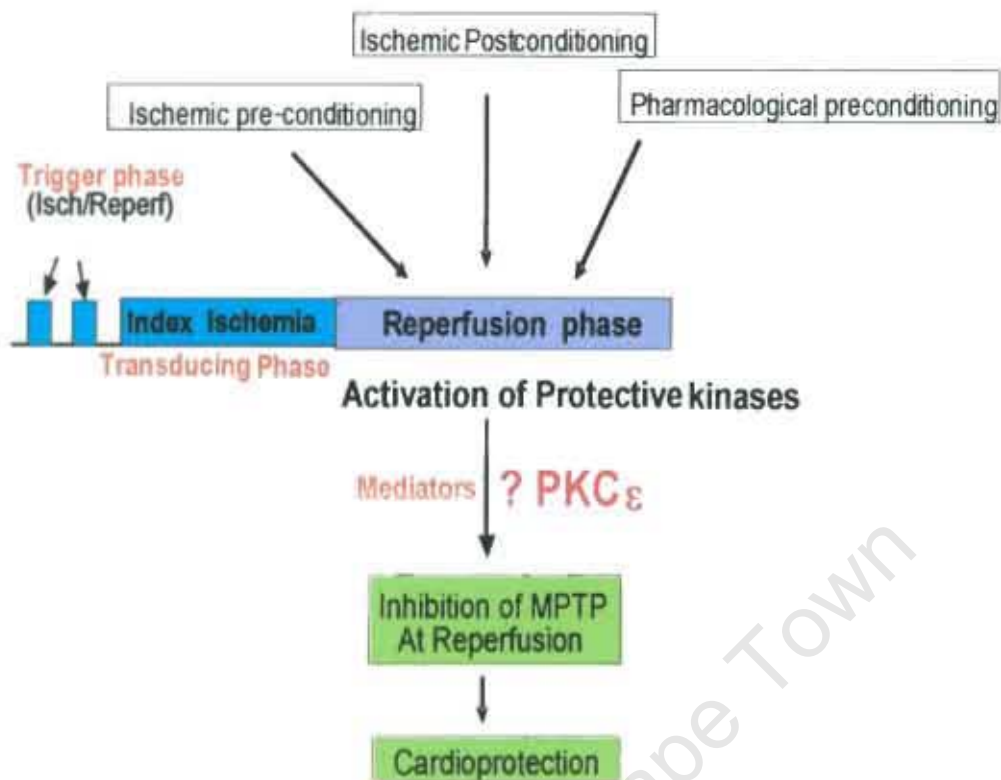


Figure 1-6. Proposed signaling pathway involved in cardioprotection

Interpretation of Hausenloy [65], who proposed that ischemic preconditioning, ischemic post-conditioning and pharmacological preconditioning all converge at a common point and activate the same protective kinase signaling pathway at reperfusion.

PKCε is also known to activate ERK1/2, a pro-survival pathway. Furthermore, it can inactivate the proapoptotic proteins Bad and Bax, and activate the antiapoptotic-signaling pathway of Akt [77] (Fig.1-7).

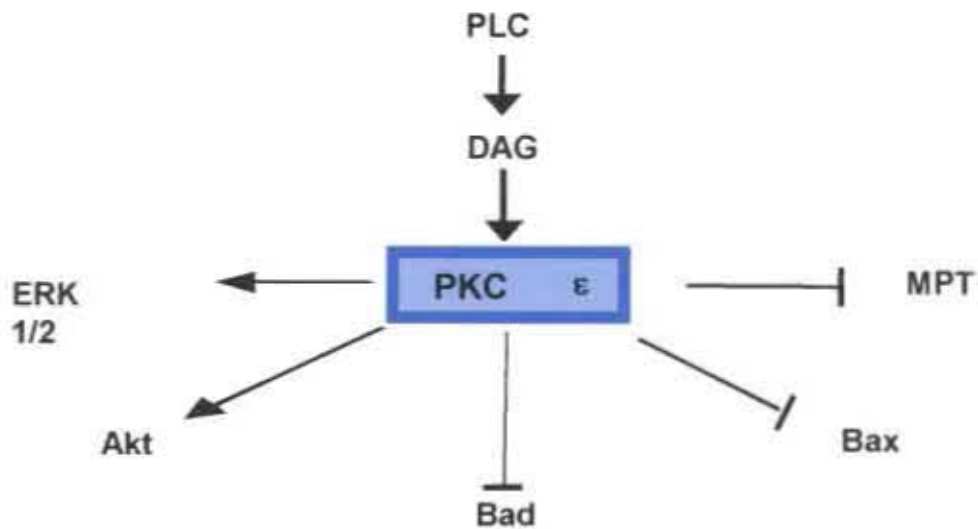


Figure 1-7. PKC ϵ protective signaling pathways (modified from Baines et al., 2005)
 PLC- Phospholipase C, DAG - Diacylglycerol

Interestingly, continuous delivery of a peptide PCK ϵ selective agonist, $\psi\epsilon$ RACK, induced cardioprotection both *in vivo* and *in vitro*, with fewer lethal arrhythmias during ischemia–reperfusion.[78] This intervention has obvious clinical potential, particularly in the early hours of myocardial infarction, as ability to ameliorate or control ischemic damage and the cell death process would be a distinct advantage. There is thus indication that PKC ϵ exerts its protective effect at the mitochondrion, ameliorating the effects of oxidant stress and maintaining maximal energy levels. It is therefore necessary to further explore the signaling pathways that regulate mitochondrial function in the heart by exploring possible

mechanisms of action of PKC ϵ , one of the major kinases involved in cardioprotection.

D. MITOCHONDRIA – BACKGROUND AND OVERVIEW

Mitochondria have classically been considered the “powerhouses” of the cell, primarily responsible for the continuous supply of ATP to fuel intracellular processes, thereby ensuring cell survival. The ATP comes mainly from the breakdown of fatty acids (FAs), glucose and lactate.[79] This is of importance in tissues with a high oxidative capacity, for example heart and skeletal muscle, where energy supply must be increased on demand in response to stress or exercise. The normal human heart produces and uses ~ 3.5 – 5 kg of intracellular ATP per day to perform its normal functions.[80] Moreover, when stressed or exercising, additional energy demands are made which need to be met in order to ensure optimal contractility.

In the light of its central role in energy production, any loss of mitochondrial function would have a significant impact on cell viability. Altered mitochondrial function will result in diminished energy production, perturbed ion homeostasis and ultimately loss of function within the cell for e.g. reduced contractility and disruption of ion flux leading to intracellular Ca²⁺ accumulation.[71, 81, 82] In agreement, perturbed mitochondrial function has been directly implicated in numerous pathologies for e.g. cardiomyopathies, heart failure, blindness, ataxia,

and hepatic dysfunction.[10, 21] Mitochondria therefore play a pivotal role in sustaining myocardial energetic requirements and the heart's contractile reserve.

However, recent studies have increasingly highlighted an additional role for the mitochondrion. For example, it has now emerged that mitochondria also mediate the processes leading to controlled cell death (apoptosis).[71, 83-85]

Mitochondria are tiny complex semiautonomous organelles ($\approx 2 \mu\text{m}$ long and $0.5 \mu\text{m}$ wide), thought to have been absorbed into eukaryotic cells by an endosymbiotic event.[86] Mammalian mitochondria contain their own circular DNA (mtDNA). Human mitochondrial DNA is composed of 16,569 bp encoding 13 of the respiratory complexes, 2 rRNAs and 22 tRNAs, sufficient to translate all the codons (Fig.1-8).[87] The remaining sub-units of the respiratory complexes and all the other mitochondrial proteins are nuclear-encoded. Intriguingly, cells therefore depend on mitochondria for their energy supply while mitochondria require the cell's transcriptional machinery for their survival. The latter concept is supported by the remarkable overlapping gene sequence of most mitochondrial genomes examined thus far.[87]

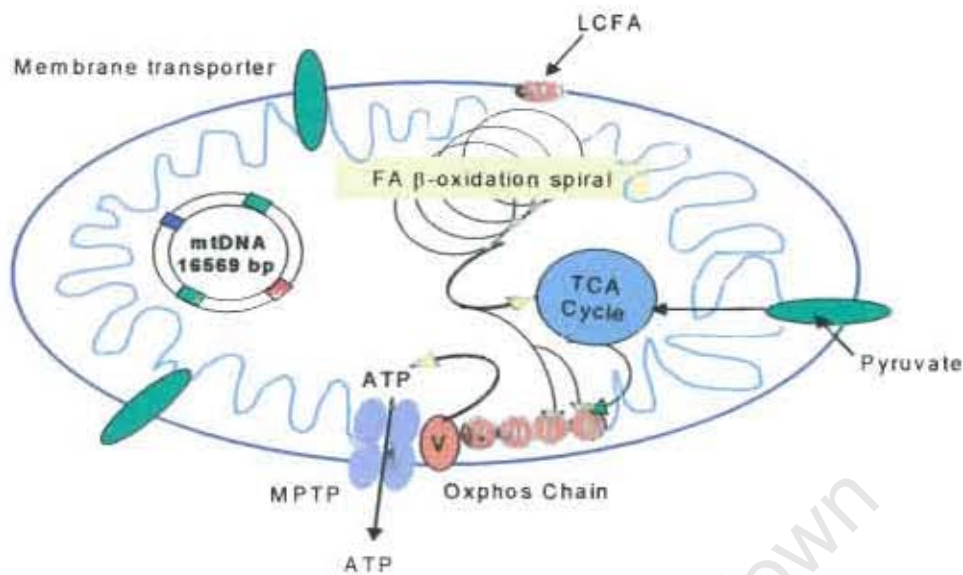


Figure 1-8. Simplified schematic of a mitochondrion

Mitochondria are oval, double membrane organelles containing a circular genome and numerous vital enzyme complexes: fatty acid oxidation (FA β -oxidation spiral), tricarboxylic acid cycle (TCA) and the oxidative phosphorylation (Oxphos) chain. The β -oxidation spiral and the TCA feed reducing equivalents into the oxidative phosphorylation chain to generate ATP. Membrane transporters import or export molecules to and from the mitochondrion. For example, long chain fatty acyl CoAs (LCFA) are imported into the mitochondrion via the rate-limiting fatty acid transfer enzyme carnitine palmitoyl transferase (CPT1). The membrane permeability transition pore (MPTP) is involved in active transport of ATP and other molecules, as well as apoptosis after an appropriate stimulus.

During 1952-1953, electron microscope studies by Frijthof Sjöstrand and George Palade[88] revealed structural details previously unknown i.e. mitochondria have a double membrane dividing them into distinct compartments (the intermembrane space and matrix, confined by the inner mitochondrial membrane).[86] The outer membrane is smooth while the inner membrane is highly convoluted with folds, called cristae. These are thought to be necessary to bring interacting proteins into closer proximity and to allow for volume changes without rupture, as occur during energizing of mitochondria or during oxidative stress.[89] At about the same time (1948-1950), Albert Lehninger and Eugene Kennedy discovered that

mitochondria contain the respiratory assembly for oxidative phosphorylation spanning the inner mitochondrial membrane, the enzymes of the citric acid cycle as well as those required for fatty acid β -oxidation within the matrix (Fig. 1-9). [88]

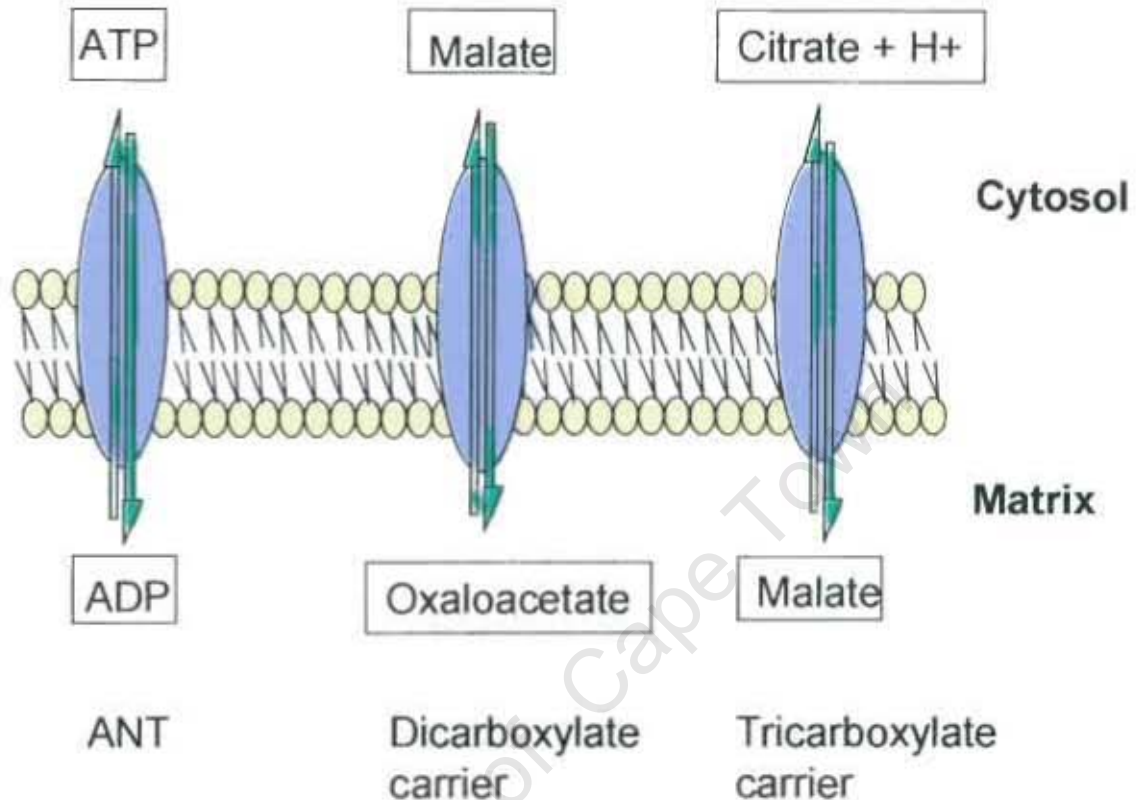


Figure 1-9. Specific membrane transporters

Adenine nucleotide translocase (ANT) exports ATP from the mitochondrion into the cytoplasm and simultaneously imports ADP for re-phosphorylation. The dicarboxylate carrier imports oxaloacetate in the form of malate to allow it to cross the outer mitochondrial membrane while the tricarboxylate carrier imports citrate in the form of malate.

The outer mitochondrial membrane is permeable to most small molecules via a relatively non-specific channel located within the MPTP allowing free access to molecules up to 1500 kDa.[90] However, the outer membrane does contain some specific transporters/carriers as well i.e. the dicarboxylate and tricarboxylate carriers and ANT (Fig.1-9). On the other hand, the inner mitochondrial membrane is largely impermeable, especially to ions and polar molecules since its main function is to maintain the electrochemical gradient formed across the inner

mitochondrial membrane. The electrochemical gradient is composed of the proton gradient and the membrane potential and is utilized to drive the synthesis of mitochondrial ATP.

E. MITOCHONDRIAL ENERGY PRODUCTION

1.8.1 Tricarboxylic acid cycle (TCA)

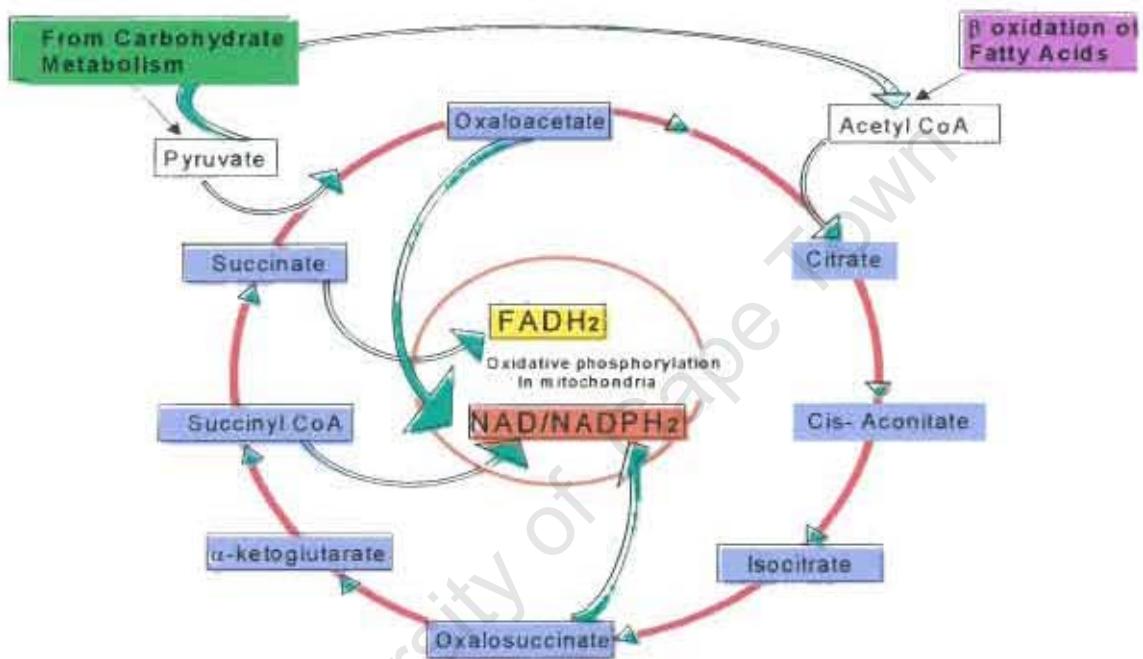


Figure 1-10. Tricarboxylic Acid (TCA cycle)

The complete combustion of a single molecule of glucose generates ~32 molecules of ATP to the cytosol, whereas complete combustion of one molecule of the long-chain fatty acid palmitate generates ~105 molecules of ATP.[80] All the rate-limiting enzymes of the TCA cycle are calcium-activated and, as mitochondria are the calcium stores for the cell, it raises the possibility that the rate of ATP synthesis via oxidative phosphorylation is influenced by the rate of

calcium uptake (Fig. 1-10).[21] The cycle also plays an important role in the provision of intermediates for protein biosynthesis for e.g. amino acids are formed from α -ketoglutarate or oxaloacetate and porphyrins from succinyl CoA.

1.8.2 Cytosolic reducing equivalents



Figure 1-11. Glycerol-3-phosphate shuttle Glycerol 3-phosphate is oxidized to dihydroxyacetone phosphate in the cytosol, generating reduced NADH_2 . The NAD^+ must be rapidly recycled to sustain glycolytic flux, thus the electrons are transferred across the mitochondrial membrane via glycerol 3-phosphate, which readily diffuses into the mitochondrion. This reaction in the cytosol is catalyzed by cytosolic glycerol 3-phosphate dehydrogenase (glycerol 3-PDH). The glycerol 3-phosphate is reoxidized at the outer edge of the inner mitochondrial membrane (IMM) by the mitochondrial glycerol 3-PDH, which utilizes FAD^+ rather than NAD^+ as its electron acceptor. The high-energy electrons are transferred to the electron carrier Q and enter the oxidative phosphorylation chain as QH_2 .

The reducing equivalents (NADH_2 , FADH_2 , NAD^+ and FAD^+) and their high-energy electrons produced by glycolysis cannot simply enter the mitochondria, as the inner membrane is impermeable to these charged molecules. They need to be recycled quickly for glycolysis to continue, so the high-energy electrons contained in the NADH_2 and FADH_2 are transferred across the membrane via a number of shuttles for e.g. the glycerol 3-phosphate shuttle (Fig. 1-11). An

electron pair from glycerol 3-phosphate is transferred to a flavin adenine dinucleotide (FAD) group in the glycerol 3-phosphate dehydrogenase enzyme, embedded in the outer wall of the inner mitochondrial membrane. The reduced flavin (FADH_2) transfers its electrons to coenzyme Q10, which then enters the respiratory chain. The cost of this shuttle is one molecule of ATP per two electrons transported and the net gain for the mitochondrion is 1.5 molecules of ATP.

The malate-aspartate shuttle is an alternative shuttle in the heart and liver for NADH_2 importation into the mitochondrial matrix (Fig. 1-12). Two transmembrane carriers and four enzymes mediate this reaction. Electrons are transferred from NADH to oxaloacetate to form malate, which traverses the mitochondrial membrane and is reoxidized by NAD^+ in the matrix to form NADH_2 . The NADH_2 thus formed enters the oxidative phosphorylation chain at complex I to be utilized for ATP formation.

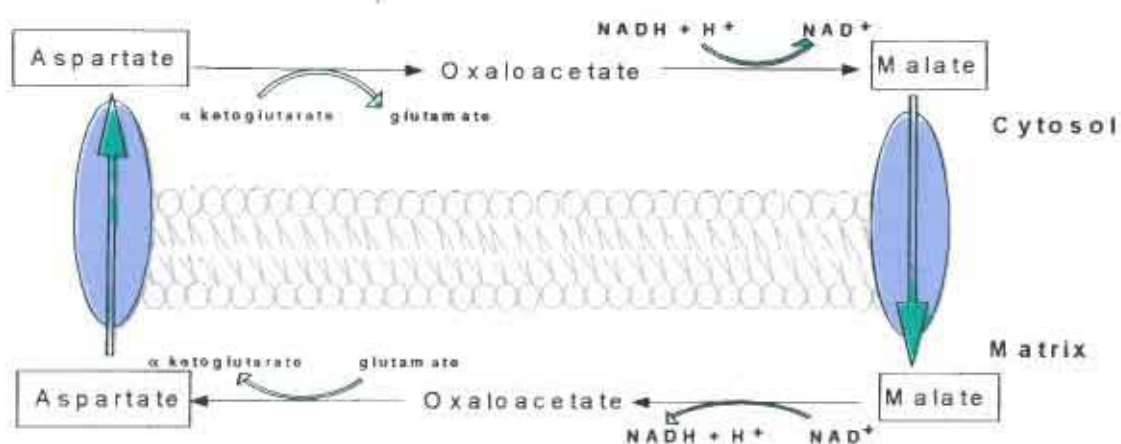


Figure 1-12. Malate aspartate shuttle

In this shuttle electrons are transferred from NADH₂ in the cytosol to oxaloacetate to form malate, which readily diffuses across the inner mitochondrial membrane into the matrix. Here it is reoxidized by NAD⁺ to form oxaloacetate and NADH₂. The oxaloacetate cannot cross the mitochondrial membrane so it is transaminated to aspartate, which can readily diffuse back into the cytosol.

The oxaloacetate remaining in the matrix cannot cross the membrane, so it is transaminated to form aspartate, which easily diffuses through the mitochondrial membrane to repeat the cycle.

1.8.3 Fatty acid β -oxidation

Oxidation of long- and medium-chain fatty acids (FAs) takes place in the mitochondrial matrix. However, before β -oxidation, FAs need to be activated. This involves an ATP-dependent esterification with coenzyme A, a reaction catalyzed by acyl CoA synthase (ACS). This reaction results in the substitution of a FA carboxylic acid terminus with a CoA thioester. Activated FAs are then transported into the mitochondrial matrix via the carnitine palmitoyl shuttle. Here, the rate-limiting step is catalyzed by carnitine palmitoyl transferase 1 (CPT1)

which catalyzes the initial step in the import of FA-CoA transport by its conversion to a carnitine ester, acyl carnitine.[91] Two CPT isoforms have been characterized in the heart i.e. the muscle isoform (mCPT1) and the liver isoform (ICPT1).[91] However, mCPT1 predominates in the heart. This isoform is usually expressed in tissue with a high capacity for FA oxidation i.e. skeletal muscle, cardiac muscle and brown adipose tissue.[91] Acyl carnitines are subsequently transported across the inner mitochondrial membrane by carnitine acyl translocase (CAT). On the matrix side of the inner mitochondrial membrane, CPT-II converts the acyl carnitine back to FA-CoA, enabling FAs to enter the mitochondrial FA β -oxidation spiral. The enzymes of the β -oxidation spiral are loosely organized into a multi-enzyme complex. Once entered, the activated FAs only leave the complex when fully oxidized. At each step in the oxidation, they are simply displaced by fresh substrate and move on to the next enzyme.[9]

Long-chain acyl-CoA dehydrogenase (LCAD) or medium-chain acyl-CoA dehydrogenase (MCAD) catalyzes the initial oxidation step of long- or medium-chain fatty acids, respectively (step 1, Fig. 1-13). The following steps are catalyzed by enoyl-CoA hydratase, L-3-hydroxyacyl CoA dehydrogenase and 3-oxoacyl CoA thiolase, respectively (steps 2-4, Fig. 1-13). As it passes through the four-enzyme sequence, the activated FA loses two carbons in the form of acetyl CoA and generates both reduced NAD and reduced FAD, which enter the oxidative phosphorylation chain at complexes I and II, respectively.

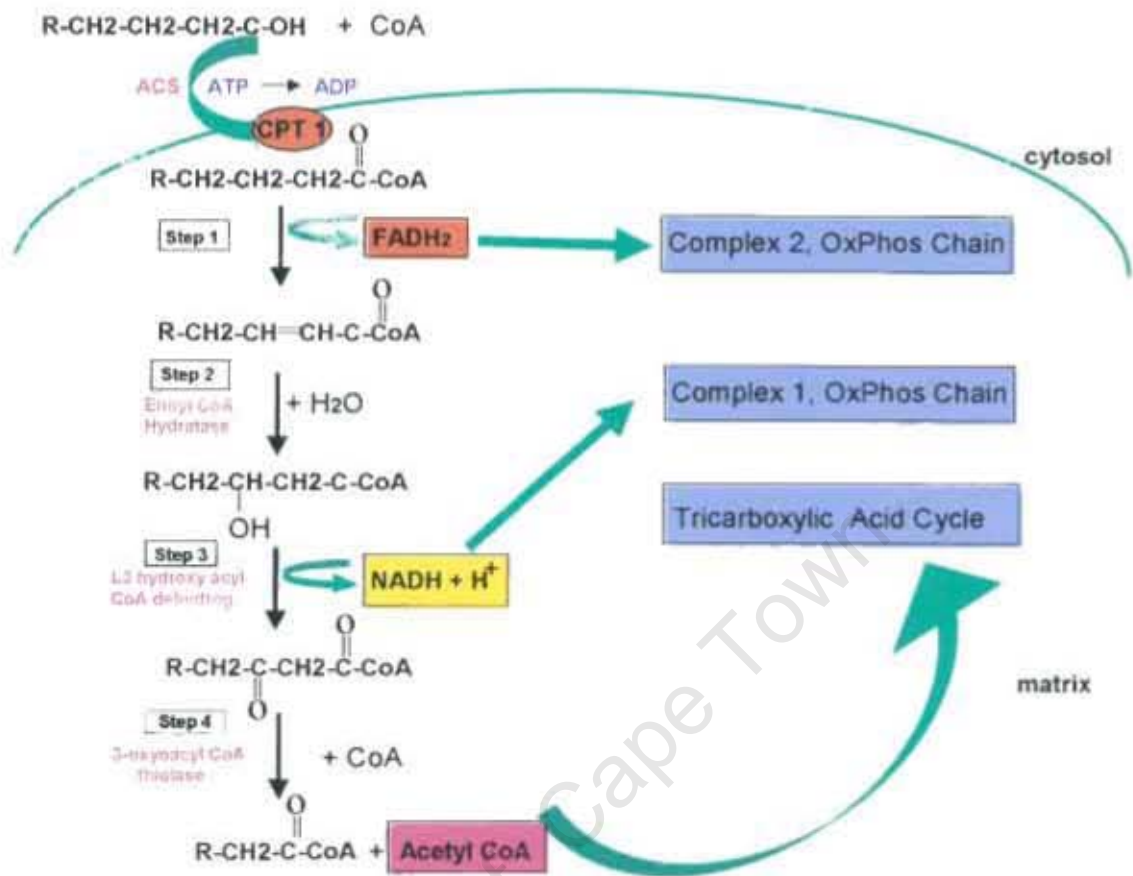


Figure 1-13. Fatty acid β -oxidation spiral

This diagram illustrates the fatty acid β -oxidation sequence occurring in the mitochondrial matrix.

The high-energy electrons move down the oxidative phosphorylation chain, ultimately generating mitochondrial ATP. The acetyl CoA produced enters the citric acid cycle, generating additional high-energy electrons in the form of NADH₂ and FADH₂. These reducing equivalents then also donate their electrons to the oxidative phosphorylation chain in the mitochondrial membrane to generate additional ATP. The shortened FA re-enters the FAO spiral and the

1.8.4 Oxidative phosphorylation

The respiratory chain consists of four protein complexes (I, II, III and IV) as well as ATP synthase (complex V). Electrons move from complex I (NADH-CoQ reductase) and complex II (succinate-CoQ reductase) to complex III (CoQ-cytochrome c reductase) via coenzyme Q (Fig. 1-14). Cytochrome c then transfers electrons to complex IV (cytochrome c oxidase), which simultaneously catalyzes the oxidation of four reduced cytochrome c molecules and the four-electron reduction of molecular oxygen. The transfer of electrons is coupled to a proton gradient across the inner mitochondrial membrane and leads to pumping of 10 protons from the matrix to the outer edge of the inner mitochondrial membrane. The proton concentration is thus lower in the matrix, creating a proton electrochemical gradient. It is this "proton-motive force" that drives the synthesis of ATP at complex V. Here, three protons are pumped back into the matrix at the conversion of this electron transfer potential to the phosphoryl transfer potential of ATP to facilitate the release of the ATP molecule.[92] Mitchell was the first to postulate this "chemiosmotic hypothesis" in 1961.[93]

simultaneously exporting ATP (Fig. 1-14).[90, 94] As an additional control, there is also a feedback inhibition of respiration: when ATP consumption is diminished, respiration also decreases. This is inhibition accomplished by the uncoupling proteins (UCPs), a family of mitochondrial transporters present in the inner mitochondrial membrane. This uncoupling function is energetically sensible, as it prevents ATP overproduction and exhaustion of the coenzymes required for cellular respiration.[95]

Mammals are able to generate heat to maintain body temperature by the uncoupling of oxidative phosphorylation. This is important in hibernating animals, in newborns and in animals adapted to survive prolonged exposure to cold conditions. Brown adipose tissue (BAT) is especially rich in mitochondria and specialized for non-shivering thermogenesis. There is a high proportion of uncoupling protein 1 (UCP1 or thermogenin) in the inner mitochondrial membrane of these mitochondria.[96] UCP1 is a dimer of approximately 33 kDa subunits, resembling the ATP-ADP translocase. It forms a short-circuit by diverting the protons from the inter-mitochondrial membrane space back into the matrix. This pathway is activated by free FAs released by the hydrolysis of triacylglycerols in response to hormone signals.

Three additional isoforms of uncoupling protein have been identified. UCP2 is found in a wide variety of tissues and has close homology with UCP1 while UCP3 is localized to skeletal muscle and brown fat.[97] UCP5 has been identified more recently and is ubiquitously expressed.[98-100]

UCP2 and UCP3 are thought to be involved in energy homeostasis, as the genes in humans and mouse have been mapped to an area of the chromosome that controls obesity. UCP2 is expressed in pancreatic islets and pancreatic beta cells. An overexpression of UCP2 in beta cells blunted insulin secretion.[101] Furthermore, Zhang et al.[102] demonstrated an increase in ATP levels and a net increase in insulin-induced glucose secretion in the islets of UCP2 knock-out mice.[102] These findings established UCP2 as a negative regulator of insulin secretion and suggested a role as an uncoupler.[95] However, Arsenijevic et al.[103] showed that UCP2 may also be involved in mitochondrial ROS production.[103] Moreover, a recent study by the Marban laboratory[104] have shown that overexpression of UCP2 in cardiomyocytes protects against ROS, suggesting that UCP2 may indeed have an antioxidant function in the heart.

UCP2 and UCP3 are expressed in cells involved in intermediary metabolism, particularly fatty acid metabolism: adipose tissue, skeletal muscle and macrophages.[95, 105] It is now generally accepted that all UCPs function as fatty acid anion transporters.[106, 107] Involvement of UCP3 in fatty acid metabolism was established by Clapham et al.[108] in transgenic mice overexpressing UCP3 in skeletal muscle. These mice were lean and resistant to diet-induced obesity and diabetes. Moreover, UCP3 is down regulated with hypoxia, along with other FAO oxidation regulatory genes like the FA transcriptional regulator peroxisome proliferator-activated receptor alpha (PPAR α) and carnitine palmitoyl transferase 1 (CPT-1), the enzyme responsible

for importing activated FAs into the mitochondrion for β -oxidation.[80] This is consistent with the switch in metabolic profile that occurs in response to chronic hypoxia. The heart responds to the oxidant stress by re-expression of the fetal gene program and utilization of the fetal substrate glucose. Concomitantly, FAO oxidation enzymes are down regulated and the glucose oxidation pathways up regulated to protect the stressed myocardium. However, UCP2 appears not to be involved in the regulation of proton leak from oxidative phosphorylation during oxidant stress and appears to play no part in the metabolic gene switching which occurs in response to the oxidant stress. These data therefore suggest a role for UCP3 in regulating fatty acid oxidation and UCP2 functioning as an antioxidant in the heart.[109-111] However, further studies are required to delineate the precise fundamental role of these UCP isoforms in the heart.

Energy consumption in the heart can be divided into several categories:

- non-beating (basal) metabolism, which accounts for ~ 25% of the total energy flux
- Excitation / activation energy, which accounts for another 25%
- Cross-bridge cycling utilized in contraction, which accounts for 50% of the ATP consumption.[112]

Estimates of the oxidative capacity of large mammalian hearts (dog, pig) suggest that the exercising heart operates at approximately 80-90% of the maximum.[113-115] Thus, these hearts have little reserve for aerobic ATP synthesis. Under conditions of maximum exercise, alternate sources for ATP

synthesis, such as glycogen and phosphocreatine, become quantitatively important.[113-115]

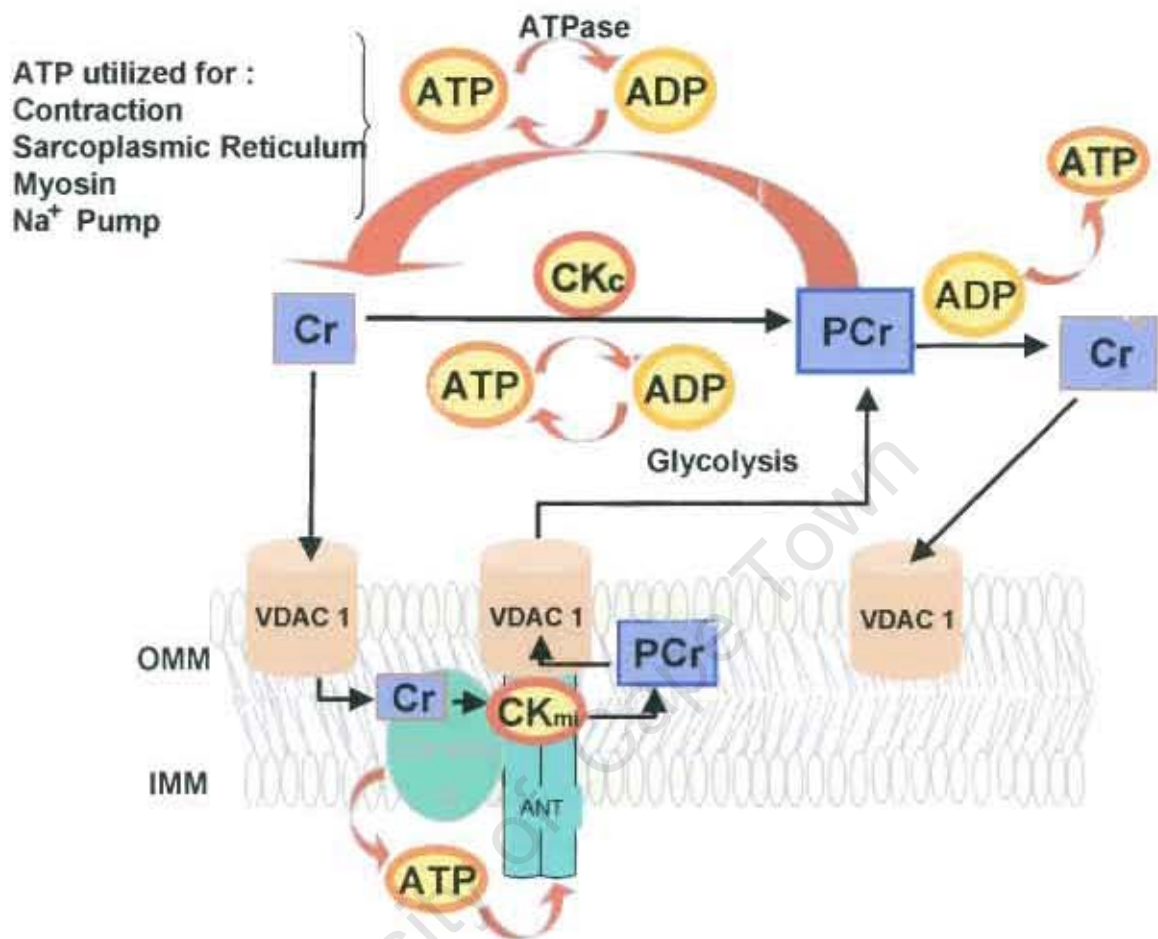


Figure 1-15. Phosphocreatine shuttle

PCr - phosphocreatine, OMM - outer mitochondrial membrane, IMM - inner mitochondrial membrane, CK_{mi} - mitochondrial creatine kinase, CK_c - cytosolic creatine kinase, Cr - creatine.

To ensure a continuous supply of ADP to facilitate ATP production, a repetitive cycling of phosphocreatine (PCr) is also essential, as it represents the prime intracellular energy reserve and therefore influences ADP stores directly.[115]

There is a specific mitochondrial isoform of creatine kinase (CK_{mi}) associated with the elements of the permeability transition pore at the inner mitochondrial membrane [115] Here, creatine kinase catalyzes the conversion of creatine (Cr)

to PCr within the mitochondrial membrane, utilizing the ATP manufactured within the oxidative phosphorylation chain (Fig. 1-15). The PCr generated can easily diffuse into the cytosol through VDAC 1/2 in the mitochondrial outer membrane and is converted back to ATP in the cytosol by the cytosolic creatine kinase (CK_c). ATP thus formed is utilized for contraction and for driving membrane pumps and the contractile apparatus.[113] Some of the cytosolic CK_c is functionally coupled to glycolysis, so that during periods of anaerobic work and recovery, it preferentially accepts glycolytic ATP to replenish the large PCr pool. Creatine re-enters the mitochondrion via VDAC 1/2 to complete the PCr shuttle, having donated its high-energy phosphate group to ADP to form ATP.

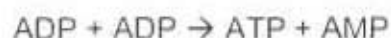
It would appear that the active transport of ATP from the mitochondria into the cytosol is sufficient while intracellular energy requirements are not too high. However, as soon as there is a greater demand for ATP, the PCr shuttle is able to provide for this extra surge as the response is more immediate and does not depend on active binding of ADP, diffusion of protons and active release of the newly formed ATP.[112, 113, 115] There are also two other forms of ATP supplementation which are often neglected:[112, 113]

- Substrate level phosphorylation, as in glycolysis



This reaction generates a net 2 ATP per molecule of glucose oxidized to pyruvate

- Adenylate kinase catalyzes the reaction



Although several adenylate kinase isoforms have been identified thus far,[113, 116] adenylate kinase 1 is predominantly expressed in the heart.[112] It has been demonstrated that this reaction forms an important part of the cytosolic ATP pool maintenance. In support, adenylate kinase 1-deficient mice have an increased flux through the PCr shuttle and glycolysis in an attempt to maintain their ATP stores.[114, 117] Moreover, these animals utilize more ATP per contraction than normal mice and have a lower tolerance to ischemia and hypoxia.[113, 116]

1.9 Perturbed mitochondrial energy production

Mitochondrial malfunction can lead to a host of pathological states. This is easily understood, as these organelles are vital to energy generation. In **pressure overload hypertrophy** and end-stage **heart failure**, several studies have demonstrated impairment of cardiac FAO and oxidative phosphorylation.[10, 113, 118-120] Conversely, FAO is increased and glucose utilization is decreased in the insulin resistant and **diabetic hearts**. Moreover, there appear to be defects in oxidative phosphorylation in the hearts of diabetic rodents.[10, 121-123] In the early stages of the disease the high rates of oxidative flux lead to mitochondrial oxidative damage and eventual impairment of respiration due to reactive oxygen species (ROS) production. In addition, a non-synchrony between FA uptake and mitochondrial FAO rates could lead to accumulation of lipid in the cardiac tissue, exacerbating and perpetuating mitochondrial damage (referred to as "lipotoxicity") [10, 124, 125] as they depolarize cardiac mitochondria by creating

non-specific pores in the mitochondrial membranes as well as uncoupling oxidative phosphorylation.[126, 127]

At the genetic level, some mutations impair NADH utilization, whereas others interfere with electron transfer to CoQ. Manifestations of these mutations could include blindness and various cardiomyopathies (Table 1-1).

Disease	Mutation	Cardiac phenotype	Other Phenotype
Kearns-Sayre Syndrome	mtDNA mutation	Dilated cardiomyopathy (DCM)	Ophthalmoplegia, retinal degeneration
Leber optic neuropathy	mtDNA mutations	Conduction defects	Vision loss
Complex 1 deficiency	Complex 1 subunits	Hypertrophic Cardiomyopathy (HCM)	Encephalopathy, Vision loss, lactic acidosis
Leigh Syndrome	OxPhos genes	HCM	Encephalopathy
FAO disorders	VLCAD, LCAD	HCM	Hypoketotic hypoglycemia Hepatic dysfunction
Friedrich's Ataxia	Frxataxin	HCM	Cerebellar ataxia

Table 1-1. Mitochondrial mutations and pathological manifestations (From Russell, 2005[10]) VL/LCAD- very long or long chainacyl dehydrogenase

There are several mechanisms by which perturbed mitochondrial function may lead to cardiac remodeling:

1. Depressed energy production due to oxidative phosphorylation defects could lead to energy starvation (for e.g. diabetes or heart failure).
2. Lipotoxicity associated with diabetic cardiomyopathy may precipitate mitochondrial dysfunction and programmed cell death (apoptosis).

3. Overt oxidative stress, leading to mtDNA rearrangements and oxidative damage, evidenced by a high rate of apoptosis (dilated cardiomyopathy, heart failure, diabetic heart).
4. Mitochondrial proliferation in response to a chronic stimulus (hypoxia, pressure overload) could interfere with the expression of structural and sarcomeric proteins, leading to impairment of sarcomeric assembly and function.[10]
5. When hearts are subjected to ischemia, the rate of ATP synthesis by glycolysis increases in an attempt to compensate for the lack of oxygen and decreased substrate supply to maintain intracellular high-energy phosphate stores for contraction. The creatine kinase (CK) reaction velocity declines by ~ 75%, affecting contractile performance and ATP turnover. Simultaneously, the rate of ATP production via oxidative phosphorylation decreases to ~ 1/6 of its former rate. Although the rate of ATP synthesis from glycolysis increases during ischemia, the total high-energy phosphate concentration (ATP + PCr) increases only slightly, indicating a markedly increased utilization. With prolonged ischemia the ATP production from glycolysis is insufficient to maintain contractility and function ceases.[113]
6. In order to salvage myocardial tissue after an ischemic episode, rapid reperfusion is necessary. However, this carries the additional risk of reperfusion-induced injury, further exacerbating the injury caused by ischemia. The existence of such a phenomenon can be proven by interventions made directly at reperfusion, thus altering the severity of

post-reperfusion injury.[8] Most of these interventions are aimed at preventing MPTP opening, as this is the major cause of reperfusion-related myocyte death.[128, 129] The use of cyclosporine A (CsA) or sanglifeherin A at reperfusion to prevent pore opening significantly reduces reperfusion-related myocyte cell death.

7. When animals are exposed to chronic hypoxia, there is up regulation of peroxisome proliferator-activated receptor γ coactivator 1 (PGC-1). Two PGC-1 isoforms has thus far been identified i.e. PGC-1 α and PGC-1 β . PGC-1, regarded as a "master" transcriptional regulator, activates expression of transcription factors regulating mitochondrial function i.e. nuclear respiratory factors (NRFs) and mitochondrial transcription factor A (mtTFA). These nuclear regulatory proteins in turn activate genes encoding constituents of the electron transport chain, fatty acid β -oxidation, anti-oxidant enzymes and uncoupling proteins 2 and 3.[123, 130] For example, PGC-1 α stimulation of NRF1 results in induction of mitochondrial respiratory genes and mitochondrial biogenesis.[127, 131] Interestingly, PGC-1 also regulates expression of several fatty acid oxidation genes. However, in this instance PGC-1 recruits different transcriptional co-activators for e.g. PPAR α that is not associated with the induction of mitochondrial respiratory genes. Thus, with chronic hypoxia PGC-1 may induce mitochondrial respiratory genes and mitochondrial biogenesis to enhance mitochondrial energy production. Furthermore, due to the hypoxia-induced reduction of PPAR α levels [132, 133] FAO

genes are not induced by PGC-1, consistent with a metabolic switch from FAO to glucose oxidation in an attempt to maximize ATP generation with the limited oxygen available.

8. Hypertrophy

Initially, hypertrophy is thought to be an adaptive response to a cardiac stress:

- Pressure overload: as in hypertension, where the heart has to pump against an increased vascular resistance and muscle mass increases as a result.
- Volume overload also causes hypertrophy, but via a different mechanism to pressure overload. Volume overload causes increased end-diastolic pressure and the myocytes elongate, yet retaining the ratio mitochondrial volume to cell volume.
- Ischemic heart disease: Persistent infarction results in non-contracting and potentially expanding scar tissue. As a result, there is both an increased volume and pressure load caused by the increased volume load. Remodelling of the entire left ventricle ensues, in proportion to the infarct size. Early post-infarct remodeling is beneficial and promotes survival, but has deleterious long-term hemodynamic consequences. [Opie 2006]

1.10 Mitochondria control cell death

Mitochondria also play a central role in programmed cell death (apoptosis), which may be initiated in response to various stress signals. The apoptotic cascade is

triggered as a result of MPT that occurs due to a change in the permeability of the mitochondrial membrane in response to a stress signal i.e. an oxidant or metabolic stress (\downarrow ATP and pH, \uparrow P_i and Ca^{2+}). [9] Preceding apoptosis there is supply/demand mismatch: PCr and mitochondrial ATP decrease due to the action of the F1F0 ATPase which consumes ATP during ischemia [134, 135] in an attempt to rescue the mitochondrion. Moreover, there is a reduction in mitochondrial oxidative phosphorylation resulting from a decline in the electrochemical gradient across the inner mitochondrial membrane. These conditions result in the activation of a multiprotein complex in the mitochondrial membrane i.e. the MPTP (Fig. 1-16).

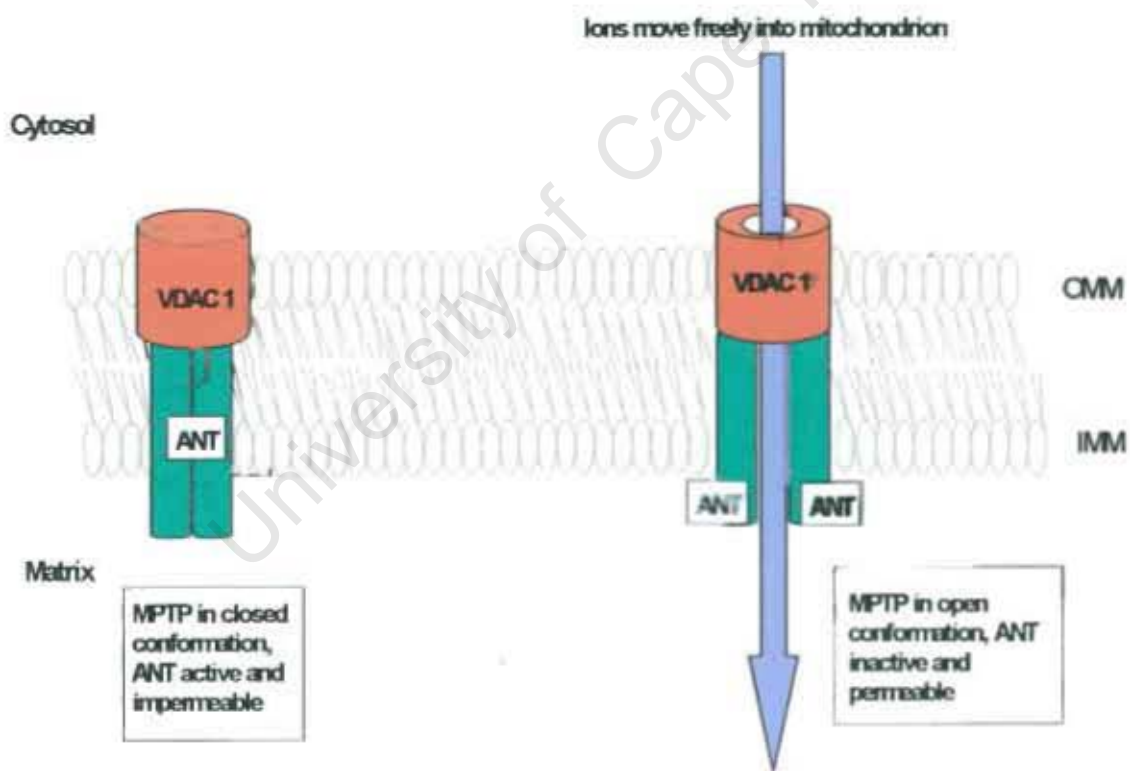


Figure 1-16. Mitochondrial permeability transition pore (MPTP)

These pores span the double membrane and are located where the inner and outer membranes are in closest proximity. [71-74]

It is generally accepted that the pore is composed of VDAC1/2 on the outer mitochondrial membrane and ANT on the inner mitochondrial membrane. Under normoxic conditions with adequate oxygen and energy supply, VDAC 1/2 allows the diffusion of most small molecules, whereas ANT is impermeable to all charged molecules and ions, thus controlling the movement of ions and solutes into the mitochondrion. [75, 136-139]

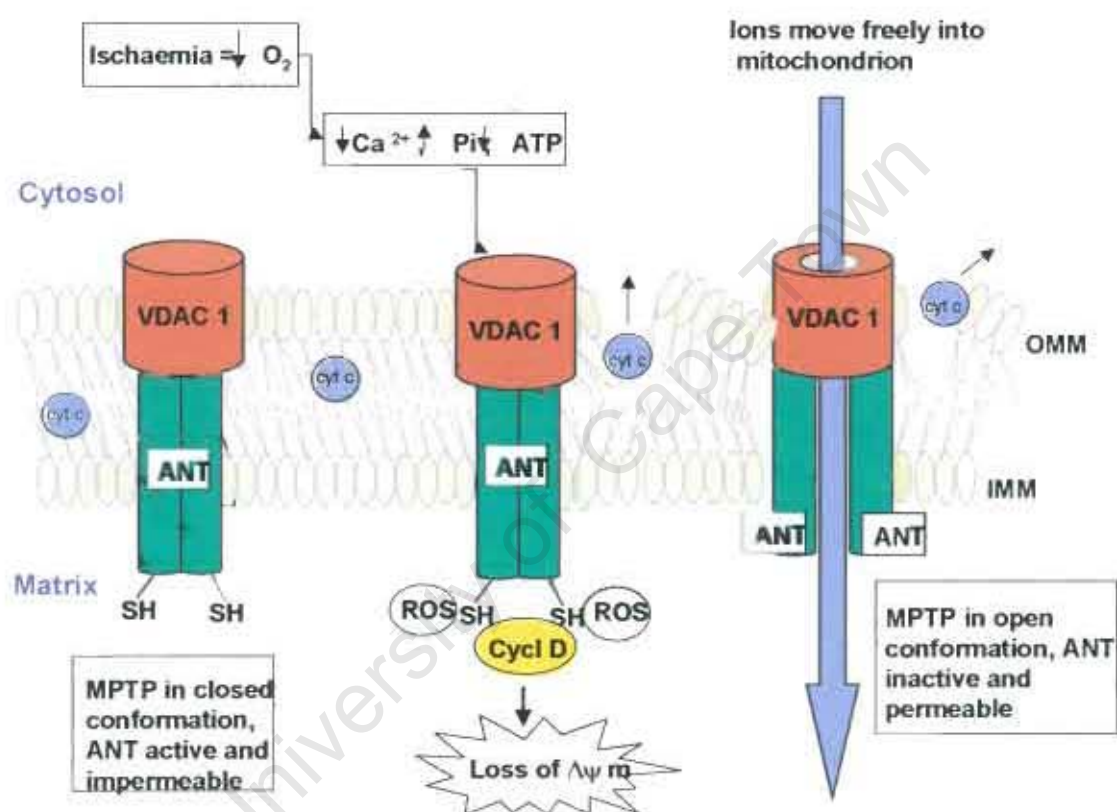


Figure 1-17: Regulation of the mitochondrial permeability transition pore in response to oxygen lack

$\Delta\psi_m$ – mitochondrial inner membrane potential; cyt c – cytochrome c, a constituent of the oxidative phosphorylation chain, normally situated at the outer edge of the inner mitochondrial membrane but released into the cytosol after outer membrane rupture; it triggers the apoptotic cascade.

Members of the Bcl-2 family of cytosolic proteins (Bcl-2, Bcl-x_L, Bad, Bid, BIM, BNIP3) form homo- or heterodimers that interact with VDAC 1/2 to either

promote or inhibit apoptosis. Bcl-2 and Bcl-x_L are antiapoptotic, whereas the other members are proapoptotic.[84, 140, 141] These proteins are key regulators of the mitochondrial response to apoptotic signals and finely control the process of apoptosis by the regulation of the release of mitochondrial mediators of the apoptotic program. [142-144]

After a trigger event, completion of the pore requires permeabilization of the outer mitochondrial membrane. ANT, spanning the inner mitochondrial membrane, undergoes a conformational change triggered by the action of calcium and ROS on its regulatory molecule cyclophilin D. ROS attacks the vulnerable sulphhydryl groups on the ANT protein complex, causing a conformational change and creating a channel to VDAC 1/2 (Fig. 1-17). The altered ANT interacts with VDAC 1/2, situated across the outer mitochondrial membrane, to cause its conformational change,[90, 145] thereby creating an opening through the double membrane large enough to permit the passage of molecules up to 1500 kDa in size directly into the matrix. This uncontrolled influx leads to swelling of the mitochondrion and rupture of the outer membrane, thereby releasing cytochrome c into the cytosol and initiating the apoptotic cascade and cell death.[90, 146] ANT cannot undergo a cyclophilin D-mediated conformational change while there is sufficient ADP and ATP in the mitochondrion, because these adenine nucleotides bind to ANT and resist conformational change. The most recent publications indicate that cyclophilin D and the permeability transition is required for Ca²⁺ and oxidative damage-induced

cell death, but has possibly only a secondary role in Bcl-2-regulated cell death.[77, 147]

However, it has been proposed that there can be apparent "pore formation" without ANT. Kokoszka et al.[148] generated an ANT transgenic mouse in which both ANT1 and ANT2 is specifically knocked out in the liver.[148] Hepatocytes and mitochondria were isolated from these mice and MPTP activation investigated in response to stress. Although more calcium was required to trigger MPTP than in the wildtype cells, loss of membrane potential and cytochrome c was demonstrated following a trigger event, indicating that ANT is not essential for MPTP formation.[148] This is in contradiction to previous evidence[90, 149] and fails to explain increasing amounts of atractyloside (ANT inhibitor) required to halt oxidative phosphorylation before and after an oxidant stress.[130]

Recently, a new regulator of mitochondrial apoptosis has been proposed: the mitochondrial apoptosis-induced channel or MAC.[144] It was discovered by directly patch-clamping mitochondria isolated from FL5.12 cells, in which apoptosis was induced by the withdrawal of interleukin-3, a stimulus known to activate the intrinsic pathway. Furthermore, recent publications[150-153] indicate that cytochrome c release can occur in the absence of mitochondrial depolarization and without the loss of outer membrane integrity. This suggests that a more selective permeabilization mechanism than outer membrane rupture may be operating, like the mitochondrial apoptosis channel or MAC.[144] This channel is also regulated by Bcl-2 and may act alone or in concert with transient

MPTP opening, to relocalize BAX to the mitochondria, remodel the cristae or to release proapoptotic mediators like cytochrome c from the mitochondrion and commit the cell to die.[150, 154].

Phospholipases hydrolyze the ester bonds in glycerophospholipid molecules to release FAs. As a result of the action of phospholipase 2 α on the cell membranes, non-specific pores form, resulting in the insertion of FAs into the membrane and the creation of "fatty acid pores". However, these pores are not regulated in the same way as the permeability transition pore and their creation and demise is considerably more random.[126, 127, 155]

There is an alternative model proposed for pore formation i.e. the protein-misfolding model.[71] Here, it is proposed that the conditions causing MPT i.e. oxidant stress, ROS and thiol abundance cause misfolding and "holes" of native membrane proteins, thereby allowing free access to small molecules. It is proposed that chaperone proteins like Bcl-2, Bcl-x_L or heat shock proteins (HSP) initially block such holes. However, as intracellular conditions deteriorate there are too many holes and not enough chaperone proteins resulting in rupture of the mitochondrion and ensuing cell death.

MPTP opening need not be an all or nothing event. Mitochondria are strategically positioned adjacent to the endoplasmic reticulum (ER) and sarcoplasmic reticulum (SR) because they also act as calcium stores for the cell. In highly organized tissues like striated muscle and cardiac muscle, mitochondria have

limited mobility and appear to be anchored about 10 nm away from the ER and SR. Calcium uptake by mitochondria was first documented in the 1950s.[156, 157] During preconditioning and in ischemia, intracellular calcium concentrations rise and ATP concentrations decline as a result of uncoupling and decreased oxidative phosphorylation. Mitochondria sense these micro domains of high calcium and undergo RAM (a rapid calcium uptake mode) in which mitochondria closest to the high calcium take up the calcium in an attempt to alleviate this condition. Mitochondria can absorb up to 5-500 μM calcium,[81] which is far in excess of the normal intracellular calcium concentration. The high calcium content in the mitochondrion leads to mild depolarization of the membrane and transient or physiological opening of the MPTP. Transient pore opening allows for release of calcium and ROS back into the cytosol, which triggers further calcium release from the SR if released in large quantities. Alternatively, release of small quantities initiates protective cascades in the cell.[81] Influx of calcium simultaneously stimulates the tricarboxylic acid cycle, thereby producing ATP to re-establish the membrane potential. This depolarization/repolarization has recently been visualized[8] and can occur repeatedly over the course of 700 seconds, but is too rapid to be visualized on a FACS machine (of the order of milliseconds).[85]

Irreversible MPTP only finally occurs once the calcium influx exceeds the mitochondrial buffering capacity. A massive wave of depolarization occurs, cytochrome c is released and the cell undergoes rigor contracture as a result of apoptosis. Once cytochrome c is released into the cytosol, an apoptotic cascade

is initiated, which involves formation of an apoptosome containing caspase 9 among other proteins (Fig. 1-18).

The apoptosome is a cytosolic structure that facilitates caspase 9 activation. Formation of the apoptosome begins when cytochrome c is released from the mitochondrion and binds to the apoptosis protease activation factor 1 (APAF-1), causing it to undergo a conformational change that in turn facilitates binding to other APAF-1 molecules.

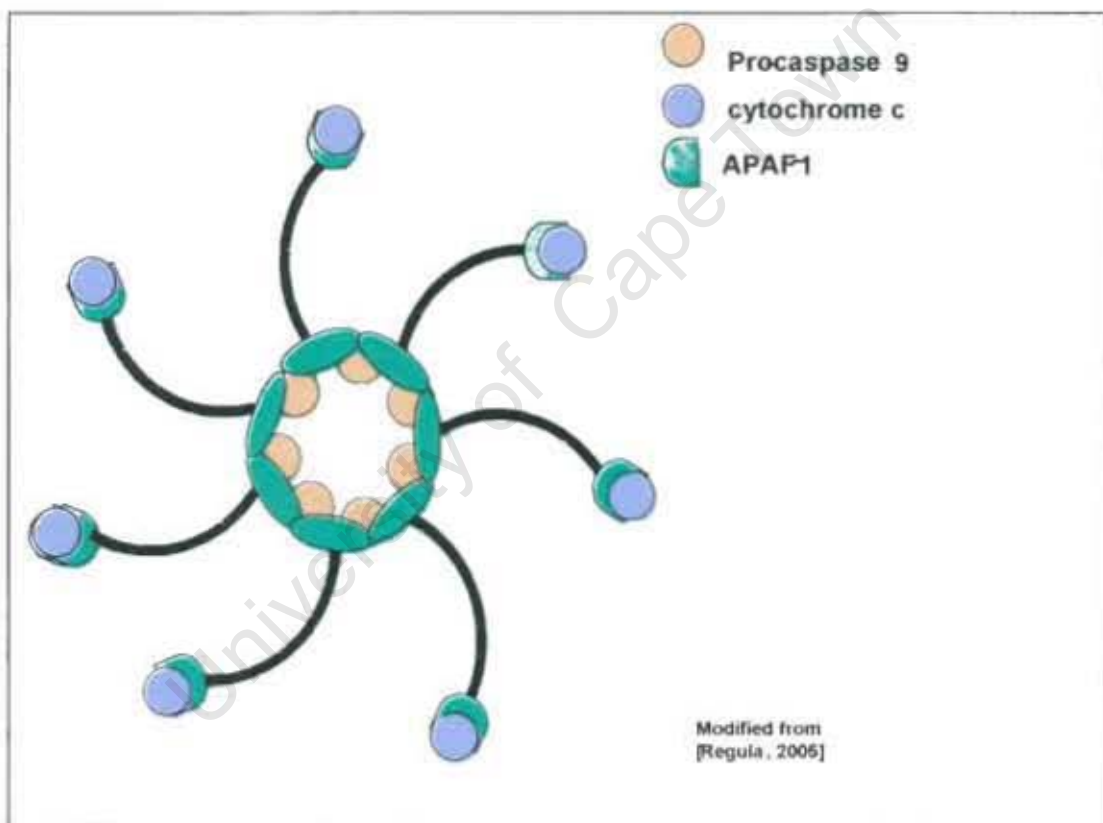


Figure 1-18 Apoptosome formation

APAF-1 – apoptosis protease activation factor 1

Stabilized by dATP, these APAF-1 molecules unite to form a wheel like structure that recruits pro-caspase 9 dimers to its core (Fig. 1.18).[158] The apoptosome

then releases caspase 9 which trigger effector caspases 3, 6 and 7, resulting in the cleavage of death substrates and apoptosis.[84] Apoptosis is not a random event. Rather, it is an ordered process in which caspases have specific targets. Intracellular structural proteins are damaged and nuclear DNA degraded, leading to shrinkage of cell contents and cell death. It is also an energy requiring process and can only occur in the presence of ATP. When the ATP supply is exhausted, cell death by necrosis follows, as this process does not require energy. There is some thought that apoptosis and necrosis are related processes i.e. apoptosis simply progresses to necrosis once the ATP supply is exhausted and that the correct term to use would be necroptosis.[71]

The signals initiating apoptosis may be either extrinsic (originating outside the mitochondrion) or intrinsic (originating inside the mitochondrion). Extrinsic stimuli could be tumour necrosis factor α (TNF- α) or Fas-ligand mediated.[159, 160] These ligands bind to the tumour necrosis factor receptors (TNFRs), triggering recruitment of the death domain (DD) containing proteins to the intracellular surface of the receptor, assembling into a death inducing signaling complex or DISC.[158] Formation of DISC facilitates recruitment and activation of caspases 8 and 10 and initiates the apoptotic cascade.

Intrinsic stimuli may include the direct effect of hypoxia, ischemia/reperfusion or oxidative stress on the mitochondrial signaling pathways. This could lead to membrane permeability transition, opening of the pore and release of cytochrome c, thereby triggering the caspase cascade.[77] The intrinsic and

extrinsic pathways at first appeared to be independent of each other, but it is now clear that cross-talk between the two pathways exists, mediated by 'BH3 domain only proteins' like Bid. Whether the trigger to the mitochondrion is intrinsic or extrinsic, the fate of unprotected ischemic myocardium just before or at reperfusion is programmed cell death or apoptosis. Stimulation or promotion of a cardioprotective signaling molecule or pathway at this point would therefore be beneficial by limiting cell death and reducing infarct size by attenuating apoptosis.[37, 64]

In light of the global burden of heart disease and the looming danger in developing nations such as South Africa, our interest has been to investigate endogenous intracellular cardioprotective mechanisms (for e.g. IPC-like mechanisms in more chronic settings) to eventually help reduce this burden. In particular, we were interested to further investigate and understand the signaling pathways that regulate mitochondrial function in the heart by exploring mechanisms of action of PKC ϵ , one of the major kinases involved in cardioprotection. Therefore, we employed mice in this study that specifically overexpress a constitutively active form of PKC ϵ in the heart.

1.11 Statement of hypothesis

Cardiac-specific overexpression of constitutively active PKC ϵ provides inherent protection against acute and chronic oxidant stress by maintenance of membrane potential and modulation of mitochondrial respiration to maintain cellular energetics (Fig. 1-19). Moreover, such protection occurs via translocation of the constitutively active PKC ϵ to the mitochondrion to interact with pore proteins, thereby stabilizing the voltage dependent anion channel and preventing any conformational changes in adenine nucleotide translocase that may lead to mitochondrial permeability transition and hence mitochondrial permeability transition pore formation and opening.

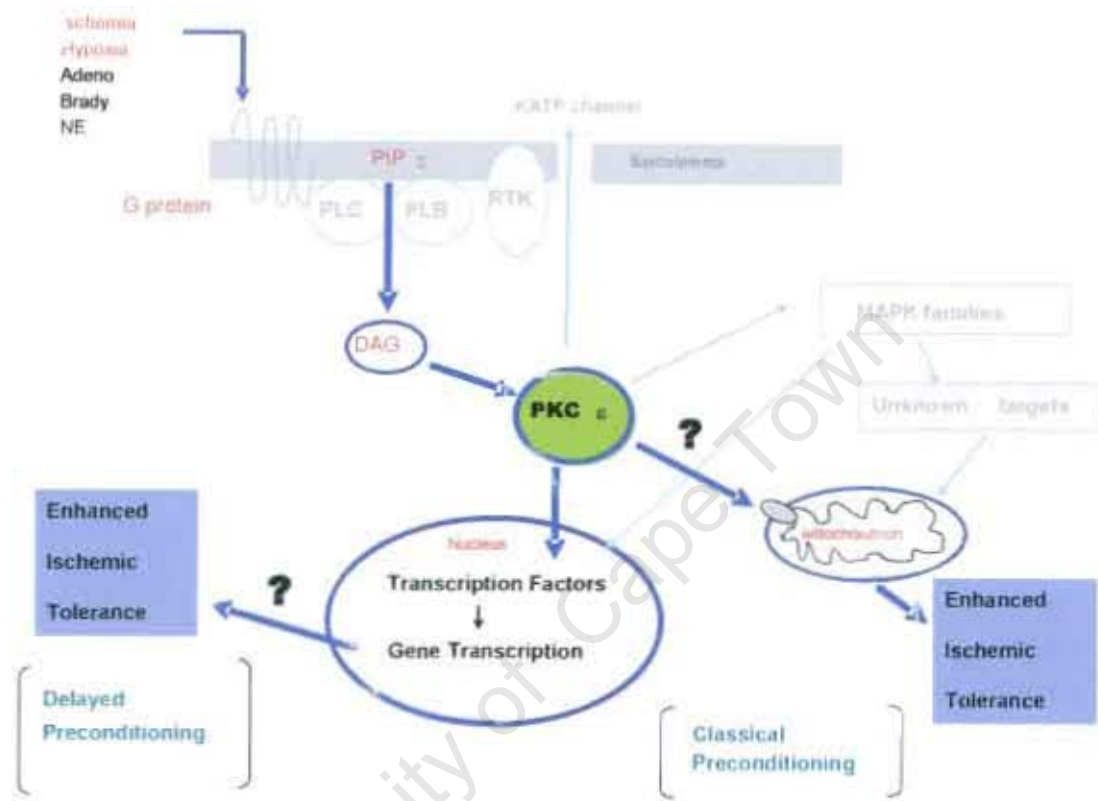


Figure 1-19: Schematic representation of hypothesis

In brief, this scheme proposes that activated PKC ϵ translocates to the mitochondrion and nucleus in response to an **acute** stimulus and interacts with components of the mitochondrial permeability transition pore, stabilizing the conformation and preventing MPT and the initiation of the apoptotic cascade.

Moreover, in response to a **chronic** oxygen lack, for e.g. hypobaric hypoxia, gene transcription pathways are induced also forming part of the cardioprotective response. In view of the association of PKC ϵ with such a wide variety of proteins, I hypothesize that there could be modulation of genes regulating metabolism as well as contractile proteins, leading to enhanced ischemic tolerance.

Adeno – adenosine, brady - bradykinin, NE-norepinephrine, PIP₂ – phosphatidylinositol, DAG – diacylglycerol, RTK – receptor tyrosine kinase

Chapter 2

Materials and Methods

University of Cape Town

2.1 Animals

2.1.1 Ethics

All animal studies performed were approved by the Animal Research Ethics Committee of the University of Cape Town, and followed the recommendations laid down in the Guide for the Care and Use of Laboratory Animals (NIH publication No. 85-22, revised 1996).

2.1.2 PKC ϵ Overexpressing Transgenic Mouse Model

The transgenic mice employed in this study were developed by Dr Peipei Ping and Professor Roberto Bolli, then of University of St Louis, Missouri, USA. Briefly a full-length PKC ϵ cDNA was cloned from a rabbit heart cDNA library. As most of the wildtype PKC ϵ resides in the cytosol and is usually self-inhibited, transgenesis with the wildtype PKC ϵ isoform might not have resulted in effective substrate phosphorylation in the membrane-particulate fraction. Thus a constitutively active PKC ϵ cDNA was generated through a single amino acid mutation (no. 159, A to E). This prevents the pseudosubstrate domain from binding to the catalytic domain, thus rendering the molecule permanently active. A linear 11.4kb DNA fragment containing the entire α -MHC promoter, the complete PKC ϵ cDNA with the mutation and a polyadenylation signal was released by digestion with *Nof1* and used for microinjection into pronuclei of

fertilized FVB mouse eggs. The presence of the transgene was screened by Southern analysis of genomic DNA extracted from tail cuttings. These mice moderately overexpress (copy number = 20) constitutively active PKC ϵ in the heart only. [160] [161] PKC ϵ transgenic mice displayed an increase of 240 \pm 15% in PKC ϵ activity compared to non-transgenic mice in the particulate fraction (Fig. 2-1, a and b). PKC ϵ protein levels were 9x higher in the heart, a 6-fold increase in the membrane to cytosol ratio (indicating activation of PKC ϵ) and a 2.5-fold increase in PKC ϵ activity in the membrane fraction.[160] There were no compensatory changes in other PKC isoforms.

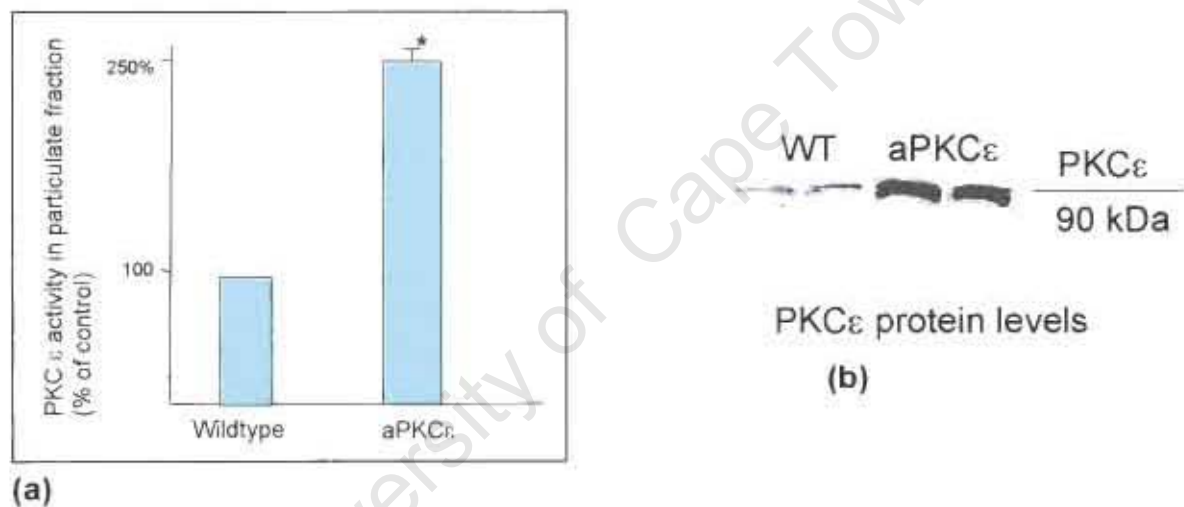


Figure 2-1, (a) and (b). PKC ϵ expression levels in aPKC ϵ mice (Adapted from Takeishi et al.[160])

2(a) indicates mRNA expression levels in aPKC ϵ mice vs WT, whereas 2(b) shows protein levels for PKC ϵ .

We have successfully established a breeding colony of transgenic PKC ϵ overexpressing mice from the original gift of 2 pairs of mice (transgene males and wildtype females), generously provided by Dr Peipei Ping, University of St Louis, Missouri, USA. For the purposes of this study, only male mice aged 9-12

weeks were utilized. Female mice were reserved for breeding or culled, if surplus.

2.1.3 Genotyping of PKC ϵ Transgenic Mouse

To distinguish wildtype from transgene animals, tail cuts were performed at weaning (2 weeks old) and genomic DNA extracted for genotyping, performed by means of the polymerase chain reaction (PCR).

2.1.3.1 DNA Extraction

Tail cuts were incubated at 55°C overnight in 400 μ l tail digestion buffer (0.5 M Tris {pH 8}, 0.1 M NaCl, 0.1 M EDTA, 1% SDS) to which 1 mg/ml proteinase K (Roche, Mannheim) had been added. Subsequently, 400 μ l phenol/chloroform mix (Sigma, USA) was added to each tube and the samples slowly inverted to mix. The digests were centrifuged at 13,500 rpm for 10 minutes (Heraeus MK202, Germany) and the bottom layer containing the cellular debris was removed using sterile barrier tips. Care was taken not to disturb the interface containing contaminating proteins. Thereafter, 200 μ l of chloroform (Sigma USA) was added to the upper aqueous phase to remove traces of phenol and samples again inverted to mix. The digests were centrifuged again at 13,500 rpm for 5 minutes and the bottom layer removed, using barrier tips. The upper aqueous phase was also microfuged again at 13,500 rpm for 5 minutes to sediment any remaining cellular debris. The combined aqueous phase was pipetted into a fresh microfuge tube, to which 50 μ l of 7.5 M ammonium acetate (to a final

concentration of 0.2 M) and 1 ml of 100% ethanol had been added. The samples were inverted to mix and the DNA, which appears as stringy precipitate, was transferred to a fresh microfuge tube containing 500 μ l of 70% ethanol. The samples were then centrifuged for 8 minutes at 13,500 rpm and the ethanol carefully decanted to prevent loss of the DNA pellet. DNA pellets were air dried until ethanol had completely evaporated, then 50–75 μ l of ultra pure RNase free water was added to dissolve the DNA. Samples were thereafter stored at -20°C for PCR analysis.

2.1.3.2 Polymerase Chain Reaction

In order to detect the transgenic PKC ϵ genetic complement, we designed specific oligonucleotide primer sequences that were synthesized by the University of Cape Town's Molecular Biology Core Facility. The following sequences, yielding a fragment of 500 bp, were employed.

Sense primer **5' - CTC GTT CCA GCT GTG GTC CAC A - 3'**

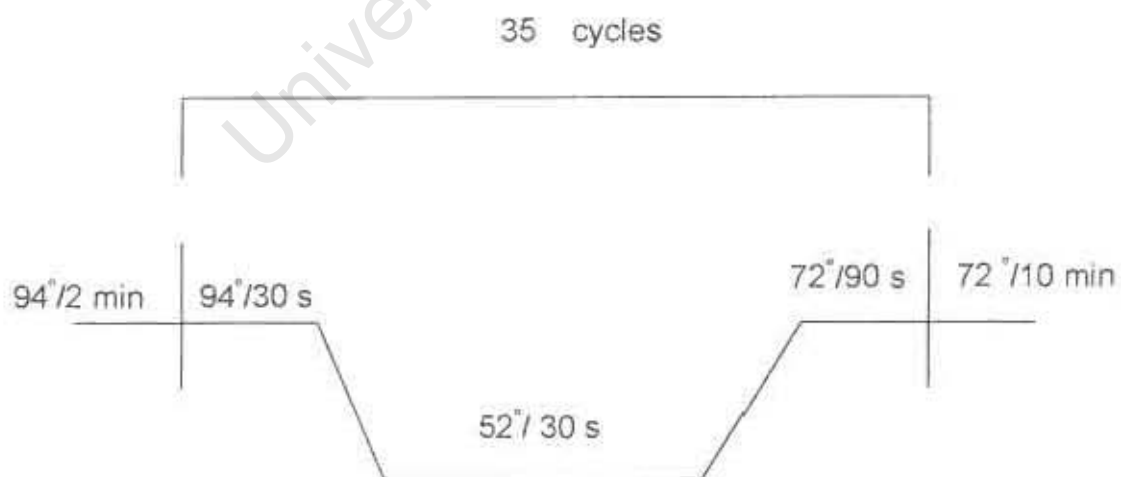
Antisense primer **3' - ACG TTG AGG GCG ATG TAG - 5'**

For each PCR run, a positive control (a previously identified transgenic mouse with distinct banding patterns), a negative control (sterile distilled water) as well as β -actin (to control for failed PCR) were included. The β -actin control yielded a DNA fragment of 490 bp.

The polymerase chain reaction included:

10x Magnesium-free Buffer	2.5 μ l	
MgCl ₂ , 25 mM	4.0 μ l	(4 mM final concentration)
dNTP mix	0.8 μ l	(220 pmol each)
β -actin primer mix	1.0 μ l	(50 pmol each)
PKC ϵ primer mix	0.25 μ l	(50 pmol each)
Taq Polymerase	0.25 μ l	(1 unit)
Sterile distilled water	15.7 μ l	
Genomic DNA	0.5 μ l	(~ 1 μ g)

The reaction was performed in a final volume of 25 μ l and all the products used for the PCR reaction were obtained from Promega (Madison, WI, USA). The DNA samples were heated to 56°C to ensure complete dissolution of the genomic DNA in the distilled water, before pipetting for PCR. The following optimized template was employed:



2.1.3.3 Agarose Gel Electrophoresis

Due to the similarity of PCR products for the β -actin control band (490 bp) and the PKC ϵ band (500 bp), a 2% agarose gel was used to ensure optimal separation. Two grams of agarose (Hispanagar, Burgos, Spain) was made up in 100 ml of 1 X Tris Acetate electrophoresis buffer (0.04 M Tris-Acetate, 0.001 M EDTA) and heated in a microwave at 70% power to dissolve completely. Once dissolved, an aliquot was measured out and ethidium bromide added to a final concentration of 0.5 μ g/ml in order to visualize the amplified DNA fragment under ultraviolet light. We also added 1 x TAE buffer was added to the gel tank before the gel combs were removed in order to prevent the wells being damaged.

Subsequently, 10 μ l of each PCR reaction was mixed with 2 μ l loading dye (Sigma, USA) and carefully loaded into the wells. To verify the size of the PCR products, 4 μ l of a 100 bp DNA ladder was run simultaneously as a marker (Roche, Germany). The gel was run at 80 V for 25-45 minutes, where after the bands were visualized on a transilluminator (UviTec, USA). PCR results were recorded using a UviTec Geldoc apparatus using UViband software v.97 (Cambridge.UK).

2.2 Ischemia/reperfusion experiments: infarct size

2.2.1 Isolated mouse heart perfusion model

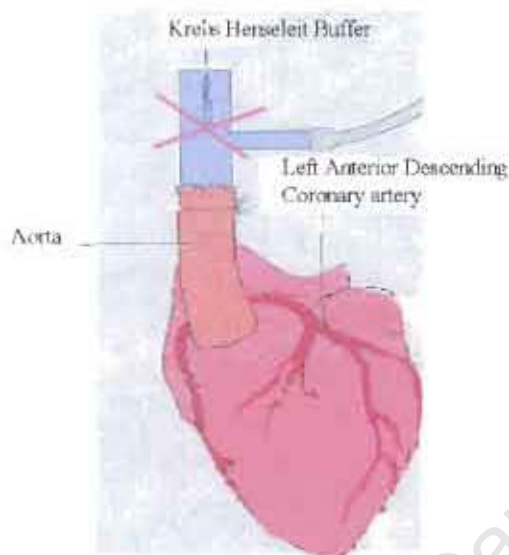


Figure 2-2: Illustration of an isolated perfused mouse heart, subjected to global ischemia by total occlusion of the aorta

In order to assess the basal protective phenotype of the $\alpha\text{PKC}\epsilon$ mice compared with their wildtype littermate controls, an isolated perfused heart model was utilized. Male mice (18-25 g) were anesthetized (pentobarbitone sodium, 60 mg kg^{-1} IP) and heparinized to prevent the blood clotting, (25 IU IP). Once an adequate level of anesthesia had been achieved, the chest was opened and the sternum and attached costal cartilage excised to give adequate access to the mediastinum. The heart was rapidly excised[162] and arrested in ice cold (4°C) Krebs Henseleit buffer and the aorta cannulated. Hearts were retrogradely perfused with a modified Krebs-Henseleit buffer (118 mM NaCl, 24 mM NaHCO_2 , 4 mM KCl, 1 mM NaH_2PO_4 , 2.5 mM CaCl_2 , 1.2 mM MgCl_2 , 0.5 mM di-sodium

EDTA, 10 mM glucose, gassed with 95% O₂ / 5% CO₂ at 27 °C) with a constant pressure of 110 cm H₂O.[162] Temperature was measured by the placement of a fine thermocouple wire (Physitemp, NJ, USA) and monitored on a Digitron 2600T temperature sensor (Torquay, UK). Global ischemia was induced by shutting off the flow to the heart by means of a stopcock through the aortic cannula. At varying ischemic times from 20-45 minutes, the heart was "reperfused" for 45 minutes, then removed for infarct size determination utilizing triphenyltetrazolium chloride (TTC) staining (section 2.2.2).

From these experiments, it was determined that 45 minutes of global ischemia followed by 45 minutes of reperfusion was required to produce an infarct in the hearts of mice overexpressing constitutively active PKC ϵ . We subsequently employed this time point for the mitochondrial anoxia/reoxygenation experiments.

2.2.2 Cardiac Functional assessment



Figure 2-3. Illustration of mouse heart perfusion model for cardiac function assessment

Hearts were excised and mounted as in section 2.2.1, then fastened by means of a 4-0 silk suture (on a 20 mm curved atraumatic needle) through the apex and a rigid lightweight lexan coupling rod to a force displacement transducer (Grass FT02C, Mass. USA). Diastolic resting tension was adjusted to 2 g and hearts paced at 600 beats per minute. The developed force was recorded on a chart recorder (Lectromed Multitrace-2, Letchworth, UK) and coronary flow rate was measured by timed collection. These parameters were utilized as measures of cardiac function for normoxic and hypoxic hearts. In addition, Dr Ellen Aasum of Tromsø University Norway, as part of a collaborative study, performed pressure/volume loops on normoxic working mouse heart preparations.

2.2.3 Infarct Size Determination



Figure 2-4. TTC staining for Infarct size estimation

TTC reacts with the NAPH in live tissue to give a brick red colour. There is no reaction in the infarct tissue, which then remains pale and allows infarct size determination by densitometric analysis.

At the end of each experimental protocol, hearts were removed from the perfusion rig and the infarct size assessed by triphenyltetrazolium (TTC) staining

as described previously.[163] Atria are trimmed off, leaving right and left ventricle, separated by the septum. The heart is incubated at 37 degrees in the 1% TTC stain, made up in phosphate buffer at pH 7.4, then sliced into 1.5-2 mm thick cross-section slices (rough measurement). Each slice includes both right and left ventricle plus septum. These slices were compressed between thin glass plates 0.5 mm apart and the sections scanned, enlarged, and infarct size assessed using computerised planimetry (Planimetry+, Boreal Software, Norway) by a researcher blinded to the groups.

2.3 Mitochondrial Respiration Studies

2.3.1 Isolation of Mitochondria

Mice were anesthetized using Euthanase (Bayer, SA) and heparin, as described in section 2.2.1. Once the pedal reflex had disappeared, indicating a sufficient degree of anesthesia, the hearts were rapidly excised and arrested in ice-cold isolation buffer (0.18 M KCl, 0.01 M EDTA, pH 7.4). Atria and connective tissue were trimmed off and the remaining tissue minced on ice using a pair of scissors. The rough homogenate was poured into a 7 ml glass homogeniser (Tenbroek, Netherlands) and rinsed 4 times with ~ 5 x w/v ice-cold isolation buffer. After visible blood had been eliminated, the tissue was quickly but gently homogenized. The homogenate was thereafter centrifuged at 700g (Heraeus Christ MK202, Germany) to eliminate larger intracellular constituents. The supernatant was transferred to a clean cold tube and centrifuged at 2000g to isolate the mitochondria using a modification of the method of Sordahl.[164] The

mitochondrial pellet was resuspended in 50 μ l of ice-cold isolation buffer and kept on ice until assayed. The above procedure was performed as quickly as possible, keeping everything on ice to ensure that the mitochondria harvested were in optimal functional condition. The entire isolation procedure usually took less than 20 minutes and mitochondria were viable for up to 4 hours after isolation. However, we routinely used mitochondrial preparations within 20 minutes. A duplicate 5 μ l sample was assayed for protein content using the Lowry protein determination method.[166]

2.3.2 Lowry Protein Determination

Duplicate 5 μ l aliquots of each sample were added to 995 μ l of sterile distilled water, followed by the addition of 1 ml of solution A (Na_2CO_3 (20 %) and $\text{CuSO}_4 \cdot 5\text{H}_2\text{O}$ (0.2 g) plus dipotassium tartrate (0.4 g) in 100 ml were mixed 1:1 to make 200 ml CTC reagent. 200 ml of 10 % SDS and 200 ml of 0.1 M NaOH were added. This mixture constitutes 600 ml of solution A). The samples were immediately vortexed to mix and incubated for 10 minutes at room temperature. Thereafter, 500 μ l of solution B (Folin's Reagent, Merck, diluted 1 in 6) was added while vortexing, as the colour complex to be assayed forms immediately. After 30 minutes incubation at room temperature the assay was read at 750 nm on a Varian 120 dual beam spectrophotometer.[166] Bovine Serum Albumin was used to construct a standard curve from 5 to 200 μ g / ml and assayed in the same manner as the samples.

2.3.3 Determination of Mitochondrial Respiration Coupling

Respiration studies were performed in a respirometer equipped with a Peltier temperature control unit (Oxytherm, Hansatech, Norfolk, UK). The 1 ml chamber contained 341 μ l of incubation buffer (250 mM sucrose, 25 mM Tris, 8.5 mM KH_2PO_4 , {pH 7.4}) at 25°C. A baseline reading was taken to verify the stability of the calibration, then 25 μ l of mitochondrial suspension (section 2.2.1) was added and a second reading taken to determine state 1 respiration. State 1 represents endogenous respiration occurring in the mitochondria. After 1 min, 20 μ l of the substrate (100 mM glutamate) was added and state 2 respiration measured. State 2 respiration is defined as respiration occurring in the absence of any ADP, therefore representing utilization of the substrate (glutamate) in the absence of ADP. Once this was stabilized, 14 μ l of 10 mM ADP (final concentration 350 μ M) was added to trigger state 3 mitochondrial respiration. State 3 is defined as the state in which phosphorylation of ADP to ATP occurs. During this state of respiration, a comparatively large amount of oxygen is consumed during the conversion of ADP to ATP. The chamber was carefully sealed at this point to allow progression to state 4 respiration. State 4 respiration is defined as the state in which all the ADP added has been phosphorylated to ATP and steady state respiration again occurs. This state is equivalent to state 2 respiration. The respiratory control index (RCI), a ratio of state 3/state 4, was calculated and samples with an RCI of less than 7 were not included in our studies. RCI is regarded as a measure of the viability of the mitochondrial population and a

value of 4 or more indicates successful mitochondrial isolation and an actively respiring preparation.

2.3.4 Determination of Basal Functional ANT Content

Atractyloside (Sigma, USA) is a plant glycoside and a potent ANT inhibitor.[166] It fixes the translocator on the cytosolic side of the mitochondrial inner membrane in the 'c' conformation, thus preventing its action. Mitochondrial oxidative phosphorylation (state 2 respiration) soon ceases.[166,167] Atractyloside binds stoichiometrically on a 1:1 basis with the ANT complex. Functional ANT content was determined by titrating the state 3 mitochondrial respiration rate with an increasing number of aliquots (10 pmol) of atractyloside until state 3 respiration had ceased. Here, the mitochondrial respiratory index was assessed as described (section 2.2.2) and after reaching state 4, the first 10-pmol aliquot of atractyloside was added. An aliquot of 10x the usual ADP concentration was immediately added to ensure that the mitochondria do not stop respiring involuntarily (due to a lack of ADP) before the atractyloside titration is complete. State 3 respiration was assessed immediately and thereafter repeatedly after addition of sequential 10 pmol aliquots of atractyloside. This was continued until state 3 respiration was completely abolished.

2.3.5 Determination of Basal Mitochondrial Proton Leak

To determine the rate of oligomycin-induced mitochondrial proton leak, oligomycin (final concentration 1 $\mu\text{g/ml}$) and an additional aliquot of ADP was added to the chamber immediately after obtaining state 4 respiration. Since oligomycin specifically inhibits ATP synthase, any oligomycin insensitive state 3 respiration that occurs will represent basal mitochondrial proton leak.

2.3.6 Determination of Total Inorganic Phosphate

Thirty μg of protein from freshly isolated mitochondria (PKC ϵ transgenic and wildtype littermate controls) was utilized to assay for inorganic phosphate. This was performed in order to approximate the ATPase activity.[169] The assay was done both in the presence and absence of oligomycin to elucidate the effects of increased basal proton leak on the ATP production / breakdown. The assay was performed using an EnzChek kit (Molecular Probes, Oregon, US) with appropriate standards and controls supplied with the kit and utilizing a Varian 120 dual beam spectrophotometer (Varian, USA) at 340 nm.

2.3.7 Rate of ATP Synthesis

The rate of ATP synthesis was determined using a modified method of Budnikhov et al.[48] Approximately 10 μg of mitochondrial protein was added to pre-warmed synthesis buffer (150 mM sucrose, 75 mM KCl, 5 mM KH_2PO_4 , 2.5 mM MgCl_2 {pH 7.4}). Mitochondria were incubated for 20 seconds at 25°C, after which 10 mM succinate was added and the reaction incubated for 60 seconds at

25°C. Subsequently, 200 µM ADP was added to initiate mitochondrial ATP synthesis. The zero time sample was removed simultaneously. Sequential samples were taken at 10-second intervals for a total period of 60 seconds and each sample injected directly into cold 2.5% trichloroacetic acid (TCA). The TCA was neutralized with 1 M Tris base and the samples were either assayed directly or frozen at -80°C for later assay. The assay was performed on a microplate luminometer (Veritas, Turner Biosystems, USA). Samples were assayed in duplicate from a standard curve constructed (in duplicate) using trisodium ATP (Roche, GMBH) from 10⁻⁵ M to 10⁻⁹ M. Ten µl of sample/standard was pipetted into each well (in duplicate), to which 175 µl double distilled water was added. 25 µl of firefly ATP reagent (diluted 1 in 2) (FL-AAM, Sigma, St Louis, MO) was added per well and the resultant luminescence data calculated as concentrations of ATP off the standard curve. The results were corrected for dilutions and for protein concentration, assayed using the Lowry method.[165]

2.3.8 FACS Analysis

Lipophilic fluorescent cationic dyes have been widely used to monitor relative inner mitochondrial membrane potential changes.[169-171] The cationic dye JC-1 (5,5', 6,6'-tetrachloro-1,1',2,2'-tetraethyl benzimidazolyl - carbocyanine iodide) (Molecular Probes, Oregon) made up to a 5 mg/ml suspension in dimethylsulphoxide (DMSO) was used to determine membrane potential. The JC-1 dye was further diluted 1:100 and 84 µl of this solution was added to the mitochondrial suspension containing glutamate and ADP at 37°C (final

concentration of JC-1 0.9 $\mu\text{g}/\mu\text{l}$). The suspension was incubated for 5 minutes at 37°C and duplicate readings taken. The JC-1 was excited at 488 nm and the monomer signal (green) analyzed at 525 nm (FL1). Simultaneously, the aggregate signal (red) was analyzed at 590 nm (FL2). As control, an aliquot of mitochondria was read unstained. After staining, the membrane potential was dissipated, using CCCP (carbonyl cyanide 2-chlorophenylhydrazone, to a final concentration of 100 mM) to confirm that we were measuring membrane potential and not mitochondrial volume or size. To confirm our results, we utilized a second potentiometric dye, DiOC6 (2',2'-dihexyloxacarbocyanine iodide). This was made up as a 1 mM stock solution in ethanol, then aliquoted and stored at -20°C. For experiments, aliquoted DiOC6 was diluted 1:1000 to yield a 1 μM solution. Forty μl of diluted DiOC6 was added to the isolated mitochondria (in incubation buffer + glutamate and ADP), to a final concentration of 9.8 nM. The suspension was incubated at room temperature for 5 minutes before it was assessed on a FACSCalibur fluorescence activated cell sorter (Becton Dickenson). The dye was excited at 488 nm and read at 525 nm as FL1. As a control, an aliquot of mitochondria was also read unstained.

2.4 Western Blot Analysis

Mitochondria were extracted, resuspended in 50 μl of isolation buffer (as previously described in section 2.2.1) and kept on ice. A duplicate 5 μl sample was taken for protein determination, using the Lowry method as described (section 2.2.2). Immediately after collection of protein samples, 2 μl of complete

inhibitor cocktail (Roche, Germany) and 25 µl of low ionising sample buffer (400 µl 10% SDS, 400 µl glycerol, 40 µl mercaptoethanol, 1.16 ml 5 mM Tris {pH 6.8} in a final volume 2 ml with sufficient bromophenol blue to make the solution pale yellow) was added to each tube. The mitochondrial samples were thereafter gently mixed and stored at -20°C.

2.5 Polyacrylamide Gel Electrophoresis (PAGE)

Sixty µg of mitochondrial protein was loaded per lane and run on a 7.5% acrylamide / bisacrylamide gel at 120 V for approximately one hour. Six µl of rainbow marker (Amersham, UK) was run simultaneously to determine the size of the candidate peptides. The gel was transferred (400 mA for 1 hour at room temperature) onto an Amersham PVDF membrane (Hybond, Amersham, UK). The membrane was fixed in methanol for 5 minutes then air-dried and stained with Ponceau stain (Sigma P7170, St Louis, MO) to quantitate and compare the loading. The membrane was placed between two acetate sheets and scanned for densitometric analysis, using the UVIBand software package.

Subsequently, the Ponceau stain was rinsed off with two 5 minute washes in distilled water, followed by one 5 minute wash in Tris buffered saline with 0.1% Tween (TBS-T). The membrane was then blocked using 3% BSA (Sigma, fr V, A7906, St Louis, Mo) in TBS-T for 1 hour, shaking gently on an orbital shaker at room temperature. Thereafter the membrane was vigorously hand washed in TBS-T for 3 x 5 minutes, then washed for 15 minutes on the shaker in TBS-T,

followed by an additional 5 minute vigorous hand wash. The blot was then probed with one of our candidate antibodies, made up in TBS-T (no milk powder or BSA added):

1. Adenine nucleotide translocator (ANT)

Primary antibody 1:500 for 1 hour (Santa Cruz Biotechnology, Santa Cruz, CA); secondary donkey antigoat 1:1000 for 35 minutes (Santa Cruz Biotechnology, Santa Cruz, CA).

2. Cytochrome c (cyt c)

Primary antibody 1:500 for 1 hour (Santa Cruz Biotechnology, Santa Cruz, CA); secondary antirabbit 1:1000 for 45 minutes (Santa Cruz Biotechnology, Santa Cruz, CA).

3. Uncoupling protein 2 (UCP2)

Primary antibody 1:40 for 1 hour (Santa Cruz Biotechnology, Santa Cruz, CA); secondary donkey antigoat 1:1000 for 1 hour ((Santa Cruz Biotechnology, Santa Cruz, CA).

4. Voltage dependant anion channel 1 (VDAC1)

Primary antibody 1:500 for 1 hour (Santa Cruz Biotechnology, Santa Cruz, Ca); secondary donkey antigoat 1:1000 for 35 minutes (Santa Cruz, SC 2020).

The membrane was probed with primary antibody for 1 hour, followed by stringent washing as described. The membrane was then exposed to secondary antibody for varying times as described earlier. The experimental parameters employed depended on the specific antibodies being utilized and were derived after troubleshooting the conditions for each antibody. Stringent washing of the

membrane followed, as described, then the blot was treated with ECL reagent (Amersham, UK). Here, 1 ml of each ECL reagent was added to the blot for 1 minute, which was drained and blotted well between two wads of paper towel and thereafter exposed to the autoradiographic film (ECL Hyper film, Amersham, UK). Films were subsequently developed, rinsed well and left to dry. After drying, developed films were aligned onto the original blots to enable us to identify the candidate peptides on the blot. Densitometric analyses were then performed using the UViband software programme. The intensities of the bands seen on the blot were corrected for protein loading against the Ponceau stained band and tabulated. As a further control, we also probed blots with VDAC1 to confirm loading. Candidate peptide levels were normalized to VDAC1.

2.6 Anoxia/Reoxygenation Experiments

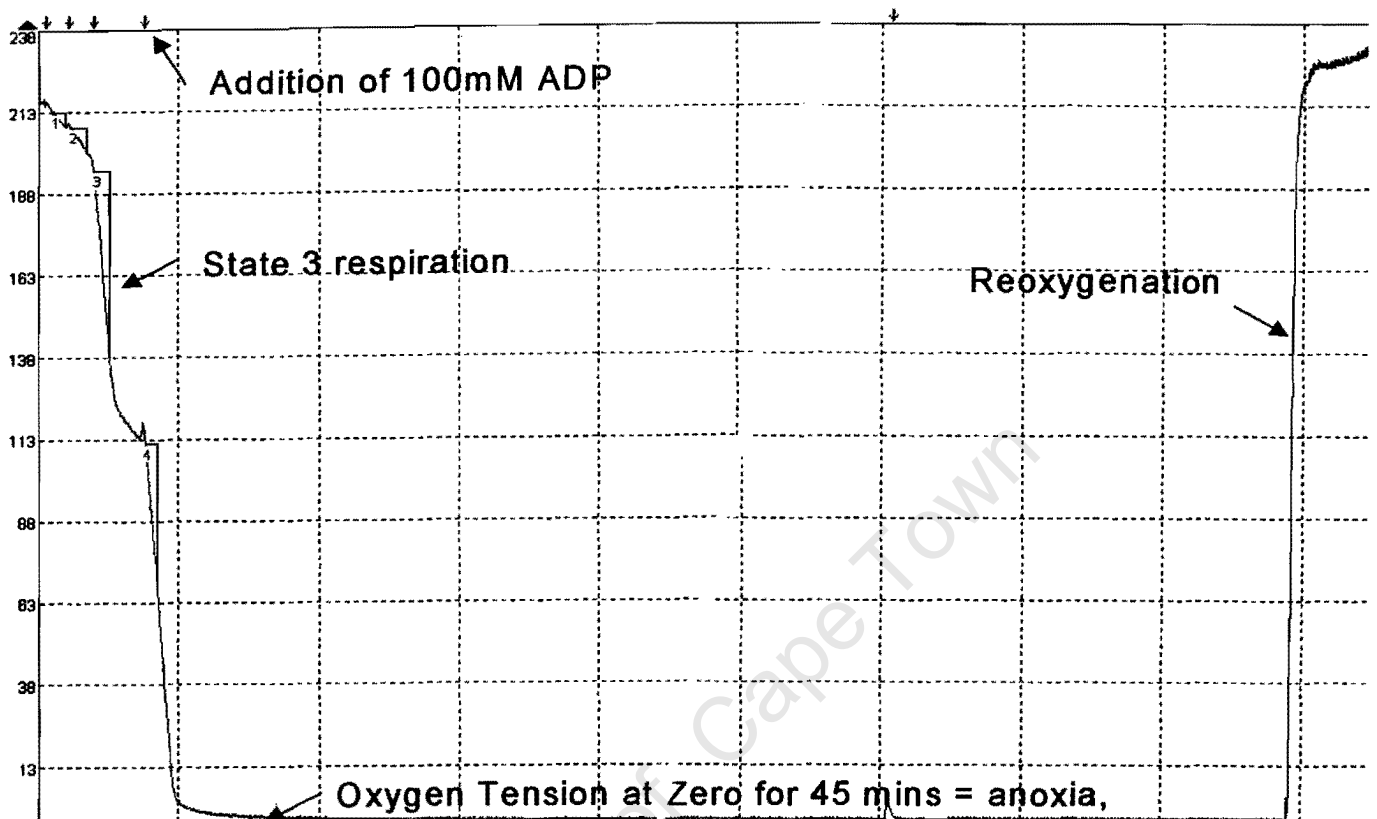


Figure 2-5: Typical trace of mitochondria subjected to ADP- induced anoxia for 45 minutes, then reoxygenated.

After mitochondria were isolated from mouse ventricular tissue, a duplicate 5 μ l sample was assayed for protein content and the mitochondrial respiratory control index was assessed as previously described (section 2.2.2). After reaching state 4, a fresh aliquot of 100 mM ADP was added to stimulate mitochondria to respire rapidly and to completely utilize the oxygen in the chamber before all the ADP is phosphorylated. The chamber was then sealed, creating an anoxic environment.

From our infarct size determination experiments (section 2.2.2) we had determined that 45 minutes of ischemia was required to induce an infarct in our transgenic mouse hearts. In the light of this, we selected the same duration of anoxic insult for the isolated mitochondrial studies. For the reoxygenation experiments, the chamber was opened after 45 minutes of anoxia and room air bubbled through the chamber until the oxygen tension was between 120 and 160 nmol oxygen. The preparation was reoxygenated for 7 minutes, during which time recovery state 2 was measured.

2.6.1 Mitochondrial endpoints

All baseline measurements (mitochondrial respiration, membrane potential determinations, rate of ATP synthesis) were also determined following anoxia-reoxygenation, in exactly the same manner and utilizing the same methodology, unless specifically stated.

2.6.2 Determination of Functional ANT Content in response to Anoxia/Reoxygenation

The procedure was the same as described in section 2.2.5, except that a fresh aliquot of 10x ADP was added together with the first 10 pmol aliquot of atractyloside upon reoxygenation. The titration continued as previously (section 2.2.4) until state 3 mitochondrial respiration was completely abolished.[166,172]

2.7 Hypobaric Hypoxia model

2.7.1 Hypobaric hypoxic chamber

Two PKC ϵ transgenic mouse strains were originally generated i.e. a moderately overexpressing phenotype (n=20 copies) and a more severely overexpressing phenotype (n=40 copies).[9] Interestingly, the high copy number transgene was associated with increased contractility and concentric compensated hypertrophy.[160;6] In light of this, part of this study was to determine whether PKC ϵ transgenic mice are also protected in response to chronic hypoxia. For this purpose, we utilized a well-characterized, specially constructed lexan hypobaric hypoxic chamber,[173] designed in-house and available in our laboratory. The chamber is 275 mm wide X 460 mm high X 1.2 m long (Fig. 2-6). The pO₂ inside the chamber was calculated according to the formula:

$$\text{pO}_2 \text{ (mmHg)} = \{0.2903 \times (\text{pressure in chamber}) - \text{vapour pressure H}_2\text{O at RT}\}[66]$$

No more than 4 small mouse cages were introduced at any one time, each containing fewer than 5 mice per cage. For this reason, carbon dioxide and water vapour build-up did not pose any problems. In addition, the system extracts only a partial vacuum.

Nine-week-old male PKC ϵ transgenic mice and their age-matched wildtype littermate controls were placed into the chamber on day one, the chamber was sealed and a partial vacuum drawn, equivalent to approximately 11% oxygen (40 kPa).

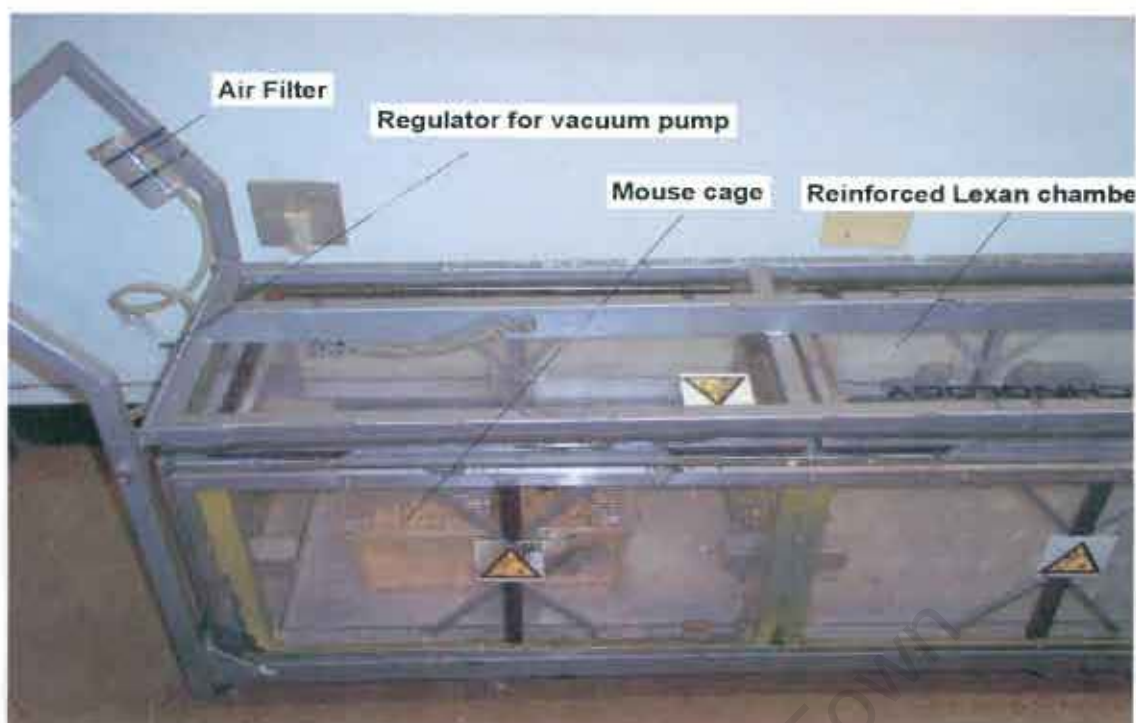


Figure 2-6: Hypobaric hypoxic chamber, developed in-house.

Age-matched normoxic animals were housed in the same area and utilized as controls. Mice were provided food and water *ad libitum*. The chamber was opened briefly every 7 days to supply fresh food and water, as well as a change of bedding. At the end of the 7 or 14 day experimental timepoint mice were removed from the chamber in small numbers, to limit "reoxygenation" and assigned to one of three groups: mitochondrial extraction for respiration studies, cardiac functional assessment and gene screening via quantitative reverse transcriptase PCR. After removal from the chamber, mice were rapidly anesthetized and sacrificed to limit the degree of reoxygenation.

2.7.2 Real Time Quantitative PCR

At the stipulated experimental time points, body weights were recorded and animals subsequently anesthetized as before (section 2.2.1). Hearts were

excised, arrested in ice-cold isolation buffer, and atria and vascular tissue trimmed off. The right and left ventricles were separated and weighed, then snap-frozen in liquid nitrogen. The tissue was stored at -80°C for gene screening using quantitative RT-PCR. The methods for the RNA extraction and real time quantitative RT-PCR have been described previously.[174] The nucleotide sequences and probes have been previously published.[130,174] The constitutive gene transcript 18 S was used to normalize the data. Internal standards were prepared using T7 RNA polymerase method (Ambion, Austin). Quantitative RT-PCR analysis was performed in collaboration with Professor Heinrich Taegtmeyer and Dr S Sharma (Houston, TX, USA)

2.7.3 Functional assessment

Mouse hearts were retrogradely perfused, as previously described (section 2.2.1) after arrest and excision in order to determine comparative contractility by measurement of developed tension and coronary flow. Hearts were paced at 600 beats per minute.

2.7.4 Mitochondrial Respiration

After arrest and excision, hearts were finely minced and mitochondria extracted as detailed previously (section 2.3.1). Subsequently, basal respiration studies and membrane potential measurements were performed on isolated mitochondria. Aliquots of isolated mitochondria were also stored at -80°C for Western blot analysis. Protein concentration was determined using the Lowry method.

2.7.5 Electron Microscopy

After removal from the hypoxic chamber, animals were anesthetized, hearts rapidly excised and arrested in ice-cold isolation buffer. A portion of the left ventricle+septum was dissected and fixed in glutaldehyde for 2-4 hrs at 4°C. The specimen was washed overnight in phosphate buffered saline, followed by 2 distilled water washes of 2 minutes each, followed by potassium osmium tetroxide for 1 hour at 4°C and a further 2 distilled water washes. Samples were then dehydrated in 0.5% uranyl acetate in 80% acetone for 20 minutes, then 90% acetone for 15 minutes, followed by 100% acetone for 20 minutes. Infiltration was performed with 50% vol/vol acetone and Spurr for 90 minutes, followed by 2 washes in neat Spurr for 1 hr at 70°C. Following dehydration the tissue samples were embedded in paraffin wax at 70°C and sectioned using an ultramicrotome. Ultra thin sections were then placed onto the copper grids and stained with heavy metals (uranyl acetate and lead nitrate). These sections were visualized at 7500x and 25000x magnification in order to compare number and structure of mitochondria in the different samples taken at 7 and 14 days hypobaric hypoxia, with their appropriate controls. The samples were visualised on a Jeol 1200 EX II electron microscope (JEOL, Japan).

2.7.6 Rate of ATP synthesis

This was performed as described in section 2.3.7.

2.8 Statistics

Results are expressed as mean \pm SEM. Significance ($p<0.05$) was determined for discrete variables by unpaired t-test, Welch corrected for multiple comparisons.

University of Cape Town

Chapter 3

Characterization of the Protective Phenotype of the activated PKC ϵ Cardiac-specific Overexpressing Mouse

University of Cambridge

3.1 Introduction

When cardiac tissue remains ischemic for more than twenty minutes, cells start to die in the ischemic area. The longer the ischemic time, the greater the tissue damage.[2] (see also chapter 1). However, reperfusion or restoration of flow also causes injury.[2-5] Any intervention that can minimize either ischemic or reperfusion injury will protect the heart: this is the principle of cardioprotection.

The heart has endogenous protective programs, which can be triggered, for e.g. ischemic preconditioning and post-conditioning.[6, 37, 175] PKC ϵ is an integral part of these endogenous protective programs [59] and our laboratory was fortunate to obtain mice overexpressing a cardiospecific activated form of PKC ϵ as gift from Dr Peipei Ping (University of California, LA. School Of Medicine, CA).

Modest activation of the epsilon isozyme of protein kinase C (PKC ϵ) confers enhanced resistance to myocardial cell death in response to ischemia in numerous species.[1, 7, 67, 68] Furthermore, functional proteomics have identified diverse intracellular signaling modules implicated in PKC ϵ orchestrated ischemia-tolerance.[3, 5, 7, 70] In addition, sub-proteome analysis has identified interactions between activated PKC ϵ and mitochondrial-enriched proteins including those governing mitochondrial oxidative phosphorylation, electron transfer, ion transport and mitochondrial permeability transition pore opening (MPTP).[3, 70] As an enhanced capacity to generate ATP would fundamentally enhance resilience to ischemia[5] and adequate ATP generation is required to prevent MPTP,[149] constitutively active PKC ϵ should promote mitochondrial

tolerance to ischemia by maintaining ATP production during an ischemic or anoxic stress. Moreover, adenosine nucleotide translocases (ANTs) are integral to ATP production[176] and are an accepted component of the MPTP.[149] Activated PKC ϵ also interacts with ANTs[70] to preserve mitochondrial oxidative phosphorylation capacity by preventing MPTP-induced inactivation of ANT. Therefore, we proposed that PKC ϵ modulates ANT functional activity as part of its cardioprotective signaling.

Before this proposal could be tested, it was necessary to establish that overexpression of cardiac-specific activated PKC ϵ had indeed resulted in cardioprotection in response to an ischemic insult. Here, PKC ϵ overexpressing and wildtype littermate control hearts were retrogradely perfused and subjected to global ischemia, followed by reperfusion.

After establishing that PKC ϵ overexpressing mice do indeed exhibit a protective phenotype, I could then proceed to test the hypothesis that activated PKC ϵ (after translocation to the mitochondrion) interacts with components of the MPTP to prevent MPT and pore formation, thereby maintaining energy homeostasis when the mitochondria are subjected to oxygen lack. Mitochondria would be isolated from mice harboring constitutively activated PKC ϵ [4] and compared with littermate wildtype control mitochondria at baseline with respect to several mitochondrial functional parameters (state 3 respiration, mitochondrial membrane potential, ANT functional content and the rate of ATP synthesis). Moreover, these

parameters were also determined in mitochondria exposed to an acute stress i.e. ADP-induced anoxia and subsequent reoxygenation.

3.2 Methods

3.2.1 Characterization of the Protective Phenotype

Transgenic mice exhibiting cardiac-specific overexpression of a constitutively active isoform of the PKC ϵ isozyme were utilized in parallel with non-transgenic age and sex-matched littermate controls.[2] Male mice were employed at age 9-12 weeks. The protective phenotype was first established by isolated heart perfusion and infarct size determination (section 2.2.3)[163] in response to global ischemia (varying exposure times). Reperfused hearts were stained with TTC at 37°C then sliced into 1.5-2 mm sections (section 2.2.3) to estimate infarct size. Intact living tissue (containing NADH) reacts with the stain to form a brick-red colour, while infarcted (non-living) cells remain colorless.[177] These serial sections of the heart are scanned for densitometric analysis. Infarct size determination by TTC staining is an accepted measure of the damage following ischemia-reperfusion. From these experiments, we determined that at least 45 minutes of global ischemia followed by 45 minutes of reperfusion was required to result in a detectable infarct in the PKC ϵ overexpressing mice. Subsequently, 45 minutes was utilized as an appropriate anoxic exposure time for the mitochondrial anoxia/anoxia-reoxygenation experiments.

Since moderate overexpression of PKC ϵ has previously been shown to be associated with hypercontractility and compensated concentric hypertrophy,[161] we also set out to confirm that mice employed in this study were functionally normal at age 9-12 weeks. Cardiac function was therefore assessed using the Langendorff perfusion method. Hearts were fastened through the apex via a rigid lightweight lexan coupling rod to a force displacement transducer (Grass FT03C, MA, USA). Diastolic resting tension was initially adjusted to 2 g and hearts paced at 600 beats per minute. The resting tension spontaneously decreased with the overall length of the experiment (stabilization time of 10 minutes and perfusion time of 20 minutes). The developed force was recorded on a chart recorder (Lectromed Multitrace-2, Letchworth, UK) and coronary flow rate was measured by timed collection (section 2.2.2).

In addition, mice were sent to Dr Ellen Aasum at the University of Tromso in Norway as part of a collaborative study. Baseline metabolic studies were to be performed to confirm the quantitative RT-PCR gene data and to do more sophisticated functional measurements (section 2.2.2)

3.2.2 Mitochondrial Functional Phenotype

Mitochondria from both PKC ϵ overexpressing mice and wildtype littermate controls were isolated as previously described (section 2.3.1). Baseline respiration coupling was measured polarographically at 25°C (section 2.3.3) [165]. ANT functional content (section 2.3.4) and baseline inner mitochondrial membrane potential (section 2.3.8) were also determined. Aliquots of

mitochondrial protein were mixed 1:1 with low ionizing sample buffer plus a complete protease inhibitor cocktail (see section 2.4) and stored at -80°C for SDS-PAGE analysis of mitochondrial pore proteins and components of the electron transport chain.

In an attempt to trigger the PKC ϵ protective program, isolated mitochondria were subjected to excess ADP-induced anoxia as an acute stress. Baseline oxidative phosphorylation was measured polarographically at 25°C,[165] whereafter mitochondria were exposed to a 45 minute excess ADP-induced anoxic insult (section 2.6). Mitochondria were retrieved by centrifugation under mineral oil to maintain an anoxic environment and thereafter rapidly resuspended in cold incubation buffer. Aliquots of mitochondria were subjected to immediate FACS analysis to determine the inner mitochondrial membrane potential after the anoxic stimulus (section 2.3.8). Employing luciferin-luciferase luminometry, the rate of mitochondrial ATP production was determined at baseline and in response to the anoxic insult.[178] The remaining mitochondrial protein was quantitated, mixed 1:1 with low ionizing sample buffer plus protease inhibitor and stored at -80°C for later SDS-PAGE electrophoresis experiments. Blots were probed for the following mitochondrial regulatory proteins (section 2.5):

cytochrome c

VDAC1 (voltage dependent anion channel 1)

ANT1 (adenine nucleotide translocase 1)

UCP2 (uncoupling protein 2)

Antibodies were purchased from Santa Cruz Biotechnology (CA, USA) and were specific for the detection of mouse, rat or human forms of VDAC1, ANT, cytochrome c and UCP2. Blots were generally of such a quality that there were seldom other non-specific bands. Moreover, if additional bands were detected they were usually located far from the size of the band expected. Recently, another researcher in our laboratory has shown localization of UCP2 to the mitochondrial membranes and matrix by immunohistochemistry of ultra-thin sections of mouse heart tissue (A Chan, unpublished data). All blots were normalized to VDAC1 to correct for loading and expression levels quantitated by densitometric analysis.

In a separate set of experiments all the above-mentioned endpoints were determined after the reoxygenation period (45 minutes of anoxia followed by 7 minutes of reoxygenation) (section 2.6.1).

3.3 Statistics

Results are expressed as mean \pm SEM. Significance ($p < 0.05$) was determined for discrete variables by Students' unpaired t-test, Welch corrected for possibly different standard deviations.

3.4. Results

3.4.1 Characterization of protective phenotype

Densitometric analysis of the TTC stained ischemia-reperfused hearts revealed a 40% decrease in infarct size in response to 45 minutes of global ischemia / 45 minutes of reperfusion in hearts overexpressing activated PKC ϵ compared to wildtype hearts (32% vs. 19% when expressed as percentage of area at risk; $p < 0.003$) (Fig. 3-1).

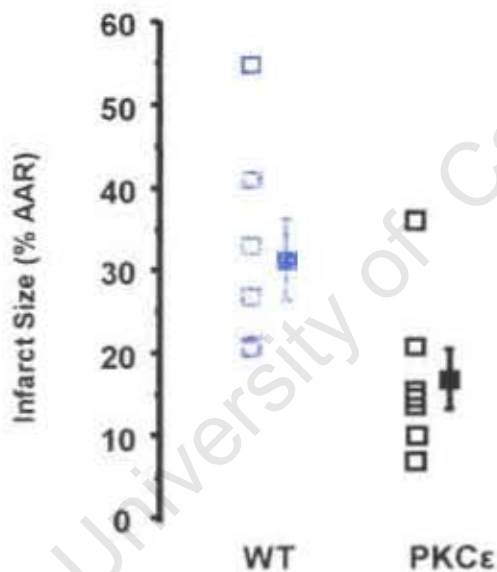


Figure 3-1. Infarct size in response to ischemia-reperfusion

There was a significant reduction in infarct size in activated PKC ϵ mouse hearts in response to ischemia reperfusion, expressed as a percentage of the area at risk ($p < 0.003$). Isolated perfused hearts were exposed to 45 minutes global ischemia and 45 minutes reperfusion. Infarct size was then determined by TTC staining of the whole heart, which was then frozen and sliced into 1.5-2 mm thick slices and scanned for densitometric analysis of the infarct as a proportion of the area at risk ($n=12$).

PKC ϵ overexpressing hearts were functionally identical to WT control littermates measured in retrogradely perfused hearts paced at 600 bpm (coronary flow, developed force, resting tension) (Fig. 3-2)(Table 3-1).

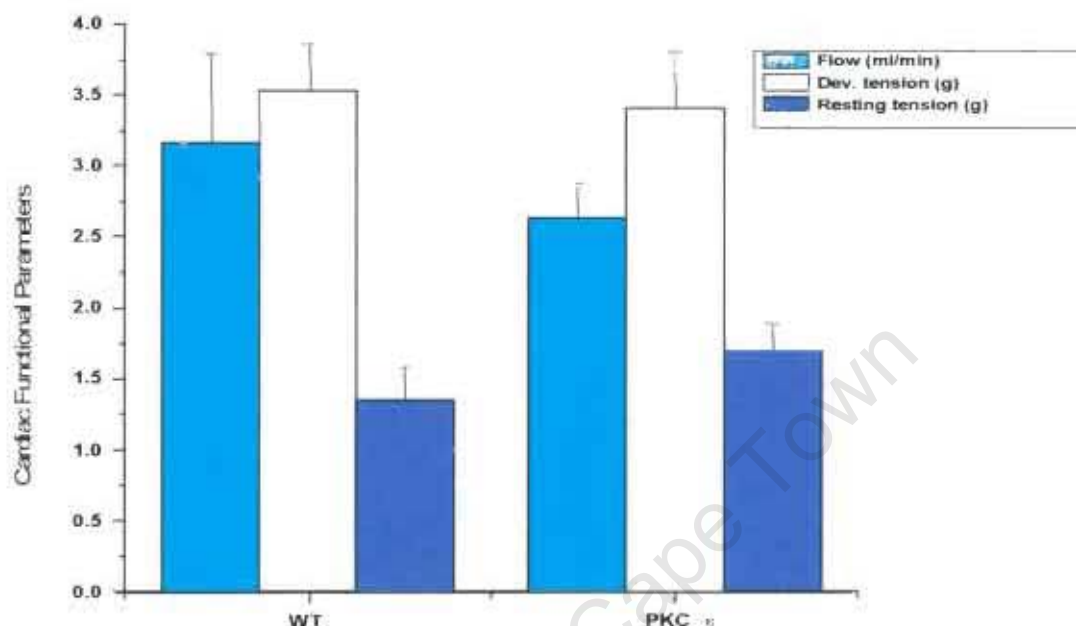


Figure 3-2. Assessment of baseline cardiac function

Baseline cardiac function was assessed on retrogradely perfused isolated mouse hearts. Hearts were fastened by means of a suture through the apex to a lexan rod connected to a force transducer. The resting tension was set at 2 g and the hearts contracted against this force to create the measured developed tension. Coronary effluent was collected at the start, halfway (after 10 minutes) and at the end of the perfusion experiments (20 minutes). As a representation of the complete perfusion experiment, values are given only for the 10 minute perfusion time point (n=8).

	Wildtype	PKC ϵ
PSP (mmHg)	76.9 \pm 0.8	74.9 \pm 1.6
HR (beats/min)	337 \pm 14	330 \pm 14
AF (ml/min)	9.8 \pm 0.6	9.4 \pm 0.5
CF (ml/min)	3.3 \pm 0.4	2.7 \pm 0.2
CO (ml/min)	13.1 \pm 0.8	12.1 \pm 0.6
RPP	25960 \pm 1305	24883 \pm 1447

Table 3-1. Working heart baseline cardiac function assessment

These measurements were performed on isolated working mouse hearts and there were no significant differences between the groups (n=7 for WT and n=9 for aPKC ϵ)
PSP= systolic pressure; HR= heart rate; AF= aortic flow; CF= coronary flow; CO=cardiac output;
RPP= rate pressure product.

There was no evidence of hypertrophy (Fig. 3-3a) or a change in body weight (Fig. 3-3b) in aPKC ϵ compared to WT mice.

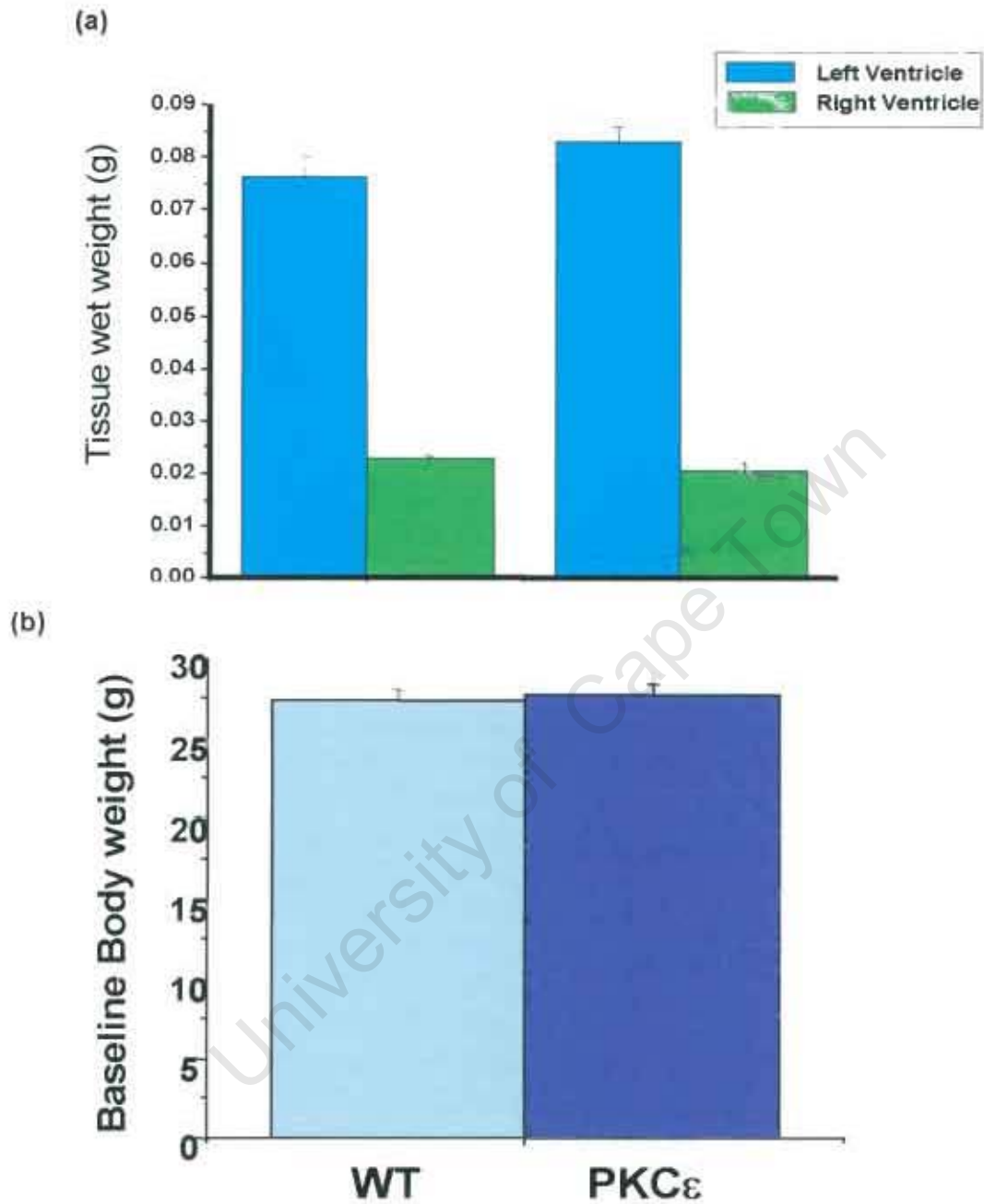


Figure 3-3a & 3-3b. Comparison of PKC ϵ overexpressing baseline heart and bodyweights with WT
There was no significant difference in heart and body weights between the two groups (n=12)

3.4.2 Mitochondrial functional phenotype

At baseline, we found no significant changes in mitochondrial respiratory parameters between PKC ϵ overexpressing and WT mice (Table 3-2).

	State 3 natomO ₂ /min/mg protein	State 4 natom O ₂ /min/mg protein	RCI	ADP/Δt nmol ADP/sec/mg protein	ADP/O nmol ADP/ natom O ₂ /mg protein
WT	186 \pm 46	28 \pm .06	7.10 \pm .44	256 \pm 71	5.82 \pm 1.27
APKC ϵ	217 \pm 54	24 \pm .05	7.5 \pm .68	306 \pm 97	7.79 \pm 3.10

Table 3-2. Basal mitochondrial respiratory parameters

State 3 respiration is mitochondrial oxygen consumption stimulated by ADP and reflects the conversion of ADP to ATP in the presence of adequate oxygen. State 4 respiration represents mitochondrial oxygen consumption after ADP phosphorylation is complete. ADP/ Δ t represents the quantity of ADP phosphorylated per second during state 3 respiration and ADP/O is the ratio between the nanomoles of ADP phosphorylated and the nano atoms of oxygen consumed during state 3. (n = 12 for all measurements).

Two distinct potentiometric dyes i.e. DiOC6 and JC-1 (see section 2.3.8) were utilized to measure the inner mitochondrial membrane potential. Suitable controls (CCCP and oligomycin, section 2.3.8) were used to ensure that measurements taken actually corresponded to changes in membrane potential. There was significant hyperpolarization of the inner mitochondrial membrane in the aPKC ϵ group compared to their wildtype littermate controls (p<0.003 for DiOC6; p<0.0001 for JC-1) (Fig. 3-4).

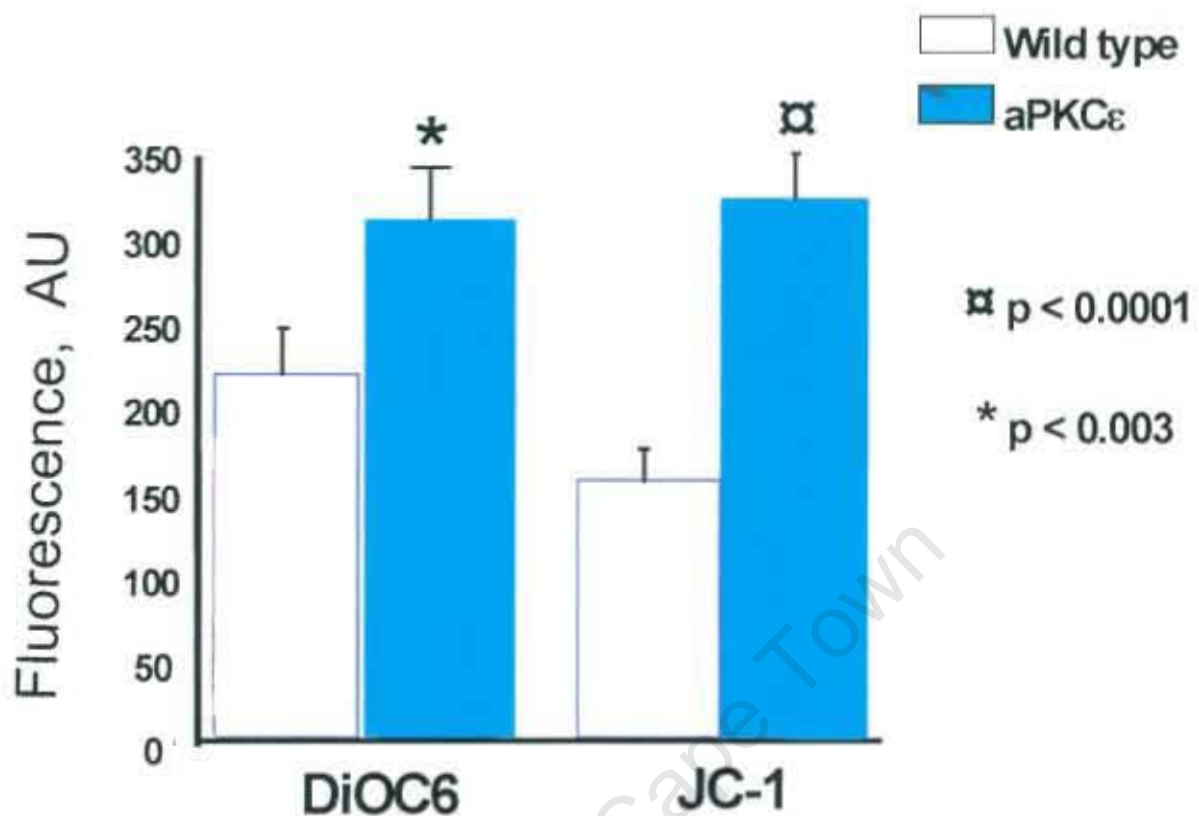


Figure 3-4. Baseline mitochondrial membrane potential

DiOC6 and JC-1 are two potentiometric dyes specifically utilized for measurement of mitochondrial membrane potential. Activated PKC ϵ mitochondria exhibited significant hyperpolarization of the inner mitochondrial membrane compared to the wildtype littermate controls with both dyes, indicating increased potential to generate ATP. α $p < 0.0001$, * $p < 0.003$, (n=8).

ANT is a key component in maintenance of intracellular bioenergetics (chapter 1) as it imports ADP into the mitochondrion for phosphorylation whilst exporting ATP to the cytosol. Preservation of ANT functional content would therefore be important during oxygen lack for e.g. ischemia or anoxia. ANT is also a potential target for PKC ϵ , being a component of the MPTP, whence PKC ϵ translocates when activated. Thus, we assessed functional ANT content in aPKC ϵ mice vs.

wild types at baseline. Here, ANT functional content was similar between the two groups (Fig. 3-5).

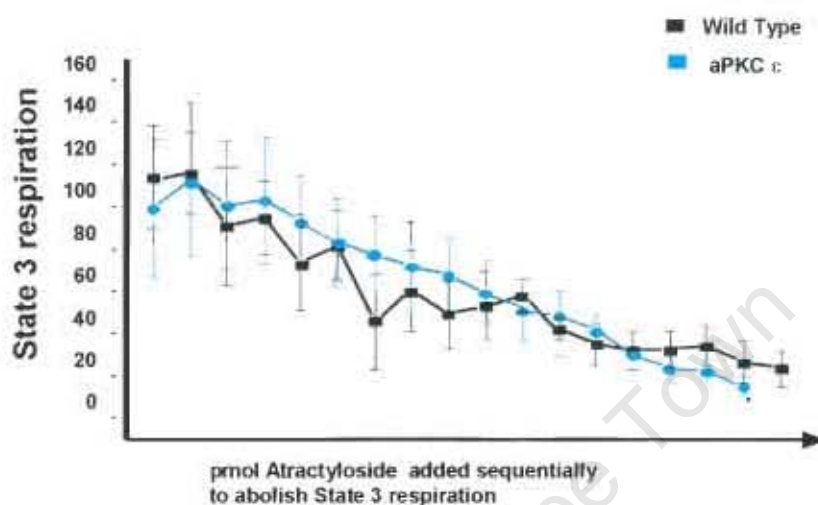


Figure 3-5. Baseline functional adenine nucleotide translocator (ANT) content

Atractyloside binds to ANT in the inner mitochondrial membrane in a one-to-one ratio, fixing the ANT in the inactive "c" conformation and inhibiting its biological action as an ADP importer/ATP exporter. As the dose of atractyloside increases and more ANTs are inactivated, the respiration rate drops continuously until respiration ceases when all ANT has been inactivated. The quantity of atractyloside required to completely abolish state 3 respiration is an index of the amount of functionally active ANT present in each population of mitochondria (n=12).

Increased ATP levels may also result from decreased ATP hydrolysis. In light of this we also determined levels of inorganic phosphate (P_i), the by-product of ATP hydrolysis. No difference was found in the inorganic phosphate levels between the two groups at baseline (Fig. 3-6). However, addition of oligomycin ($1\mu\text{g/ml}$) (inhibitor of ATP synthase) to the assay mixture lead to decreased P_i levels in the wildtype mitochondria but not the aPKCε mice ($p < 0.03$ aPKCε vs. wildtype) (Fig.

3-6). Oligomycin inhibits ATP synthase (enzyme catalyzing ATP formation) but not F1F0 ATPase (enzyme catalyzing ATP breakdown). Increased inorganic phosphate in the wildtype mitochondria is not surprising, as the existing ATP is hydrolyzed to maintain intracellular bioenergetics. However, the α PKC ϵ protective program ensures maintenance of mitochondrial ATP synthesis despite the oligomycin-induced inhibition of ATP synthase. I speculate that this may occur by PKC ϵ preventing the oligomycin-induced inhibition of ATP synthase. Alternatively, it may prevent the action of F1F0 ATPase.

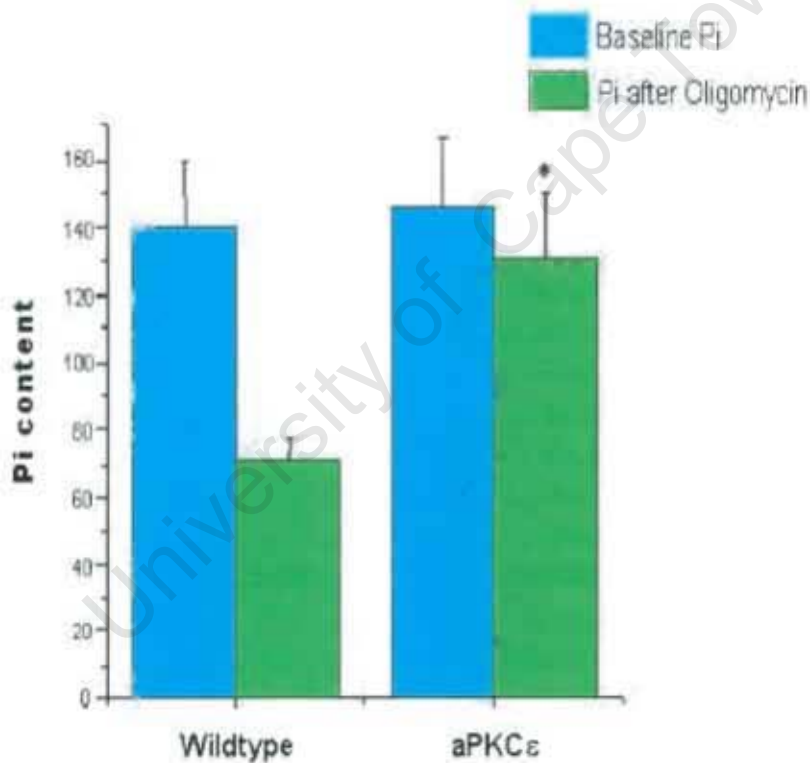


Figure 3-6. Baseline inorganic phosphate (P_i) levels in isolated mitochondria

There was no significant difference in the basal levels of P_i. However, after oligomycin exposure there was a significant reduction in the P_i levels of the wildtype mitochondria (*p < 0.03), whereas levels were maintained in the α PKC ϵ population. This indicates an enhanced capacity in the α PKC ϵ mice to produce mitochondrial ATP (n=6).

In agreement, the activated PKC ϵ mitochondria displayed increased rate of ATP synthesis at baseline compared to wildtype littermate controls ($p < 0.0001$ at time zero, $p < 0.003$ for all the other time points) (Fig. 3-7).

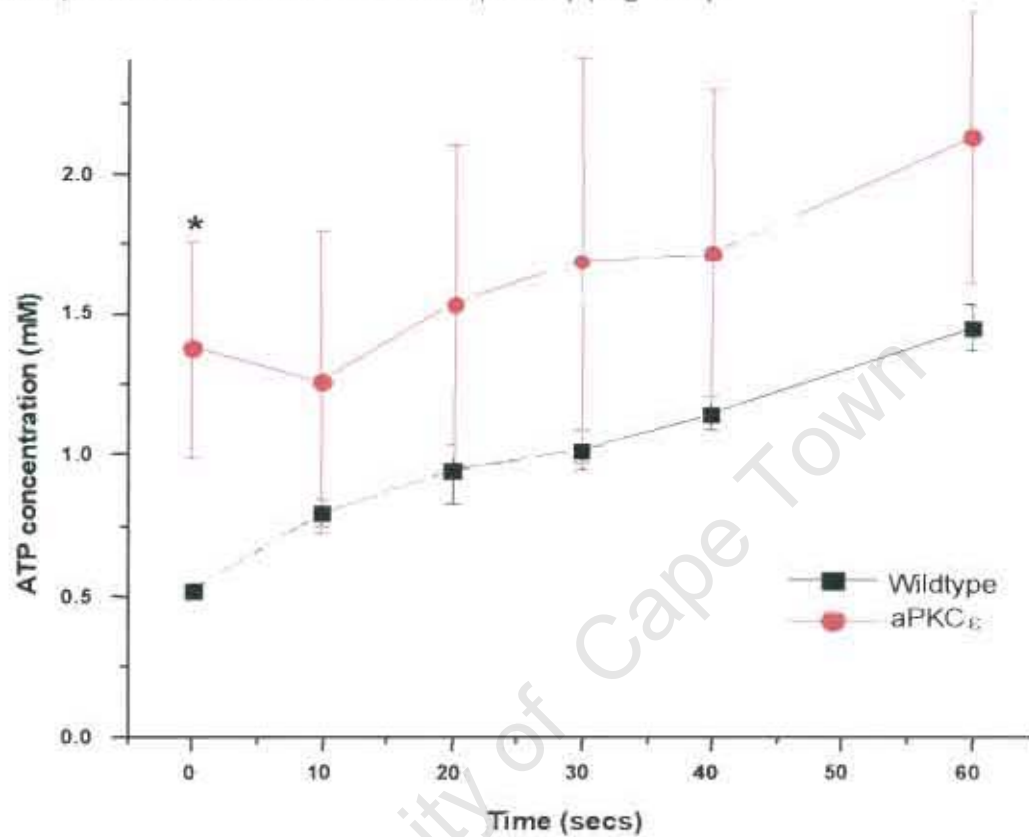


Figure 3-7. Baseline rate of ATP synthesis

Rate of ATP synthesis was measured in isolated unstimulated mitochondria, using a luciferin-luciferase assay method according to the method of Budnikhov.[88]. Rates were similar, but the activated PKC ϵ mice had a higher overall concentration of ATP (* $p < 0.0001$ at time zero, $n = 5$).

To gain some insight into mechanisms underlying these observations, we also determined expression levels of peptides regulating intracellular bioenergetic capacity. At baseline, cytochrome c, VDAC1, ANT1 and UCP2 peptide levels were not significantly altered (Figs. 3-8a - 3-8d). These findings were confirmed by densitometric analysis (data not shown).

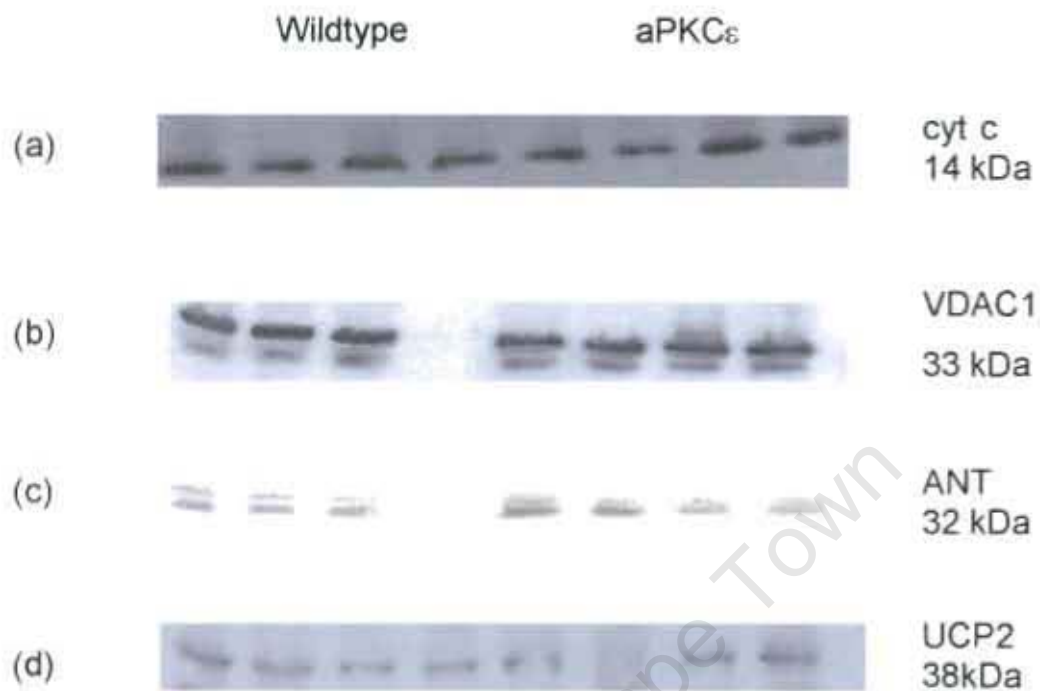


Figure 3-8. Representative baseline Western blot of mitochondrial regulatory proteins

Mitochondrial protein was extracted and mixed 1:1 with low-ionizing sample buffer plus a complete inhibitor cocktail to prevent proteases damaging proteins. Sixty micrograms of mitochondrial proteins were loaded per lane and run on a 7.5% polyacrylamide gel for approximately 1 hour at 160 volts, to ensure good separation of the target proteins. There was no discernible difference in protein levels of the selected pore component proteins between the two groups (n=6).

3.4.3 Acute Oxidative Stress

I then proceeded to investigate mitochondrial bioenergetic capacity of aPKC ϵ mitochondria in response to anoxia-reoxygenation. After state 4 steady state respiration had been reached, isolated mitochondria were subjected to excess ADP (100 mM), thereby increasing respiration until all the oxygen in the

polarographic chamber had been utilized. The chamber was then sealed. This resultant "anoxic" state was utilized to mimic anoxia. Mitochondria were exposed to either 45 minutes of anoxia, or 45 minutes of anoxia followed by 7 minutes of reoxygenation. At reoxygenation (7 minutes of reoxygenation following 45 minutes of anoxia) the activated PKC ϵ mitochondria exhibited 44% recovery of state 3 respiration, compared to only 28% in the WT ($p < 0.001$) (Fig. 3-9).

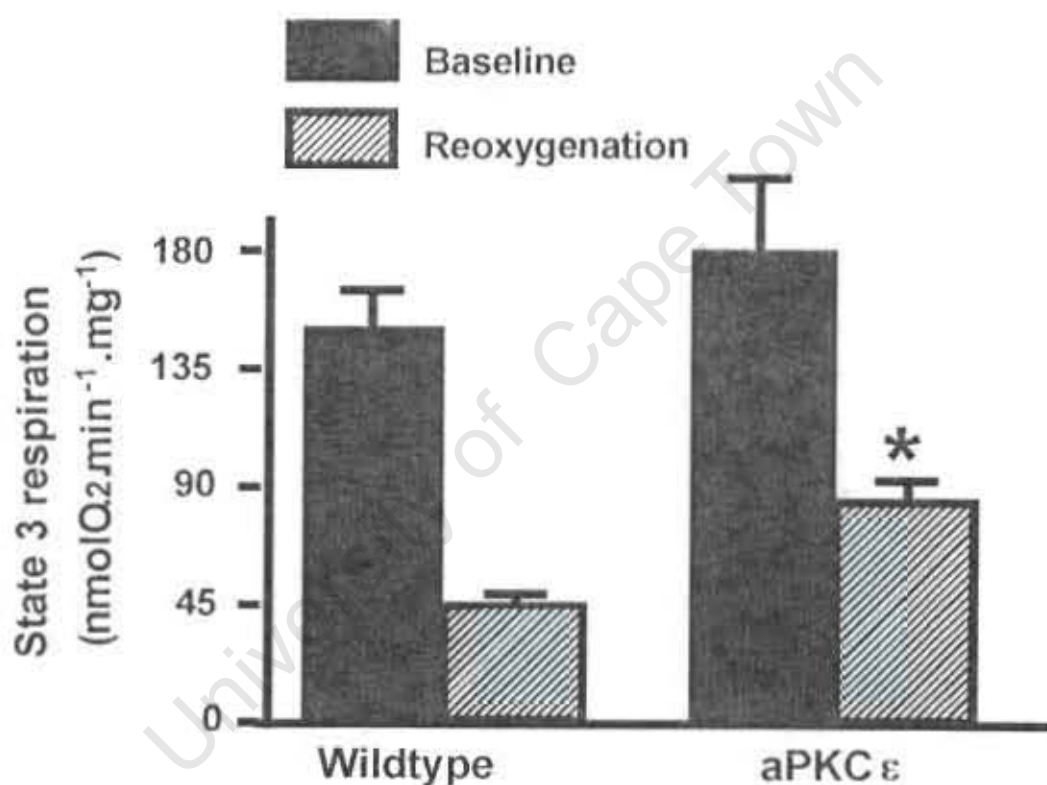


Figure 3-9. Mitochondrial respiration after excess ADP-induced anoxia and reoxygenation

Basal respiration levels were measured as previously described. After state 4 respiration had been reached, anoxia was induced in the chamber by the addition of 100 mM ADP, forcing mitochondria to continue to respire and exhaust all the oxygen in the chamber. The chamber was then sealed and the anoxia maintained for 45 minutes, followed by 7 minutes of reoxygenation. State 3 respiration was re-measured after "reoxygenation" and expressed as a percentage of the basal state 3 respiration. The aPKC ϵ mitochondria were more resistant to this stress ($*p < 0.03$ vs. wildtype), as indicated by improved recovery of state 3 respiration after reoxygenation ($n = 8-14$).

The hyperpolarization exhibited at baseline by the activated PKC ϵ mitochondria was maintained after 45 minutes of anoxia compared to the wildtype (* $p < 0.001$ for JC-1 dye) (Fig. 3-10).

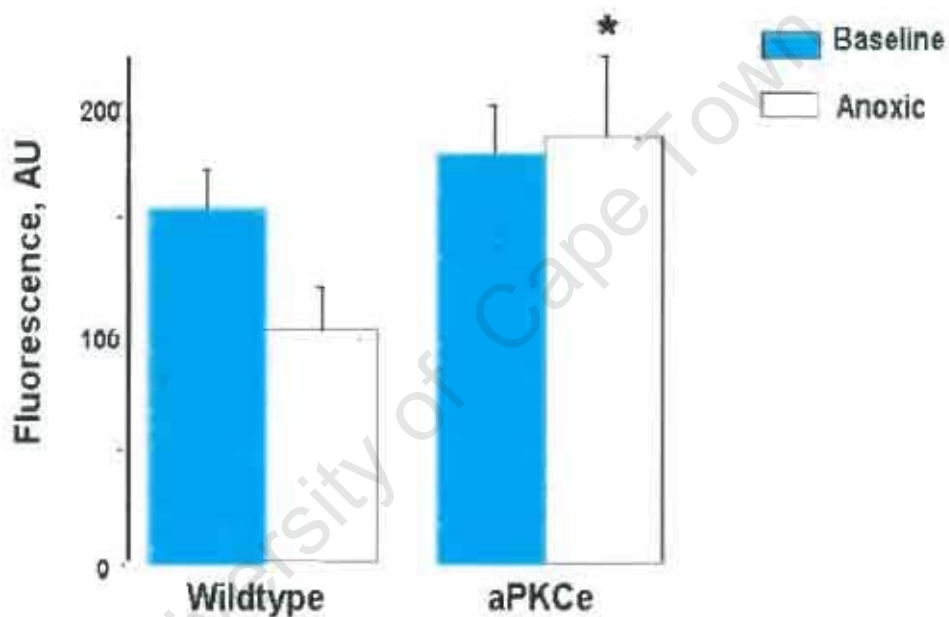


Figure 3-10. PKC ϵ overexpressing mice maintain mitochondrial membrane potential in response to excess ADP-induced anoxic stress (JC-1)

Mitochondrial membrane potential was measured immediately after the 45-minute anoxic period using the potentiometric dye JC-1. Mitochondria were aspirated from the polarographic chamber and injected under mineral oil into a reaction vessel to maintain the anoxic environment. The mitochondria were then loaded with dye and membrane potential measured as quickly as possible on the fluorescence-activated cell sorter. There is a significant reduction in inner mitochondrial membrane potential in the wildtype population after the anoxic insult compared to aPKC ϵ (* $p < 0.003$ vs. WT, $n=8$).

In agreement, membrane potential was also maintained after anoxia-reoxygenation when using a second potentiometric dye i.e. DiOC6 ($p < 0.001$ vs. WT) (Fig. 3-11). These data suggest reduced membrane permeability transition and MPTP opening in the PKC ϵ mice.

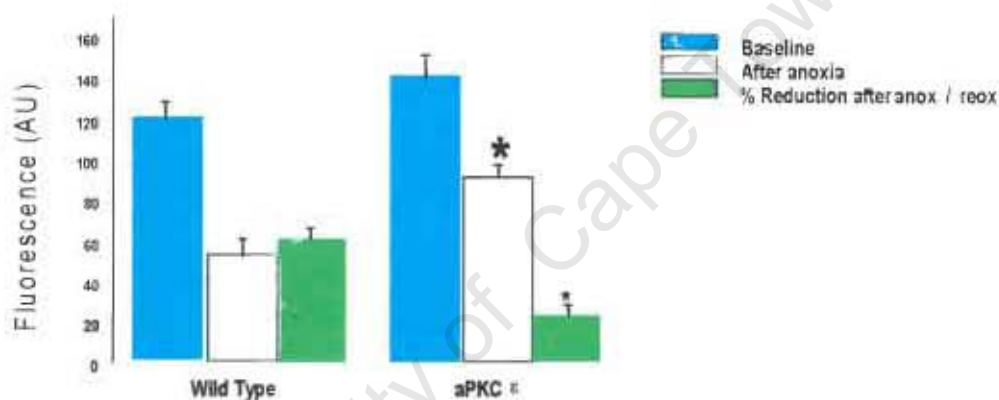


Figure 3-11. PKC ϵ overexpressing mice maintain mitochondrial membrane potential in response to excess ADP-induced anoxia/reoxygenation stress (DiO6)

Mitochondrial membrane potential was measured using the potentiometric dye DiOC6 immediately after the 45-minute anoxia-7 minute reoxygenation period. Mitochondria were loaded with dye and membrane potential measured as quickly as possible on the fluorescence-activated cell sorter. Mitochondrial inner mitochondrial membrane potential decreased in the WT population after anoxia reoxygenation, compared to their PKC ϵ overexpressing littermates. This coincides with the maintained state 3 respiration in the PKC ϵ mice after the anoxic insult, compared with the WT mitochondria. (* $p < 0.001$ vs. WT, $n=8$).

Further evidence for reduced MPTP in the aPKC ϵ mice is provided by the ANT functional content data. Here, ANT functional content was maintained in the aPKC ϵ mitochondrial population ($p < 0.0001$ vs. WT) (Fig. 3-12) following anoxia-reoxygenation, while decreasing in the WT littermate mitochondria.

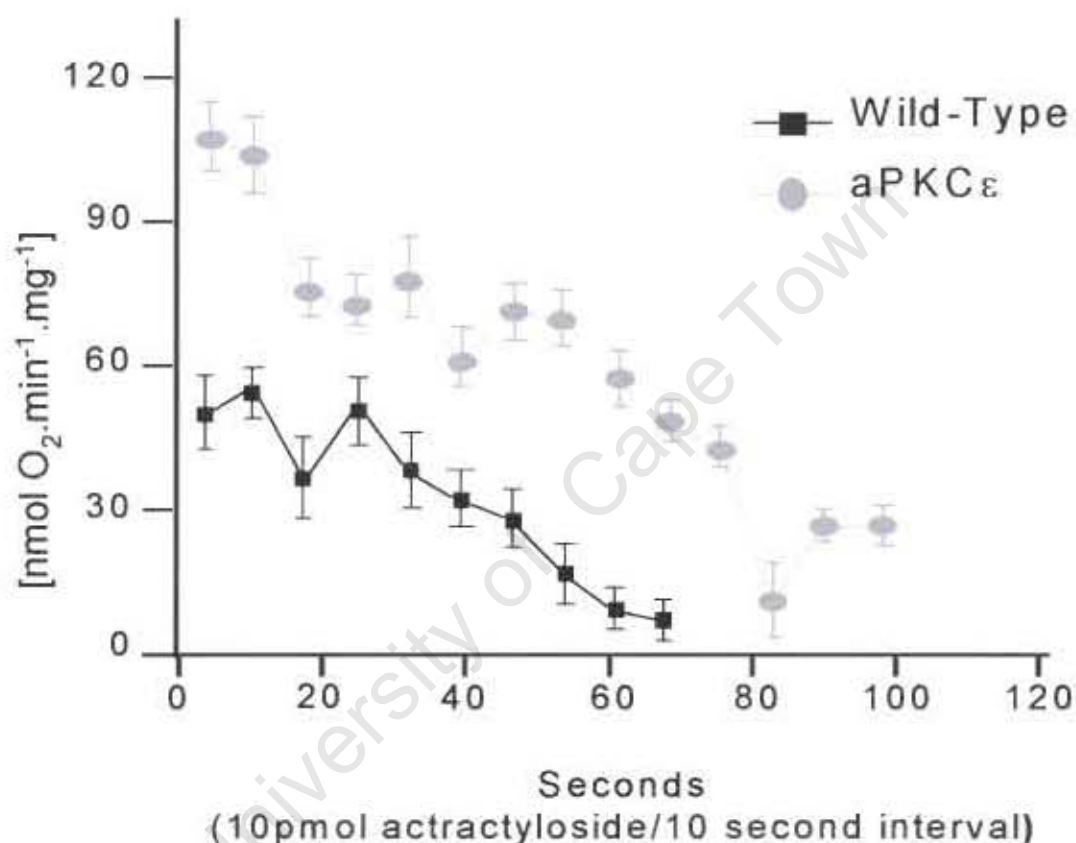


Figure 3-12. Functional ANT content after ADP-induced anoxic stress

Atractyloside binds to ANT in a one-to-one ratio, fixing the ANT in the inactive "c" conformation and inhibiting its biological action as an ADP importer-ATP exporter. As the dose of atRACTYLOSIDE increases and more ANTs are inactivated, the respiration rate drops, until respiration ceases. The quantity of atRACTYLOSIDE required to completely abolish state 3 respiration is an indication of the amount of functionally active ANT present in each population of mitochondria. More atRACTYLOSIDE was required to completely abolish state 3 respiration in the aPKC ϵ mitochondrial population after anoxia-reoxygenation than in the WT ($p < 0.0001$). This correlates with a higher functional ANT content and reinforces our finding of increased state 3 respiration as well as an increased ability to synthesize ATP after the anoxia-reoxygenation stimulus ($n=6$).

Moreover, after anoxia-reoxygenation the activated PKC ϵ mitochondria retained their ability to synthesize ATP, whereas the rate of ATP synthesis was reduced in the wild type mitochondria subjected to the same anoxic stress ($p < 0.03$ vs. WT) (Fig. 3-13).

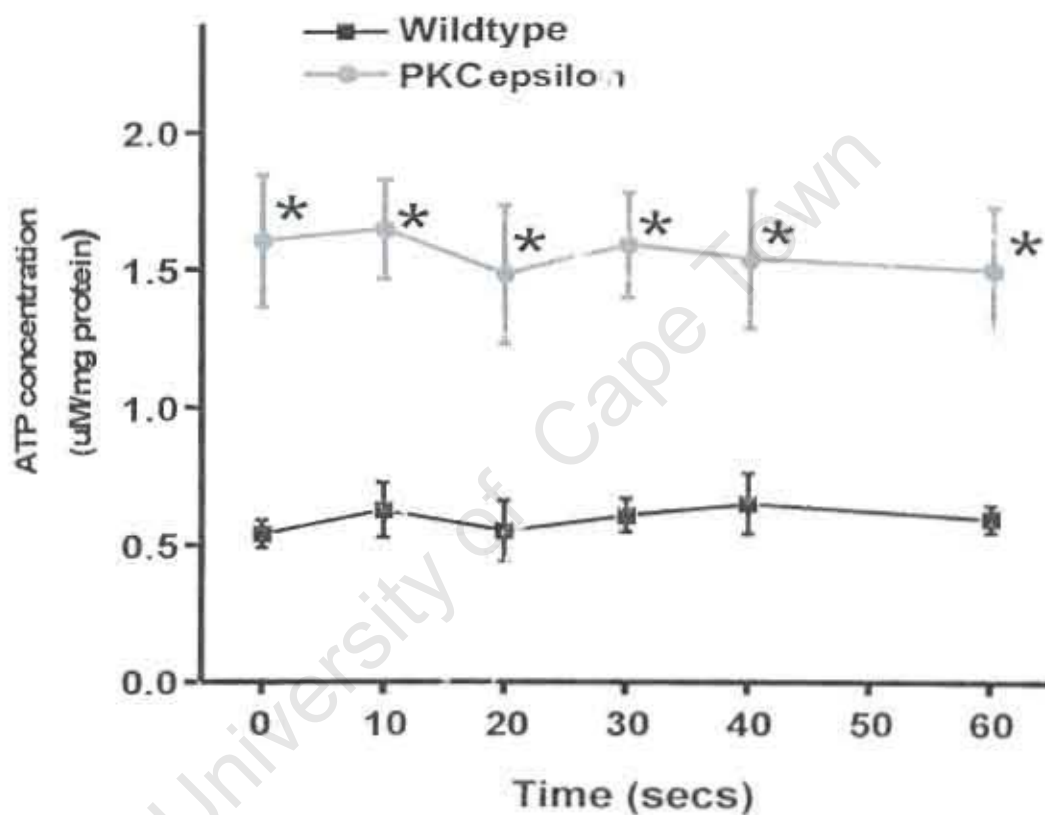


Figure 3-13. Rate of mitochondrial ATP synthesis after ADP-induced anoxia/reoxygenation stress

Rate of ATP synthesis was measured by luciferin-luciferase luminometry, according to the method of Budnikhov.[48]The activated PKC ϵ mice produced significantly more ATP subsequent to an ADP-induced anoxia/reoxygenation stimulus than corresponding wildtype littermate controls ($p < 0.03$ for each time point, $n=6$).

Cytochrome c is a component of the electron transport chain, situated in the inter-mitochondrial membrane space. When mitochondria undergo membrane permeability transition pore opening and the matrix swells due to unregulated influx of solutes, the outer membrane ruptures and cytochrome c is lost into the cytosol. Loss of cytochrome c adversely affects oxidative phosphorylation and is a useful indirect marker of MPTP opening. We demonstrated earlier that protein levels of cytochrome c at baseline were similar (Fig. 3-8a). However, after ADP-induced anoxia/reoxygenation there were decreased cytochrome c levels in the wildtype compared with to the aPKC ϵ mitochondrial extract ($p < 0.002$) (Figs. 3-14 and 3-15).



Figure 3-14. Mitochondrial cytochrome c protein levels

There was no difference in the basal mitochondrial cytochrome c content of either group (Figure 3-8a). There was, however, a significant difference in cytochrome c content in the mitochondria of constitutively activated PKC ϵ mice after the ADP-induced anoxia/reoxygenation stress, compared to the WT population. ($p < 0.0002$) Loss of cytochrome c from within the mitochondria is indicative of membrane permeability transition and pore opening, meaning that WT mitochondria had more damage as a result of the insult. The activated PKC ϵ mitochondria retained their cytochrome c, therefore were protected against membrane permeability transition and pore opening ($n=6$).

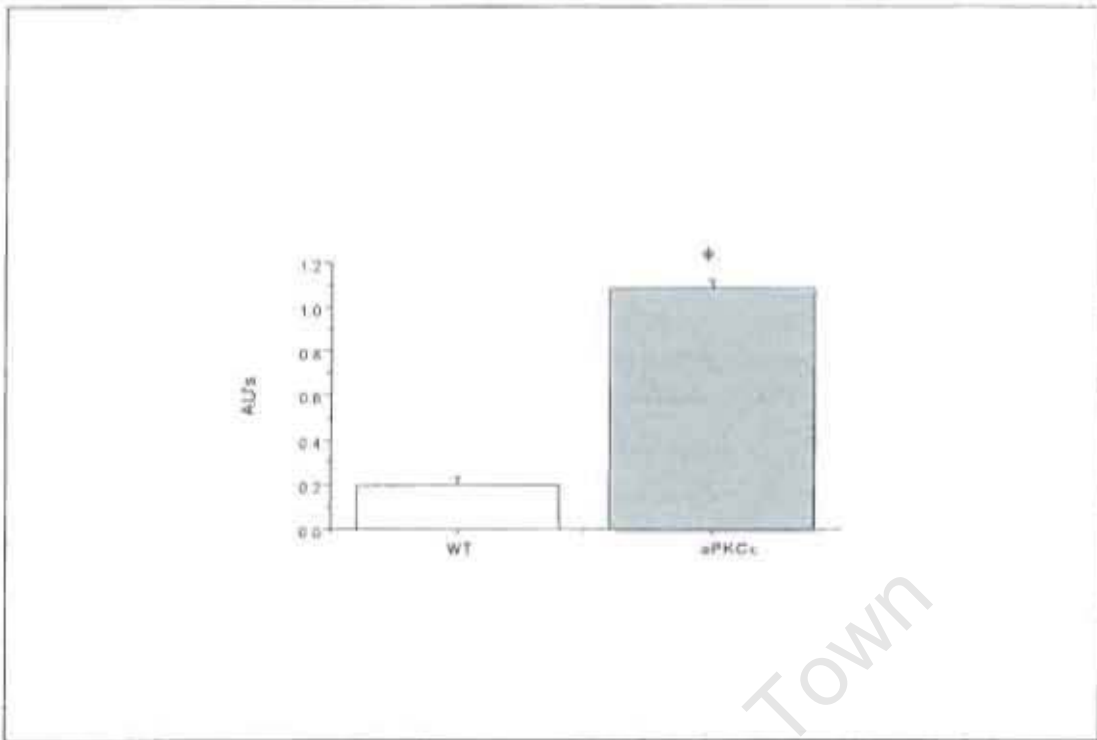


Figure 3-15. Densitometric analysis of cytochrome c levels

The Western blots performed after anoxia-reoxygenation (Figure 3-14) were scanned and analyzed densitometrically. Each sample was normalized for loading to VDAC1. There was a reduction in the quantity of cytochrome c in the wildtype mitochondria compared to the activated PKC ϵ mice, indicating greater release into the supernatant after anoxia/reoxygenation ($p < 0.0002$). AU – arbitrary units

3.5 Discussion

The major findings reported in this chapter are as follows:

1. Hearts from PKC ϵ overexpressing mice are cardioprotected, having a 40% reduction in infarct size compared to wildtype hearts subjected to similar ischemia/reperfusion stress.
2. PKC ϵ overexpressing hearts subjected to retrograde Langendorff perfusion or working heart perfusion were functionally identical to WT

littermate controls. Furthermore, at baseline aPKC ϵ and WT mice had similar right and left ventricular as well as body weights.

3. At baseline, mitochondria isolated from mice overexpressing constitutively active PKC ϵ possess:

- Identical functional parameters to wildtype (similar state 3 and 4 respiration, ADP/ Δt , ADP/O ratio).
- Hyperpolarized mitochondrial membrane potential
- Similar peptide levels for the key mitochondrial proteins measured (ANT, VDAC1, cytochrome c, UCP2)
- Similar functional ANT content
- Increased ATP rate of synthesis

4. PKC ϵ mitochondria subjected to an ADP-induced anoxic stress, followed by reoxygenation exhibited:

- Increased recovery of respiration after exposure to anoxia and to anoxia-reoxygenation
- Maintained hyperpolarization of inner mitochondrial membrane
- Increased functional ANT content
- Increased rate of ATP synthesis
- Increased retention of cytochrome c

These findings were sufficiently novel to merit publication as a brief communication in *Journal of Molecular and Cellular Cardiology*. [130]

Reduction in infarct size

To confirm that overexpression of cardiac-specific activated PKC ϵ resulted in a protected cardiac phenotype, TTC staining was employed to assess infarct size. PKC ϵ mice exhibited a marked reduction in infarct size (Fig. 3-1), indicating that overexpression of PKC ϵ had conferred protection against an acute ischemia-reperfusion insult. However, it should be borne in mind that this method of estimating ischemia-reperfusion damage may have limitations since it relies on detection of NADH to indicate living tissue. The temperature at which the staining is done is also very important and may lead to errors if not strictly adhered to. Despite these limitations, estimation of infarct size by TTC staining is an accepted method to quantitate the degree of ischemia-reperfusion damage.[59, 64, 177] Our data are in agreement with others who showed improved functional recovery after ischemia reperfusion in mice overexpressing PKC ϵ mice.[69, 179, 180]

Baseline cardiac function

It has been previously reported that modest cardiac-specific overexpression of PKC ϵ results in concentric compensated hypertrophy and a degree of hypercontractility at 9-12 weeks of age.[161] In light of this, I next established whether the contractile function of the PKC ϵ overexpressing mice was similar to wildtype control mice. The data show that contractile function was not altered in aPKC ϵ mice (Fig. 3-2). Furthermore, aPKC ϵ mice exhibited no hypertrophy (Fig. 4-3a and b) at baseline. However, I realize that the method employed to

estimate cardiac function is a limitation of this study i.e. developed force is not ideal. Ideally, we would have preferred to determine cardiac contractile function using pressure volume loops. The equipment to perform this technique is presently not available to us, so these measurements were performed by Dr Ellen Aasum of the University of Tromso in Norway, as part of a collaborative agreement. The more sophisticated methods also showed no functional difference at baseline between the WT and aPKC ϵ hearts. Similarly, additional parameters are required to confirm our ventricular weight measurements as an index of cardiac hypertrophy. In future, we are planning to determine the expression levels of atrial natriuretic peptide (ANP), a well-known gene marker of cardiac hypertrophy.

Mitochondrial phenotype at baseline

Baseline function was similar in mitochondrial populations isolated from hearts of either group, suggesting no difference in basal mitochondrial phenotype. However, mitochondrial membrane potential ($\Delta\psi_m$) measurements demonstrated that mitochondria from the PKC ϵ overexpressing mice were hyperpolarized compared to wildtype controls. Since a hyperpolarized inner mitochondrial membrane indicates a higher proton concentration in the intermembrane space (proton-motive force), our data suggest that PKC ϵ overexpressing mice possess an enhanced ATP generating capacity at baseline. In agreement, we found that hyperpolarized mitochondria from the PKC ϵ transgenic mice produced more mitochondrial ATP than their wildtype littermates, as shown by the baseline rate

of ATP synthesis measurements. To investigate the mechanisms underlying increased bioenergetic capacity in PKC ϵ transgenic mice, functional ANT content was measured. Here, the functional ANT content in both mouse strains was similar. Since increased ATP levels may also result from decreased ATP hydrolysis we next determined inorganic phosphate (P_i) levels, a by-product of ATP hydrolysis. Again, we found no difference between PKC ϵ transgenic mice and wildtype controls. However, the addition of oligomycin caused a significant decrease in P_i levels in the wildtype mitochondria compared to aPKC ϵ mitochondria. Oligomycin inhibits ATP synthase (catalyzes production of ATP from ADP), but has no effect on F1F0 ATPase (catalyses ATP hydrolysis). These data indicate decreased ATP turnover in the wildtype mitochondria, which could be an attempt to conserve intracellular energy stores. Subsequently expression levels of several mitochondrial regulatory peptides were measured in PKC ϵ transgenic and wildtype control mice. Cytochrome c, VDAC1, ANT1 and UCP2 peptide levels were similar in both groups. Thus, the increased rate of ATP synthesis could not be attributed to increased levels of a number of functional proteins involved in mitochondrial ATP production.

Mitochondrial phenotype after exposure to an acute ADP-induced anoxic stress

As activated PKC ϵ overexpression enhanced myocardial tolerance to acute ischemia and also possessed hyperpolarized mitochondria, I hypothesized that mitochondria from the mice overexpressing activated PKC ϵ would also be more resilient to an ADP-induced anoxic stress. Here, aPKC ϵ overexpressing mouse

mitochondria displayed improved ADP-dependent respiration after anoxia and also anoxia/reoxygenation, recovering to 40% of baseline compared to the wildtype that showed only 18% recovery. Hyperpolarization of the inner mitochondrial membrane and ANT functional content was sustained during this time compared to wildtypes.

When mitochondria undergo membrane permeability transition (MPT), the pore opens and the inner mitochondrial membrane loses its electric potential, meaning the proton motive force is reduced and hence also the ability to produce ATP.[181] In this instance, ANT has undergone irreversible conformational change and is no longer functional, resulting in increased influx of solutes into the matrix and rupture of the outer mitochondrial membrane, with release of cytochrome c into the cytosol.[90] Cytochrome c is an important component of the electron transport chain, hence oxidative phosphorylation and ATP production is impaired following loss of cytochrome c. In addition, its release into the cytosol may lead to the recruitment of caspases and initiate an apoptotic cascade, committing the cell to programmed death. At baseline there was no difference in cytochrome c peptide levels. However increased cytochrome c levels were found in the aPKC ϵ mitochondria after the anoxic stimulus, indicating that, unlike wildtypes, aPKC ϵ mitochondria had not lost cytochrome c through MPT.

These findings are based on the use of isolated mitochondria i.e. separated from other relevant signaling pathways. Therefore, one may argue that it would be

more physiological to have used skinned fiber bundles or permeabilized cells in this instance. However, activated PKC ϵ is translocated to the mitochondrion and its protective effects at this location are an inherent part of the hypothesis put forward in this study. Percoll gradient purification of the mitochondrial fraction did not dislodge PKC ϵ from the mitochondria, nor alter its activity, leading to the speculation that maybe PKC ϵ is situated in the inner membrane space, or else very strongly bound to the outside.[182] Indeed, employing whole permeabilized cells or skinned muscle bundles may have limited the exploration of the PKC ϵ protective mechanisms. Since there is lack of clarity regarding this issue, permeabilized cells, skinned fibres and isolated cardiomyocytes may form part of the future research plans for this interesting signaling molecule.

In summary, my data show that PKC ϵ plays a pivotal role in cardioprotection in response to an acute stress. The data suggest that PKC ϵ translocates to the mitochondrion where it phosphorylates VDAC1 resulting in hyperpolarized mitochondria and reduced MPTP opening. Moreover, we propose that PKC ϵ plays a role in maintenance of ANT functional activity. Together, these adaptations increase mitochondrial ATP synthesis capacity, thereby providing cardioprotection to the organism in response to acute stress. Although we did not actually determine PKC ϵ subcellular distribution in this study, others have previously reported this. One of the earliest references to address the issue of subcellular redistribution of PKCs upon activation was Ping et al.[69] This study showed differential translocation of different PKC ϵ isoforms to the particulate

fraction upon stimulation by preconditioning, but did not pinpoint the location of PKC ϵ at this time. Baines et al. in 2003 [183] showed that activated PKC ϵ was translocated to the mitochondrion, where it interacted with components of the permeability transition pore. Recently, Costa et al.[182] showed that PKC ϵ is translocated to the mitochondria with activated PKC ϵ overexpression.

My data are in agreement with others who proposed that modulation of the mitochondrial permeability transition pore may be involved in ischemia/reperfusion injury[3] The precise mechanisms whereby PKC mediates cardioprotection are not completely delineated. However, Baines et al.[3] hypothesized that protein-protein interaction between PKC ϵ and mitochondrial pore components might modulate pore function and thus engender cardioprotection. Moreover, coimmunoprecipitation and GST-based affinity pull-down from mouse cardiac mitochondria showed interaction of PKC ϵ with components of the pore, namely VDAC, ANT, and hexokinase II (HKII). VDAC1, ANT1, and HKII were present in the PKC ϵ complex at ~ 2%, 0.2%, and 1% of their total expression, respectively [3]. In addition, *in vitro* studies demonstrated that PKC ϵ directly binds and phosphorylates VDAC1.[3] Incubation of isolated cardiac mitochondria with recombinant PKC ϵ also resulted in a significant inhibition of Ca²⁺-induced mitochondrial swelling, an index of pore opening.[3] Furthermore, cardiac-specific expression of active PKC ϵ in mice, which is cardioprotective, greatly increased interaction of PKC ϵ with the pore components and inhibited Ca²⁺-induced pore opening[3] In contrast, cardiac expression of

kinase-inactive PKC ϵ did not affect pore opening.[3] Lastly, administration of the pore opener atractyloside significantly attenuated the infarct-sparing effect of PKC ϵ transgenesis.[3] Collectively, these data demonstrate that PKC ϵ forms physical interactions with components of the cardiac mitochondrial pore, in turn inhibiting the pathological function of the pore and thereby contributing to PKC ϵ - induced cardioprotection. Our future work will include experiments to further investigate these interactions i.e. between PKC and MPTP constituents in the heart in response to acute oxygen lack.

3.6 Conclusion

Together, these data demonstrate that modest cardiac specific overexpression of constitutively active PKC ϵ results in enhanced bioenergetic capacity in response to acute anoxic stress. This biochemical response may occur, in part, via maintenance of ANT functional activity and prevention of MPTP opening in response to oxygen lack. These findings support the concept that therapeutic interventions that aim to conserve cardiac mitochondrial bioenergetic capacity hold significant promise to promote myocardial tolerance to ischemic injury.

Chapter 4

A Cardioprotective Role for Constitutively Active PKC ϵ in response to Chronic Hypobaric Hypoxia

4.1 Introduction

Hypoxia is caused by reduced supply of arterial oxygen to tissues and leads to an imbalance between oxygen supply and demand.[184] Some of the most common causes of hypoxia are:

1. **ischemic hypoxia**, due to a reduction in coronary blood flow.
2. **systemic hypoxia**, caused by a fall in arterial pO_2 .
3. **a combination of either 1 or 2 , or both , with an increased oxygen demand.**[185]

To sustain metabolism and energy homeostasis, organisms have developed various adaptive regulatory mechanisms to cope with acute and chronic hypoxia. The human body has five specific hypoxia-response mechanisms to deal with hypoxic stress.

Elevating O_2 uptake by lungs to compensate for O_2 shortage	[186]
Gas exchange efficiency in lungs increases	[187]
Increase in general vascular sensors (HIF-1, VEGF)	[188-190]
Increase in erythropoietin to increase red blood cell production	[191-193]
Transcriptional regulation of hypoxia sensitive genes e.g. glycolytic enzymes	[194-196]

Table 4-1: Hypoxia response mechanisms in the human body.

Exposure of non-acclimated mammals to these conditions leads to a period of acclimatization involving angiogenesis.[197,198] erythropoiesis.[199] switching preferential substrates for the heart from FAs to carbohydrates,[195,200] and hyperventilation.[196] The vasoconstrictive effect of hypoxia on pulmonary arteries results in pulmonary hypertension, thereby increasing load on the right ventricle.[186]

Similarly, in diseased states like chronic obstructive pulmonary disease, patients are also relatively hypoxic, due to pulmonary hypertension as a result of pulmonary artery constriction, making the heart work harder against an increased

pressure. In response to this persistent pressure stimulus, hearts enlarge (hypertrophy) in order to cope. To minimize cardiac damage due to hypoxia subjects hyperventilate, have increased heart rate and red blood cell count. The coronary vessels also dilate to maximize the oxygen reaching the heart.[185] At the molecular level, protective pathways are activated to ensure additional protection. For example, mitochondrial numbers increase via stimulation of transcriptional regulators activating the mitochondrial biogenesis gene program i.e. PGC-1 α and NRF-1 [201, 202]. Moreover, there is tighter coupling of mitochondrial respiration and increased efficiency of the respiratory enzymes.[131] Simultaneously there is a metabolic switch to enhanced anaerobic ATP production from glycolysis, rather than fatty acid oxidation[203-205], since glycolytic ATP is thought to maintain ion pumps and will prevent disruption of ion homeostasis [9].

Despite the apparently normal cardiac function with compensated hypertrophy, Meerson has defined several additional changes in the heart that are not readily evident.[206, 207]

1. There is an increase in myocardial mass without sufficient sympathetic nerve growth. This change predisposes to decreased norepinephrine release, associated with impaired contractility and relaxation occurring in the early phase of chronic hypoxia. Subsequently, myocardial signal transduction is impaired due to changes at the receptor level, G-coupled proteins and altered adenylyl cyclase functioning.

2. The enlarged myocardium is relatively hypoxic as the mass increase exceeds the heart's ability to vascularize this new tissue. Reserve capillaries are recruited to maximize blood flow and minimize the hypoxia.
3. Intracellular organelles like the myofibrils have poor energy provision and hence poor contraction, due to insufficient mitochondrial number compared to the tissue mass in the hypertrophied heart. This change leads to disturbance of energy homeostasis. [206,208]
4. There is a switch in contractile protein isoforms: the expression of myosin heavy chain α protein (adult isoform) is superseded by a switch to re-expression of myosin heavy chain β proteins (re-expression of fetal gene program), which gives improved contraction when oxygen is limited, but results in decreased contractile force. [209-211]

Adaptive changes in response to chronic hypoxia also include activation of intracellular signaling pathways. For example, activation of PKC ϵ has been reported for infants undergoing surgery for congenital cyanotic defects have hearts chronically perfused with hypoxic blood. Here, PKC ϵ is phosphorylated and translocated from the cytosol to the particulate fraction, along with activated p38 mitogen activated kinase (p38 MAPK). [212] In agreement, Rafiee et al. [212] found that the same kinases were activated and translocated in an experimental infant rabbit model of congenital hypoxia. Interestingly, these hearts displayed enhanced recovery (increased coronary flow and developed pressure) compared to normoxic controls in response to an ischemic insult. Treatment with specific inhibitors for PKC (chelerythrine) or p38 MAPK (SB203580) abolished the

protective effect. Thus, PKC ϵ was established as an upstream kinase activating p38 MAPK to confer protection during hypoxia and any subsequent ischemic stress.[212]

Recent studies have shown that PKC ϵ is also associated with the mitochondrion. For example, Baines et al.[3] have demonstrated co-localization of PKC ϵ with components of the mitochondrial permeability transition pore (MPTP). Moreover, they showed that PKC ϵ -mediated phosphorylation of a component of the MPTP, the voltage dependent anion channel 1 (VDAC1), leads to "stabilization" of the transition pore (closed conformation). In agreement, reconstituted mitochondrial membranes from mice overexpressing constitutively activated cardiac PKC ϵ showed resistance to MPTP opening.[3] These data agree with my earlier findings that mitochondria from PKC ϵ overexpressing mice are hyperpolarized at baseline (chapter 3). Furthermore, when subjected to an acute anoxic insult, mitochondria from mice overexpressing activated PKC ϵ maintain membrane potential and recover ADP-dependent respiration to a greater degree than matched wildtype littermates. Therefore, this protection in the transgenic mouse is probably due activated PKC ϵ translocating to the mitochondrion, maintaining membrane potential and bioenergetic capacity in response to reduced oxygen levels. These data have engendered my interest in PKC ϵ as a pivotal signaling intermediate in the chronically hypoxic heart, orchestrating cell survival programs.

It is unclear, however, how these protective mechanisms are activated in response to a chronic oxygen lack. In light of the above, our team hypothesized that mice overexpressing a constitutively activated form of PKC ϵ should be resistant to chronically reduced oxygen levels. To investigate this hypothesis, PKC ϵ overexpressing mice and their age-matched littermate controls were exposed to 7 or 14 days of hypobaric hypoxia (11% O₂) and various cardiac functional and mitochondrial respiratory parameters investigated.

4.2 Materials and Methods

4.2.1 Transgenic mouse model

Details of the mouse model have been previously described.[7] Briefly, transgenic mice exhibiting moderate cardiac-specific expression of a constitutively active mutant of PKC ϵ isozyme (aPKC ϵ) were used in parallel with littermate non-transgenic controls (WT). Mice were housed in the hypobaric hypoxic chamber and provided with food and water *ad libitum*. The chamber was opened once a week to provide fresh food, water and bedding. At the conclusion of experiments, care was taken to utilize the tissue as rapidly as possible after removal from the chamber, in order to minimize exposure to normal atmospheric oxygen and possible skewing of the data. All animals were treated in accordance with the Guiding Principles in the Care and Use of Animals and National Institutes of Health Guidelines.

4.2.2 Mitochondrial Isolation

9-week-old male mice were placed in the hypobaric chamber (11% O₂) for 7 or 14 days. Mice were thereafter anesthetized as described (chapter 2) and mitochondria rapidly extracted from both right ventricular (RV) and left ventricular (LV) tissue (modification of method of Sordahl 1971) of hypoxic and normoxic mice. A portion of LV was fixed in gluteraldehyde for electron microscopy.

4.2.3 Characterization of mitochondrial function

Baseline ADP-dependent respiration was measured polarographically at 25°C.[165] Basal proton leak was estimated using oligomycin (1µg/ml). The phosphorylation rates (ADP/Δt) and rate of ADP conversion per nmol oxygen utilised (ADP/O) were calculated from the respirometer data. Simultaneously, an aliquot of mitochondria from each of the four experimental groups was utilized to assay the rate of ATP synthesis using luciferin-luciferase luminometry, according to a modification of the method of Budnikhov.[48] Inner mitochondrial membrane potential was also estimated, as previously described (chapter 2). Oligomycin and CCCP were used as controls to ensure the fluorescence of the dyes consistently correlated with changes in inner mitochondrial membrane potential.

4.2.4 Electron Microscopy of LV tissue

A portion of the left ventricle plus septum was removed from the same hearts excised for mitochondrial isolation (section 2.3.1). The sample was approximately

2 mm X 2 mm and was immediately fixed in 2.5% glutaraldehyde, then dehydrated and embedded in paraffin wax. Thin sections were placed on grids and stained with uranyl acetate/lead nitrate (section 2.7.5) before being visualized at 7500x and 25000x magnification using a JEOL 1200 EX II electron microscope (JEOL, Japan) in order to compare number and structure of mitochondria from hypoxic and normoxic mice.

4.2.5 Heart perfusion studies

In a separate set of experiments, additional activated PKC ϵ and WT mice were placed in the hypobaric chamber for 7 and 14 days. Mice overexpressing constitutively active PKC ϵ and WT littermates exposed to hypoxia as well as matched normoxic controls were then anesthetized, hearts were rapidly excised and retrogradely perfused in the Langendorff mode.[163] Perfused hearts were paced at 600 beats per minute and functional activity (developed LV pressure)[167] was assessed using a force displacement transducer set at 2-gram tension.[163] Coronary flow and resting tension measurements were also taken. Hearts with parameters exceeding accepted control values were discarded i.e. coronary flow > 2ml/min and resting tension >2g were not included in the study.

4.2.6 Assessment of hypertrophy

Hearts were dissected and weighed after perfusion. Atria were removed and the hearts gently blotted to remove any excess perfusate. The right ventricle was

dissected free from left ventricle plus septum and weights were compared between groups to establish the degree of hypertrophy resulting from the hypoxic insult. Weights from the normoxic groups were also noted to ensure that the hypertrophy was not a function of age, but specifically in response to the hypoxic stimulus.

4.2.7 Quantitative RT- PCR

Metabolic changes were explored in transgenic mice by subjecting additional mice to 7 and 14 days hypobaric hypoxia (section 2. 7.2) Hearts were harvested (section 2.7.2), right ventricle was separated from the left ventricle plus septum, rinsed in ice-cold isolation buffer and snap frozen in liquid nitrogen. Target genes were amplified by means of quantitative RT-PCR analysis performed in collaboration with Professor Heinrich Taegtmeyer (Houston, TX, USA). The methods for the RNA extraction and real time quantitative RT-PCR have been described previously.[133] The nucleotide sequences and probes have been previously published[133, 174] and the constitutive gene transcript 18 S was used to normalize the data. Internal standards were prepared using T7 RNA polymerase method (Ambion, Austin).

4.3 Statistics

Results were expressed as means \pm SEM. Significance ($p < 0.05$) was determined for discrete variables by unpaired Student's t-test, Welch corrected for the assumption that the two groups may have different standard deviations.

4.4 Results

Prolonged exposure to hypobaric hypoxia leads to pulmonary hypertension, resulting in increased right ventricular pressure. With time, this continued pressure overload stimulus leads to right ventricular hypertrophy as an adaptive response. However, when right ventricular weights were compared, there was a significantly attenuated hypertrophic response in the activated PKC ϵ mice at 14 days hypoxia only compared with their WT littermate controls, when RV weight is expressed as a function of body weight. There was no difference in the RV or LV weights of the normoxic controls for the same time points, indicating that the right ventricular hypertrophy in the WT mice had occurred in response to the hypoxic stimulus (Figs 4-1a and b).

Figure 4-1(a)

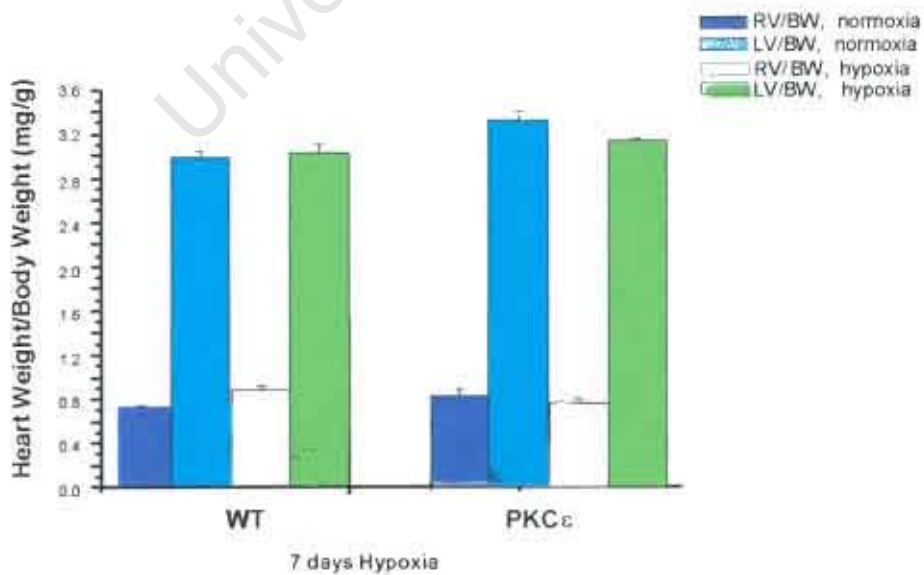


Figure 4-1(b)

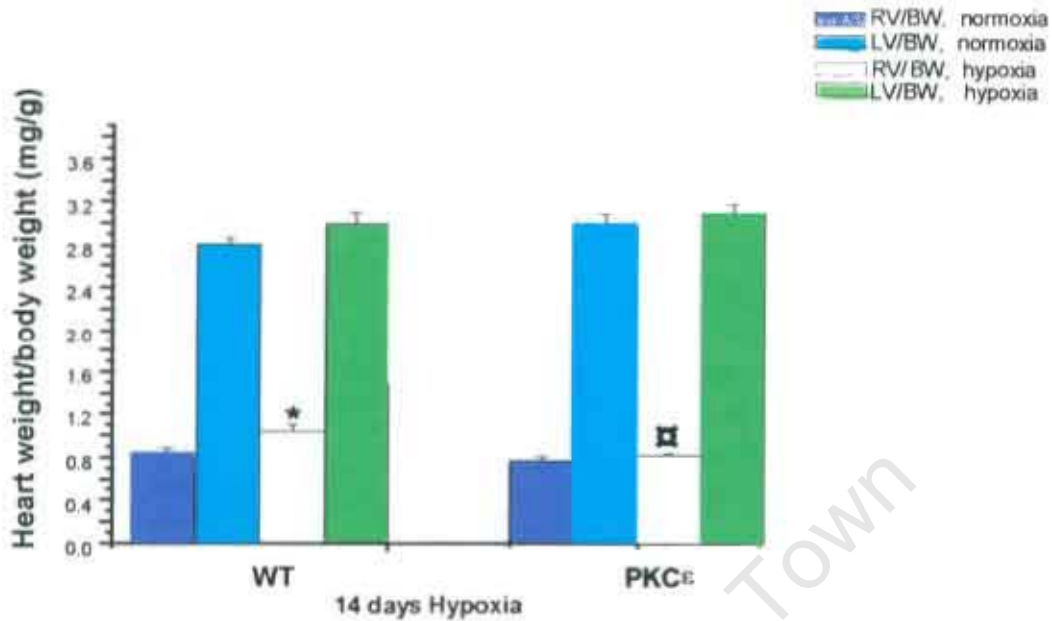


Figure 4-1a and b: Attenuated hypertrophic response in the RV of PKC ϵ overexpressing mice.

Hypobaric hypoxia causes pulmonary hypertension, which is a pressure overload stimulus. In response to the continued stimulus, the right ventricle hypertrophies as an adaptive response to the increased pressure. There is no significant change in hypertrophy after 7 days exposure to the hypobaric hypoxia. However, at 14 days hypoxia, the WT are significantly hypertrophied vs. aPKC ϵ hearts and WT normoxic controls hearts. There was no hypertrophy in the normoxic mice with age at each time point. ($\#p < 0.005$, aPKC ϵ vs. WT at 14 days hypoxia, * $p < 0.05$ WT hypoxic vs. WT normoxic at 14 days, $n \geq 12$ for each group).

However, despite the attenuated hypertrophic response in the aPKC ϵ mice, there was maintenance of cardiac function, as estimated by developed tension, resting tension and coronary flow during isolated Langendorff perfusions (Figs 4-2a & b).

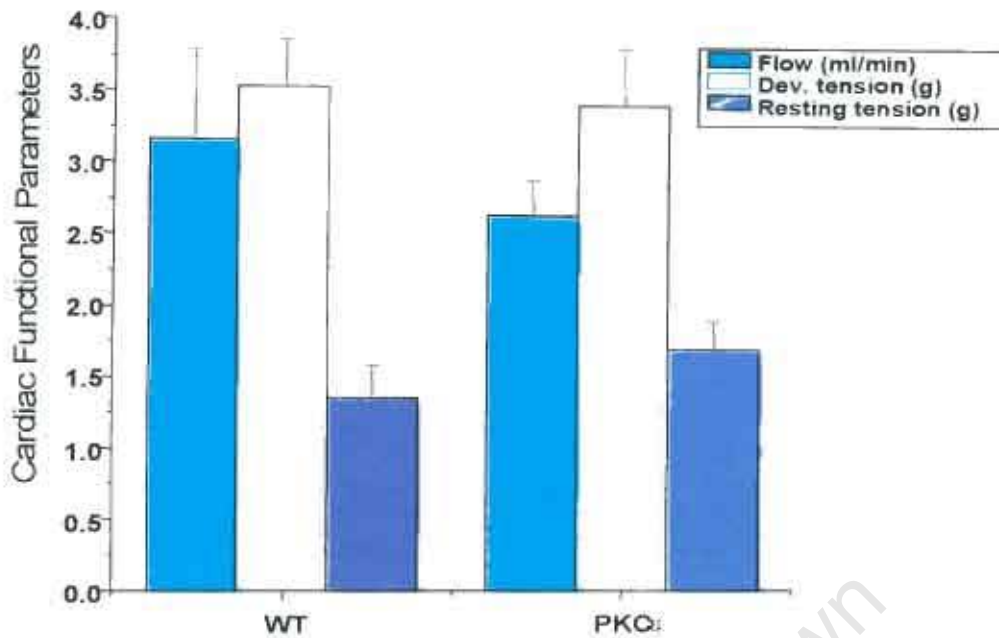


Figure 4-2a. Cardiac function after 7 days of hypobaric hypoxia

After 7 days of hypobaric hypoxia, WT and activated PKCε hearts were rapidly excised and retrogradely perfused (paced at 600 bpm). There was no significant difference in cardiac function, as evidenced by the parameters measured. (n=5 in each group).

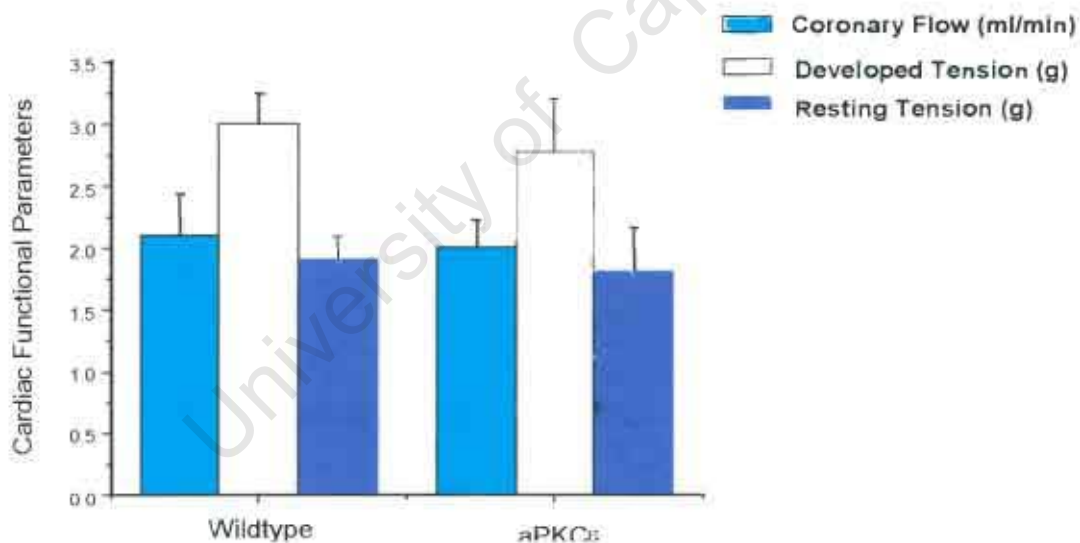


Figure 4-2b. Cardiac function after 14 days of hypobaric hypoxia

After 14 days of chronic hypobaric hypoxia, hearts were rapidly excised and retrogradely perfused in the Langendorff mode. WT and activated PKCε hearts (paced at 600 bpm) showed no significant difference in function. (n=5 in each group).

Consistent with previous experiments performed at baseline (chapter 3), there was no significant difference in baseline respiratory function between mitochondria from normoxic 7-day PKCε overexpressing and WT mice. Although

activated PKC ϵ protected mitochondria against an acute anoxic insult, there was no difference in respiratory function (state 3 and 4 respiration and RCI) between activated PKC ϵ and WT mitochondria after 7 days exposure to hypobaric hypoxia. Protection (increased state 3 respiration) was only evident after 14 days exposure to hypobaric hypoxia (Figs 4-3a and 4-3b).

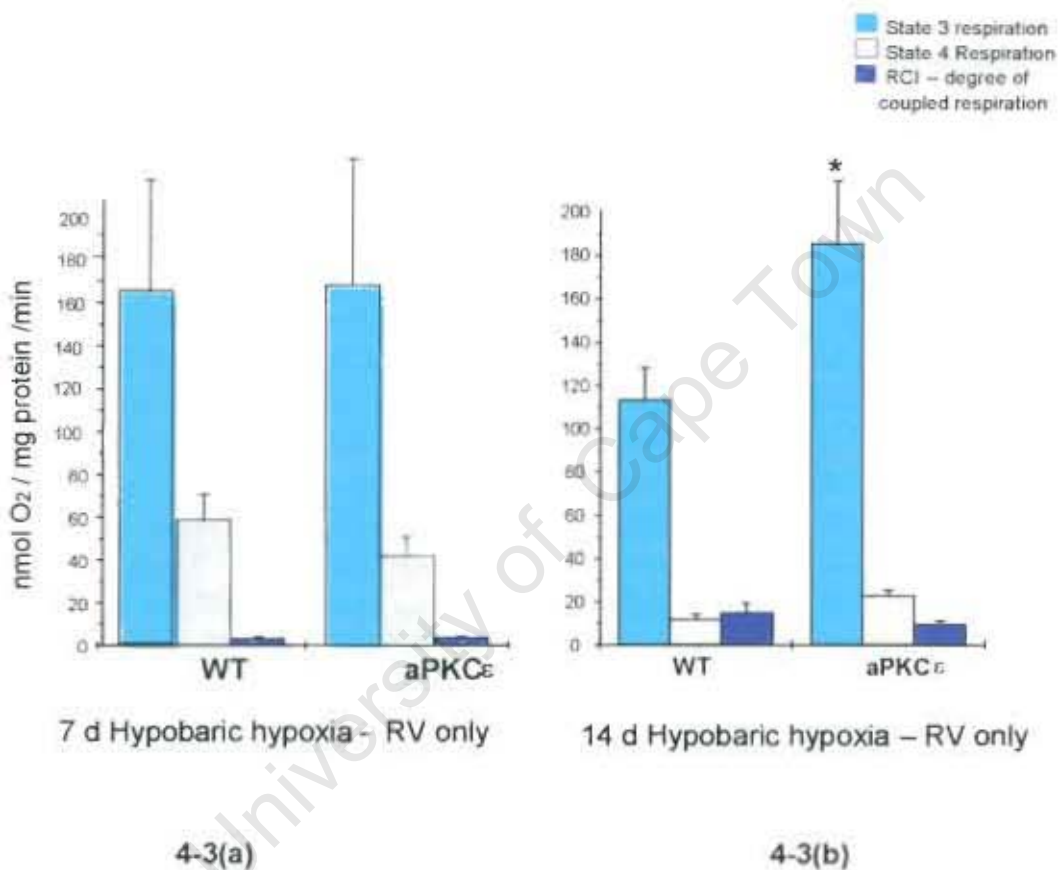


Figure 4-3a & 4-3b: Preserved mitochondrial respiration in response to 7 and 14 days of hypobaric hypoxia. At 7 and 14 days respectively, mice were anesthetized and hearts excised for mitochondrial extraction. Isolated mitochondria were assayed polarographically at 25°C and respiration rates compared. There was no difference in state 3 and state 4 respiration at 7 days, but a significant difference observed between the wildtype and transgenic heart mitochondria at 14 days (* p<0.0245, n=8), reinforcing the increased ATP production seen in the PKC ϵ mice at this time point.

Likewise, ATP synthesis in response to 7 days hypobaric hypoxia was similar in both the WT and the activated PKC ϵ mitochondria. However, after 14 days the ATP produced was significantly higher in the activated PKC ϵ mitochondria than in the matched WT littermate controls (Figs 4-4a and 4-4b, $p < 0.03$).

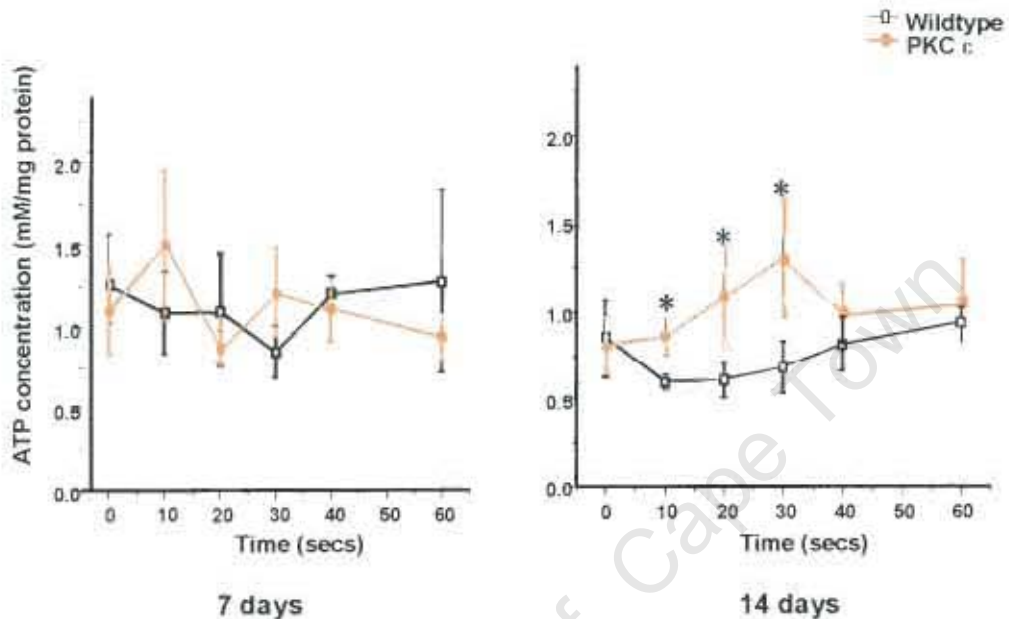


Figure 4-4, a & b. ATP synthesis in mitochondria isolated from RV in response to chronic hypobaric hypoxia.

An aliquot of mitochondrial suspension obtained for polarographic analysis was utilized to assay the rate of ATP synthesis, using an adaptation of a luciferin/luciferase method of Budnikhov.[48] At 7 days hypobaric hypoxia there was little difference in the rate of ATP synthesis between the two groups (Fig 4-4a). However, at 14 days the activated PKC ϵ mitochondria were synthesizing significantly more ATP than their WT littermate controls. (* $p < 0.03$ vs. WT at 14 days, $n = 5$ for both groups).

In light of these data, I proposed that a possible explanation for the observed maintenance of respiration and cardiac function in the WT mice compared to the innately protected PKC ϵ overexpressing mice might be mitochondrial biogenesis. Alterations in mitochondrial number and ultra structure were assessed by electron microscopic examination of sections of left ventricles of from normoxic

and hypoxic mice, as the right ventricle, which is small and comparatively thin in mice, was utilized for the protection studies shown earlier. On comparison with normoxic samples (Figs 4-5a and 4-5b), marked morphological changes were visible in the electron micrographs of hypoxic aPKC ϵ vs. WT LV tissue. (Figs 4-5c and d; 4-5e and f). The WT sections displayed higher mitochondrial numbers (rounded, larger) and the ultra structure appears in disarray.



4-5(a) WT



4-5(b) activated PKC ϵ

Figure 4-5a and b: Electron micrograph of longitudinal sections of normoxic left ventricle magnified 25000X.

In both hearts, mitochondria are arranged in an orderly fashion between the sarcomeres, which are clearly visible with their z-bands.



4-5(c) WT



4-5(d) activated PKC ϵ

Figure 4-5c and 4-5d: Electron micrograph of longitudinal sections of 7-day hypoxic left ventricle, magnified 25000X.

Mitochondria are still arranged in an orderly fashion between the sarcomeres, clearly visible with their z-bands, in the activated PKC ϵ mouse, whereas in the WT mouse (Fig 4-5c) the mitochondria have proliferated and are no longer arranged in an orderly fashion between the sarcomeres



4-5 (e) WT



4-5 (f) activated PKC ϵ

Figure 4-5(e) and (f): Electron micrograph of longitudinal sections of 14-day hypoxic LV, magnified 25000X.

Mitochondria are still arranged in an orderly fashion between the sarcomeres in the activated PKC ϵ mouse (Fig. 4-5f), whereas in the WT mouse (Fig 4-5e) the mitochondria have proliferated even more and the arrangement is more disordered.

To gain further insight into the adaptive changes observed in response to chronic hypoxia, we next performed quantitative RT-PCR on right and left ventricular tissue to assess expression patterns of several metabolic genes. Changes in RV tissue were paralleled by changes in the LV. Only RV data are shown for clarity.

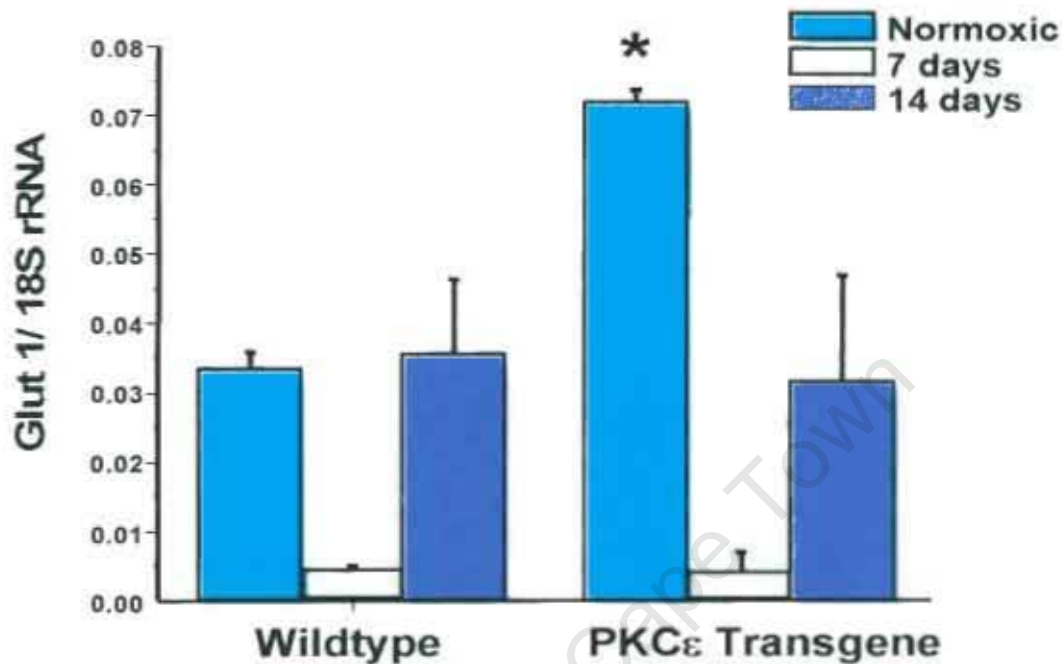


Figure 4-6. mRNA expression of GLUT 1 in RV tissue

GLUT 1 is a glucose transporter usually predominantly expressed in the fetus and neonate, whilst GLUT 4 is the predominant adult isoform. When the myocardium is exposed to a persistent stressor e.g. hypoxia, endogenous cellular protective mechanisms are activated. One of these mechanisms is re-expression of the fetal gene program, where the heart preferentially utilizes glucose as its main substrate and GLUT1 as the main transporter. Moreover, glucose utilization genes are also coordinately up regulated. At baseline (open columns), mRNA for GLUT 1 is highly expressed in the activated PKC ϵ hearts compared with the WT hearts in both RV and LV (LV data not shown, * $p < 0.0002$ vs. WT RV). However, GLUT1 mRNA expression markedly decreases at 7 days exposure to hypoxia. At 14 days the activated PKC ϵ mice express approximately half the baseline mRNA levels, whereas the WT have recovered their baseline levels. WT-wildtype, TG- transgenic PKC ϵ mouse, RV – right ventricle.

GLUT1, a constitutively expressed (fetal) isoform of glucose transporter,[213,214] was highly expressed at baseline in the activated PKC ϵ mice compared to the WT littermate controls, (Fig. 4-6), ($p < 0.0002$). The expression was reduced after 7 days hypoxia, recovering back to approximately

50% of baseline by 14 days. In the WT mice, GLUT1 expression was reduced at 7 days, thereafter increasing to baseline values at 14 days of hypoxia in the RV.

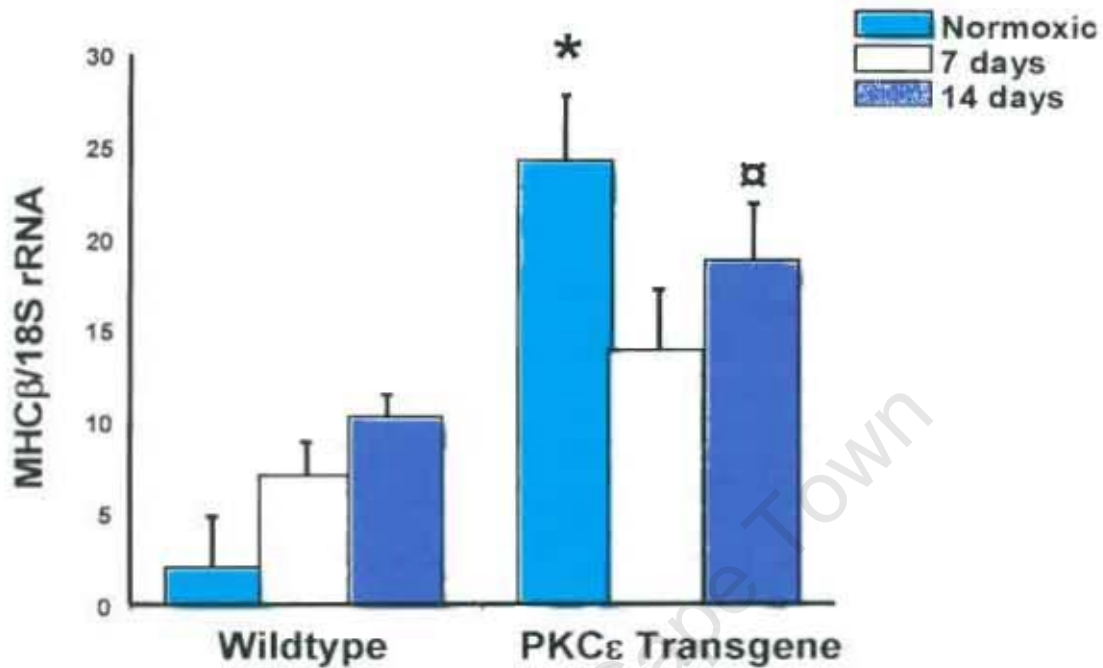


Figure 4-7. mRNA expression of MHCβ in RV tissue

There are two identified myosin isoforms in the heart: alpha myosin heavy chain (MHC α) and the slower contracting fetal isoform (MHC β). In response to the hypoxic stimulus and the resultant hypertrophy, there is a re-expression of MHC β , which allows the heart to contract at a lower oxygen cost than the α isoform. The MHC β mRNA is highly expressed in the activated PKC ϵ mice at baseline in the RV and LV, decreases at 7 days and recovers to almost 60% of its baseline value in the RV at 14 days exposure to hypoxia. However, in the WT, the expression of MHC β mRNA is extremely low at baseline compared to the PKC ϵ mice and increases with duration of the hypoxic stimulus. (* $p < 0.005$ at baseline vs WT; $\alpha p < 0.03$ at 14 days) WT-wildtype, TG- transgenic PKC ϵ mouse, RV – right ventricle.

MHC β displayed a similar pattern i.e. highly expressed in the α PKC ϵ mice at baseline ($p < 0.0005$ vs WT), decreased at 7 days and increasing again at 14 days, (Fig. 4-7), ($p < 0.03$ vs. WT). WT hearts showed progressively increased MHC β expression with increasing duration of stimulus (* $p < 0.05$ vs. baseline).

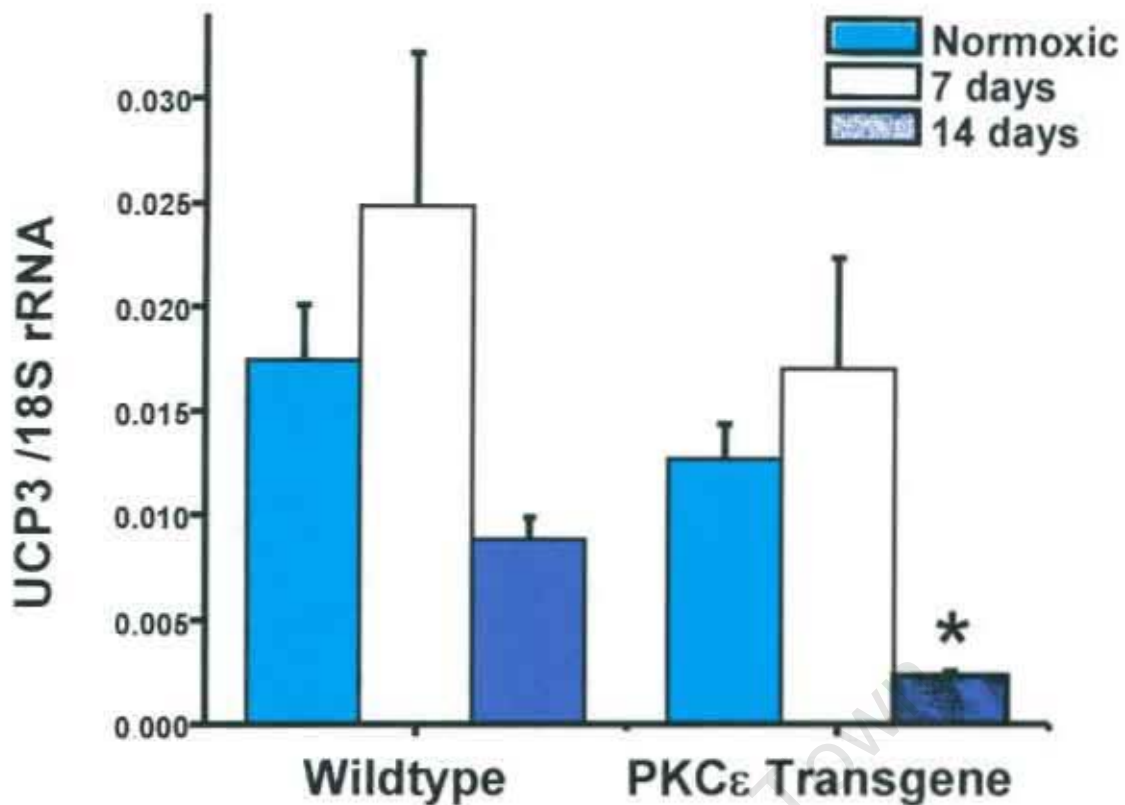


Figure 4-8. mRNA expression levels of UCP3 in RV tissue

Uncoupling protein 3 is present only in the heart, skeletal muscle and brown fat. Induction of UCP3 expression in the heart occurs postnatally, mediated by fatty acids. Its role in the heart is unclear i.e. it is linked to lipid metabolism or alternatively proposed to act as a proton transporter (lowering membrane potential) and uncoupler of oxidative phosphorylation. mRNA expression levels in both groups increased (NS) after 7 days exposure to hypoxia, then decreased at 14 days. However, the expression levels in the activated PKC ϵ mice were lower overall than in the WT, (* $p < 0.0003$ vs. WT at 14 days) WT-wildtype, TG- transgenic PKC ϵ mouse, RV – right ventricle.

Uncoupling protein 3 (UCP3) is thought to uncouple mitochondrial respiration and thereby reduce mitochondrial efficiency.[109,215,216] However, its precise functional role is not clear since it is also known to regulate fatty acid oxidation.[217-219] mRNA expression of UCP3 was not significantly different at baseline in the RV of aPKC ϵ mice compared with WT, but increased (NS) after 7 days exposure to hypobaric hypoxia in both experimental groups, then declined significantly at 14 days (Fig. 4-8).(* $p < 0.0003$ vs. WT 14 days).

PPAR α is a pivotal regulator of several FA metabolic genes and a useful marker of cardiac FA utilization.[13] PPARs bind to peroxisome proliferator response elements (PPRE) located within gene promoters of target genes after activation by their ligands.[220,221] Numerous PPARs exist - α, β, γ . PPAR α is abundantly expressed in the rodent heart[222] and is the major regulator of myocardial FA utilization pathways. PPAR α mRNA expression levels did not significantly differ between the groups at any time point although there were reduced levels at the 7-day time point. (Fig 4-9).

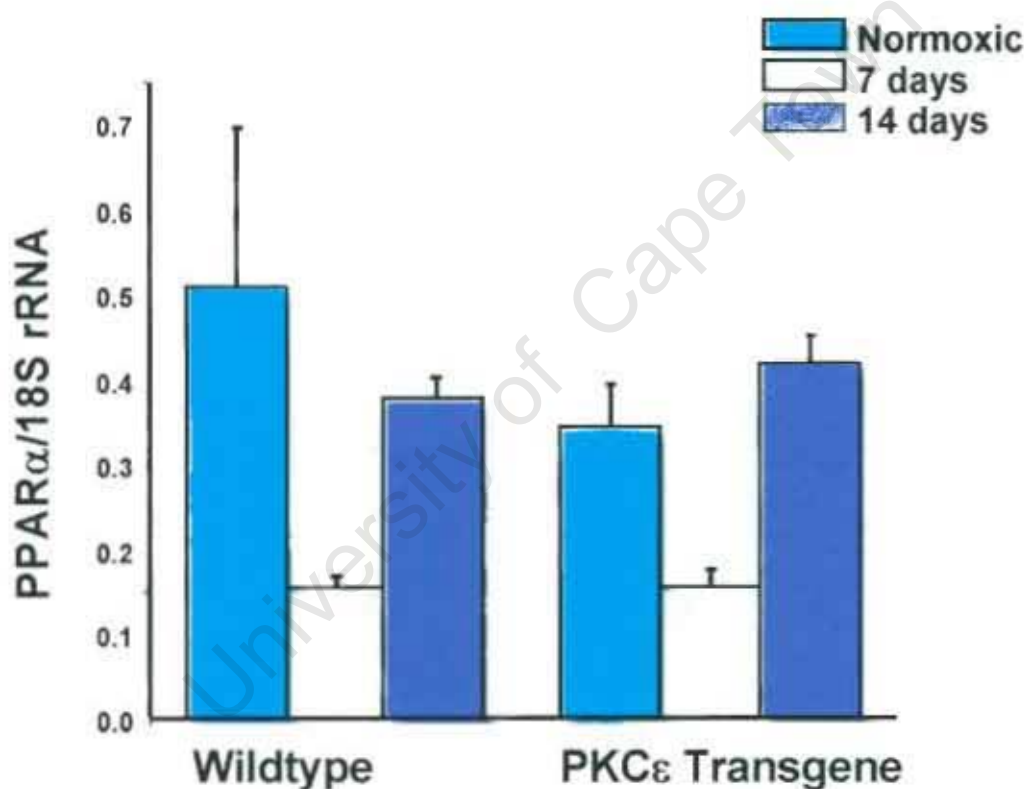


Figure 4-9: mRNA expression for PPAR α in RV tissue

No significant changes were detected in the expression levels of PPAR α at 7 or 14 days on comparison of PKC ϵ overexpressing and WT mice.

mCPT-1 is the muscle isoform of carnitine palmitoyl transferase 1 (CPT-1), also enriched in the heart. It is the rate-limiting enzyme of mitochondrial fatty acid

uptake, situated on the outer mitochondrial membrane. It is responsible for the activation and import of long chain fatty acids across the outer mitochondrial membrane. Reduced activity and expression of CPT-1 and medium chain acyl-CoA dehydrogenase, a key fatty acid oxidation enzyme, are thought to be responsible for reduced fatty acid oxidation seen in heart failure.[223] Reduced mCPT1 would therefore result in decreased mitochondrial FA import and fatty acid oxidation. mCPT1 gene expression levels were not significantly different between the groups except after 14 days of hypoxia (Fig 4-10). Here, mCPT1 levels were reduced in WT hearts in response to hypoxia and increased beyond baseline at 14 days hypoxia in the RV of PKC ϵ overexpressing mice.

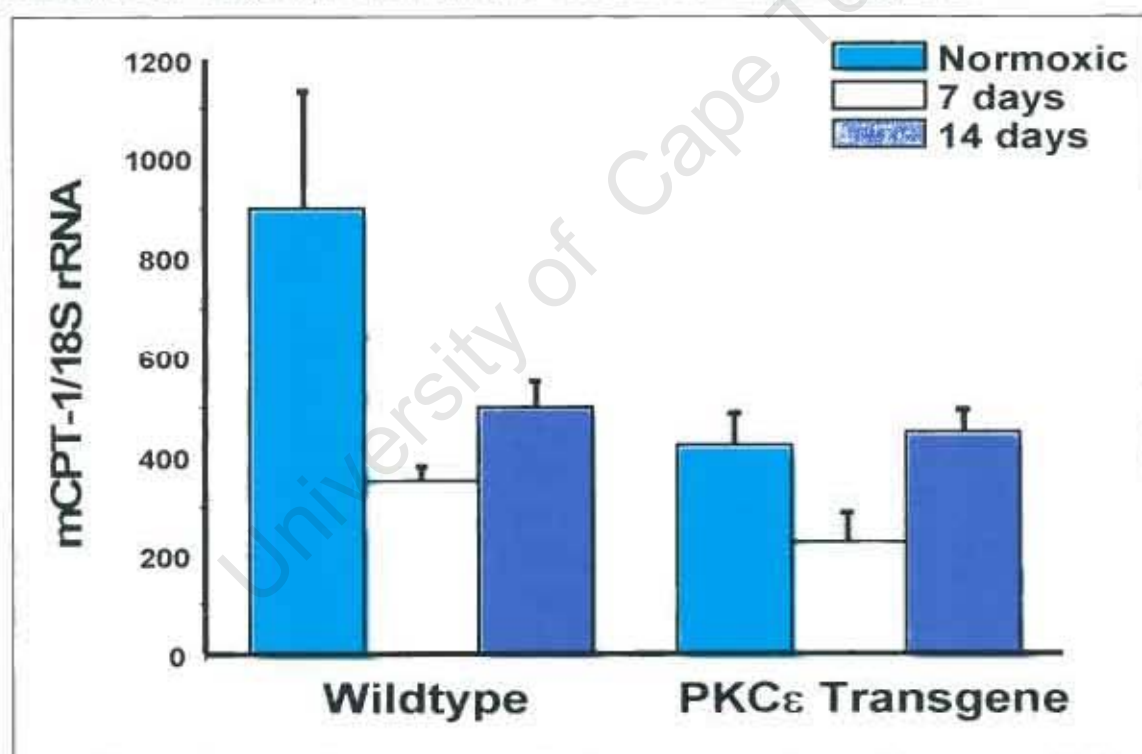


Figure 4-10: mRNA expression levels of mCPT1 in RV tissue

mCPT-1 is the muscle isoform of carnitine palmitoyl transferase 1. It is the rate-limiting mitochondrial fatty acid uptake enzyme situated on the outer mitochondrial membrane, responsible for the activation and import of long-chain fatty acids into the mitochondria for β -oxidation. Decreased expression of mCPT-1 mRNA would imply decreased fatty acid oxidation rates.

4.5 Discussion

Previous workers have shown that PKC ϵ physically associates with components of the membrane permeability transition pore, *in vivo* and *in vitro*. [3, 7, 70] In light of this, I hypothesized that PKC ϵ protects the heart by modulation of MPT and pore opening, thus maintaining ATP production and cellular homeostasis. In agreement, in this thesis I reported hyperpolarized mitochondrial membranes, an increased rate of ATP synthesis and protection against acute oxygen lack for PKC ϵ transgenic mice (chapter 3). In light of these interesting findings, I further hypothesized that similar mechanisms will protect PKC ϵ hearts against chronic hypobaric hypoxia.

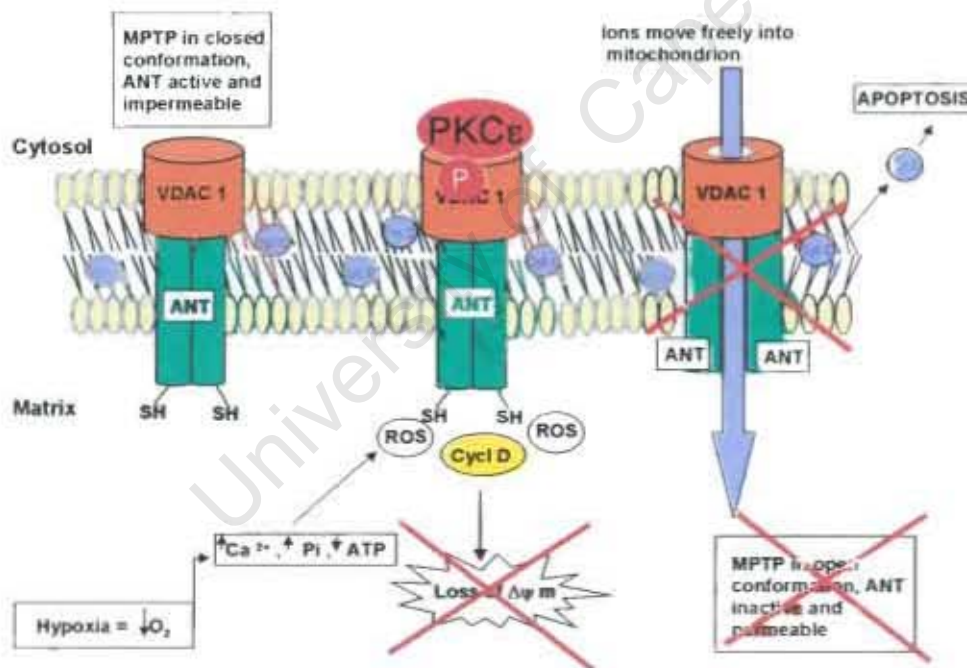


Fig 4-11: PKC ϵ protects against chronic hypoxia

In unprotected mitochondria exposed to hypoxia, calcium accumulation and ROS generation target ANT, recruiting its regulatory molecule cyclophilin D. This causes ANT to undergo a conformational change, becoming inactive and permeable, in turn triggering a change in VDAC1, facilitating pore formation and apoptosis (chapter 1). PKC ϵ phosphorylates VDAC1, stabilizing the pore and preventing MPT, pore opening and loss of cytochrome c. Oxidative phosphorylation can continue and ATP levels are maintained.

Specifically, I proposed that in response to chronic hypoxia, PKC ϵ stabilizes VDAC1, thereby preventing MPT and facilitating maintenance of cellular energetics and homeostasis (Fig 4-11). To test this hypothesis, transgenic PKC ϵ mice were exposed to 7 and 14 days of hypobaric hypoxia, respectively, and compared to WT controls. Cardiac functional parameters, mitochondrial respiratory capacity and the regulation of several metabolic genes were determined and compared with matched wildtype control mice.

The main findings of this chapter are: 1. Attenuated trophic response in the RV of PKC ϵ mice after 14 days of hypobaric hypoxia. 2. Sustained cardiac function in PKC ϵ overexpressing mice and wildtype controls after 7 and 14-day exposure to hypobaric hypoxia. 3. Increased rate of mitochondrial ATP production in the PKC ϵ mice vs. wildtypes after 14 days of hypoxia. 4. Lack of mitochondrial biogenesis in PKC ϵ hearts vs. wildtypes after 7 and 14 days of hypoxia. 5. Distinct regulation of metabolic genes in PKC ϵ vs. wildtypes in response to chronic hypoxia.

Attenuated Trophic Response in PKC ϵ Mouse

We found no robust hypertrophic response in the right ventricle of PKC ϵ hearts after exposure to 14 days of hypobaric hypoxia. These data suggest that PKC ϵ may play a role in attenuating hypertrophic signaling, which contrasts with previous studies[161, 225] supporting a role for PKC ϵ in promoting cardiac hypertrophy. However, Takeishi et al.[161] reported that mice overexpressing constitutively active PKC ϵ develop mild compensated concentric hypertrophy yet

have normal cardiac function. When the PKC ϵ transgenic mouse was constructed, several different transgenes were made expressing mild, moderate and high copy numbers of the constitutively active PKC ϵ gene. We propose that this difference may be due to differences in copy number of the mice employed in the various studies. Alternatively, we cannot rule out the possibility that a different PKC isoform may have been reduced in response to chronic hypobaric hypoxia [47, 226, 227] and this could perhaps have influenced the hypertrophic response in the RV. Further studies are required to elucidate this interesting finding of an apparent role for PKC ϵ in attenuating hypertrophy in this model of hypobaric hypoxia.

Sustained Cardiac Function in Response to Chronic Hypoxia

Contractile function was sustained in both the PKC ϵ overexpressing and wildtype hearts after 7 and 14 days exposure to chronically reduced oxygen levels, indicating that both groups had adapted to the oxygen deprivation. Moreover, despite an attenuated trophic response in the RV, PKC ϵ hearts maintain function, implying different adaptive mechanisms for the PKC ϵ and wildtype hearts. Rafiee et al.[212] have demonstrated that infant human and rabbit hearts adapt to chronic hypoxia through activation of PKC ϵ , p38 MAP kinase, and JUN kinase signal transduction pathways. In both the clinical (human cyanotic infants) and experimental (hypoxic infant rabbits) settings, hearts are protected when PKC ϵ is activated and translocated. Inhibition of PKC ϵ abrogates the protection. Furthermore, hypoxic hearts had elevated coronary flow and better functional

recovery (measured as developed pressure) than normoxic hearts after subsequent exposure to ischemia. Thus, our data are consistent with these concepts. However, the different trophic response in the aPKC ϵ mice suggests distinct protective mechanisms may operate in PKC ϵ and wildtype mice.

We are aware that cardiac functional parameters may have been more accurately measured using pressure volume loops, but the technique was not available to us at the time. We are planning to use this technique in collaboration with Dr Aasum of University of Tromsø in Norway to do follow-up perfusion studies on the hypoxic hearts to confirm these data.

Increased Rate of ATP Production in PKC ϵ Mice

To further elucidate the mechanisms sustaining cardiac contractile function subsequent to hypobaric hypoxia, we next assessed mitochondrial respiratory functional parameters. Interestingly, there was no difference in mitochondrial respiratory function between the PKC ϵ overexpressing mice and wildtype in response to 7 days of hypoxia. However, after 14 days of hypobaric hypoxia, state 3 respiration was significantly increased in aPKC ϵ compared with WT littermates. These data suggest that PKC ϵ signaling allows the cell to increase respiratory capacity in response to the chronic oxygen lack. We found increased rates of mitochondrial ATP synthesis in both the right and left ventricle of the PKC ϵ overexpressing mice compared to the wildtype. Our data are in agreement with the findings of Cross et al. [2] who also reported increased ATP synthesis in

PKC ϵ mice at baseline. Moreover, in response to ischemia- reperfusion, recovery of contractile function and rates of ATP synthesis were greater in PKC ϵ than wildtype hearts, consistent with the proposed cardioprotective role of PKC ϵ . Together, these data suggest that PKC ϵ signaling pathways provide protection against chronic oxygen lack. Here, I propose that PKC ϵ phosphorylates VDAC1/2, thereby stabilizing the pore proteins in the closed conformation. In agreement, we also found inner mitochondrial membrane potential ($\Delta\psi_m$) (preliminary data) to be significantly elevated in mitochondria isolated from aPKC ϵ mice in response to 14 days' hypobaric hypoxia. Studies in isolated mitochondria may be considered non-physiological, but nevertheless the mitochondrial studies performed in this study support my hypothesis regarding a possible mechanism of action for activated PKC ϵ during chronic oxygen lack. For future studies (see chapter 5) isolated intact adult myocytes or permeabilized fibres are being considered.

Lack of Mitochondrial Biogenesis in PKC ϵ Hearts

Electron microscopic analysis was performed to determine mitochondrial number and ultra structural changes in response to the hypoxic stimulus. Here, the wildtype hearts showed increased mitochondrial numbers in response to the hypoxic stimulus with altered ultra structural arrangements. Surprisingly, hearts from PKC ϵ overexpressing mice did not display a classic mitochondrial biogenesis response (7 or 14 days), suggesting that either overexpression of constitutively active PKC ϵ plays a role in the mitochondrial biogenesis pathway or

that the protection conferred by activated PKC ϵ makes mitochondrial biogenesis unnecessary. These data imply a compensatory mechanism in the PKC ϵ overexpressing mice in order to maintain cardiac function without hypertrophy or mitochondrial biogenesis.

Gleyzer et al.[131] have documented hypoxia as stimulating PGC1 α and NRF-1, transcription factors known to stimulate mitochondrial biogenesis. In their review article, McLeod et al.[228] documents work by various authors [207, 229, 230] demonstrating that hypoxia results in stimulation of PGC1 and NRF-1, leading to mitochondrial biogenesis and increased ATP synthesis. However, in each case the model utilized is different from ours and the hypoxic stimulus is intermittent, not sustained as in our model. Thus the stimulus employed in these instances equates more with a preconditioning stimulus. We speculate that aPKC ϵ mice do not require mitochondrial biogenesis, as they are protected by the overexpression of PKC ϵ facilitating enhanced bioenergetic capacity and stabilizing the mitochondria. In addition, we speculate that there may be a coordinate up regulation of electron transport chain components,[231, 232] further facilitating maintenance of bioenergetics in the aPKC ϵ without mitochondrial biogenesis.

Distinct Regulation of Metabolic Genes in PKC ϵ Mouse

Quantitative RT-PCR was performed on hearts from both groups for a number of FA and glucose utilization metabolic genes in order to further investigate compensatory mechanisms. Fuel substrate utilization is highly regulated during

neonatal cardiac development and at the onset of cardiac hypertrophy. The mammalian fetus lives in a relatively hypoxic environment and predominantly expresses the fetal gene program.[209] Here, glucose is the main fuel substrate utilized, GLUT1 being the major isoform present.[233] Postnatally, a switch occurs so that fatty acids become the chief energy substrate in the non-fed adult mammalian heart and the major glucose isoform expressed at this point is GLUT 4. Likewise, a reversion to fetal energy metabolism occurs with the development of cardiac hypertrophy, with simultaneous re-expression of the fetal genes and transporters. Sack et al.[233] have demonstrated co-ordinate down regulation of mRNA of fatty acid utilization enzymes like LCAS (long chain acetyl CoA synthase), MCAD (medium acyl CoA dehydrogenase), GLUT4 (the adult isoform) and phosphofructokinase with increasing LV mass in spontaneously hypertensive rats.

When mRNA expression levels of the proposed target genes mediating PKC ϵ protection were examined, the basal gene metabolic phenotype of the PKC ϵ overexpressing mice resembled (in part) a fetal expression pattern. Two "fetal-like" genes examined were MHC β and GLUT1. PKC ϵ overexpressing hearts had elevated MHC β and GLUT1 expression levels at baseline. Hashimoto et al.[234] characterized cardiac changes in myosin heavy chain-beta (MHC β), capacity for oxidative metabolism and muscle mass in hearts of rats born and raised at simulated altitudes (2200 m or 4000 m) compared to age-matched sea level controls. On the basis of electrophoretic analyses, they found that the hypoxia-

induced ventricular hypertrophy produces a significant increase in MHC β in both ventricles. Furthermore, they observed an exponential relationship between the mass of right ventricular muscle and percentages in the expression of MHC β ($r=0.928$, $p<0.001$). Moreover, later studies found a gene switch from MHC α to MHC β in response to sub-acute and chronic hypobaric hypoxia.[124, 133, 235] Mochly-Rosen et al. overexpressed constitutively active PKC ϵ using a RACK (receptor for activated c kinase) peptide[236] and reported increased MHC β mRNA expression with decreased myocyte size, yet concentric compensated remodeling. However, the explanation for differences between their findings and the current study may be due to the degree of PKC ϵ overexpression. Mochly-Rosen's group employed transgenic mice with 20% overexpression, whereas the current study used a transgenic mouse that has 15x the mRNA for PKC ϵ , 9x the protein level, and 4.2x the membrane activity of the WT mice. Similar findings were reported by Chen et al.[47] where overexpression of both PKC ϵ and PKC δ had elevated mRNA for MHC β and developed hypertrophy, yet PKC ϵ was cardioprotective and PKC δ harmful. Raised MHC β mRNA expression levels and protein were reported in an aging study of overexpressing constitutively active PKC ϵ mice at 36 weeks by Goldspink et al.[237], with evidence of heart failure at 48-52 weeks, yet normal cardiac function at 9-12 weeks. They did not comment on MHC β mRNA levels at this time point. PKC ϵ was also overexpressed using adenoviral vectors and also showed no hypertrophy, but raised MHC β mRNA levels, thus further corroborating our data.[238] These data suggest that elevated

MHC β levels represent a compensatory mechanism to sustain cardiac contractile efficiency in response to impaired oxidative metabolism.

Differential regulation of GLUT1 and GLUT4 isoforms with hypobaric hypoxia in Wistar rats has also been shown.[133, 235] In contrast, my data show that at the onset of hypoxia (7 days) GLUT1 was down regulated. As tolerance to the hypoxic stress progressed with time, the isoform expression reverted to baseline levels by 14 days. Since we did not measure GLUT4 transcript levels it is difficult to explain GLUT1 down regulation after 7 days of hypoxia. It remains a possibility that the ratio of GLUT4 to GLUT1 may be similar to Sharma et al.,[133] who found an increased GLUT1/GLUT4 ratio after 7 days of hypobaric hypoxia versus normoxic controls. Interestingly, the α PKC ϵ mice showed significantly high GLUT1 transcript levels at baseline, compared to normoxic controls. Since we did not measure GLUT4 levels, it is difficult to make a conclusive finding. However, the elevated GLUT1 levels raise the interesting possibility that PKC ϵ transgenic mice express an inherently more "fetal" gene program at baseline.

Regarding genes regulating cardiac FA metabolism, PPAR α and mCPT1 levels were reduced (NS) after 7 days of hypoxia, consistent with a switch from FAs to increased glucose utilization. However, after 14 days of hypoxia, PPAR α and mCPT1 levels returned to baseline. These data exhibit a similar trend to a previous study that showed dynamic gene regulation in the RV in response to hypobaric hypoxia.[133] Here, they found a switch to a fetal gene pattern after 7

days and a switch-back to an adult gene profile after 14 days of hypobaric hypoxia. These authors found that hematocrit levels increased by 7 days and further increased after 14 days, suggesting that some degree of normoxia may be restored at the 14-day time point.

After 14 days of hypoxia UCP3 mRNA expression levels were significantly down regulated in the overexpressing PKC ϵ mice compared to wildtype controls. If UCP3 indeed acts as an uncoupler, reduced UCP3 levels should make mitochondria more tightly coupled, hence capable of producing more ATP. This is corroborated by findings of increased rate of ATP synthesis at 14 days exposure to hypoxia. Alternatively, UCP3 has been proposed to play a pivotal role the regulation of metabolism. However, since we found restoration of the adult FA gene profile at 14 days, low UCP3 levels do not suggest that it acts to regulate FA metabolism. Additional studies are required to further investigate these possibilities.

Lastly, we are aware that changes in mRNA levels do not necessarily reflect changes in protein levels or in activity levels of proteins. I do plan to perform SDS-PAGE analysis of the protein levels of these genes as well as activity levels by measuring substrate utilization in isolated myocytes and in isolated perfused hearts.

Together, these findings support the hypothesis that PKC ϵ overexpressing mice are more resilient to a chronic hypoxic stress. Attenuation of the hypertrophic

response may play a role, but the mechanism appears to be mainly via enhanced bioenergetic capacity i.e. modulation of metabolism, increase of the MPT threshold by stabilizing the pore structure due to VDAC 1/2 phosphorylation as well as increasing the efficiency of mitochondrial ATP production via a decrease in the uncoupling of oxidative phosphorylation by UCP3.

The data also evidence different protective pathways for PKC ϵ overexpressing and wildtype mice in response to chronic hypobaric hypoxia. The wildtype hearts respond by increased mitochondrial biogenesis and right ventricular hypertrophy to maintain mitochondrial respiration and cardiac function. Conversely, PKC ϵ overexpressing mice lacked the chronic hypertrophic response in the RV, displayed no mitochondrial biogenesis, yet had an increased rate of ATP synthesis and were able to maintain cardiac function and contractility. Moreover, PKC ϵ transgenic mice also appear to be mainly glycolytic at baseline and lose this when stressed by prolonged exposure to hypobaric hypoxia.

This illustrates the complexity of in vivo PKC ϵ signalling pathways (Fig.4-12):

- 1) PKC ϵ modulates hypertrophy, possibly by direct phosphorylation of GSK3 β , a component of the protective Akt pathway and co-localized at the MPTP, PKC ϵ could also phosphorylate Akt directly [66] and could directly activate it to phosphorylate GSK3 β .
- 2) PKC ϵ modulates the mitochondrial biogenesis pathway, possibly by direct inhibition of PGC1 α and NRF-1 during hypoxia.

- 3) PKC ϵ possibly activates a protective pathway, as with acute anoxia, involving the phosphorylation and stabilization of VDAC 1/2, increased resistance to MPT during hypoxic stress coupled with an increased bioenergetic capacity which sustains intracellular ATP levels, thus maintaining cardiac function and mitochondrial respiration in response to hypobaric hypoxia.
- 4) PKC ϵ apparently also regulates transcription upon translocation to the nucleus, evidenced by the regulation of mRNA expression levels of the metabolic genes selected.

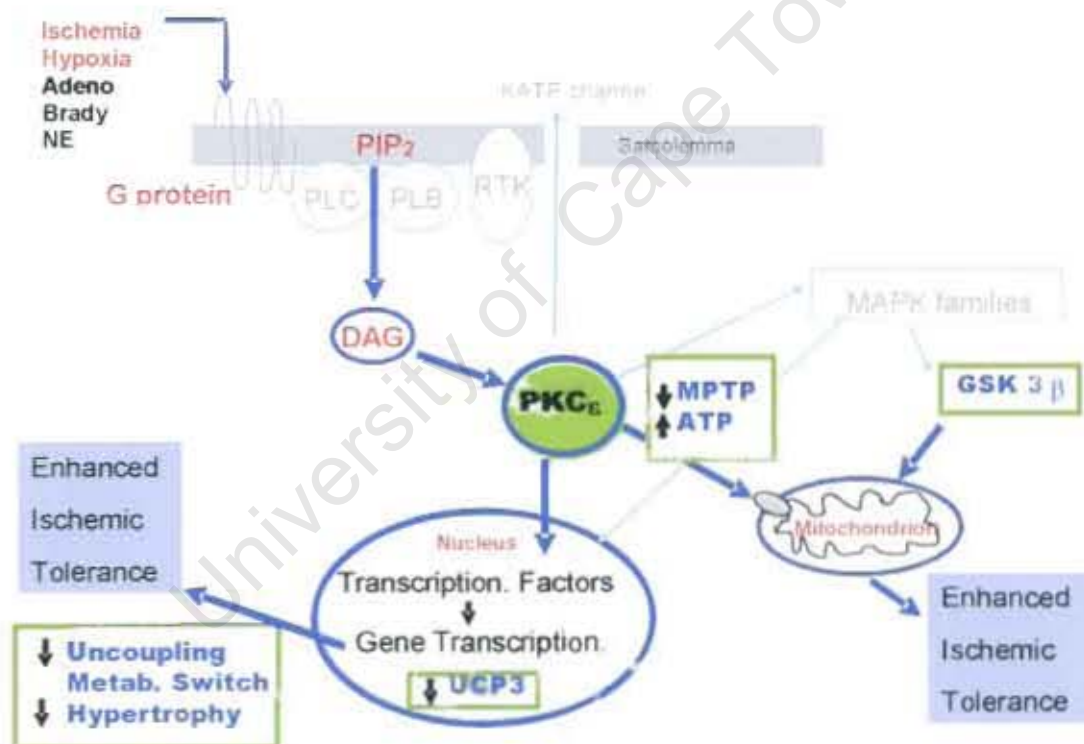


Figure 4-12: PKC ϵ activates multiple pathways to exert its protective effects on the heart

Activated PKC ϵ has been shown to phosphorylate GSK3 β , a critical downstream element of the Akt survival pathway, which facilitates glycogen production and initiates hypertrophy. It is inactivated when phosphorylated. Activated PKC ϵ translocates to the nucleus and mitochondrion, where it can modulate transcription of various genes (decrease in UCP3) and prevent MPTP by stabilizing pore components, thus maintaining optimal bioenergetics during oxidant stress.

Chapter 5

Conclusion

University of Cape Town

This thesis encompasses two major hypotheses:

1. Activated PKC ϵ is translocated to the mitochondrion and confers cardioprotection during an acute oxygen lack. The mechanism of protection is via modulation of the membrane permeability transition pore. PKC ϵ stabilizes the pore, preventing loss of membrane potential and thereby maintaining ATP production during an acute oxygen lack.
2. Activated PKC ϵ further protects against chronic hypoxia, by a) prevention of MPT and pore opening and b) translocation to the nucleus, regulating target metabolic genes.

5.1 Acute oxygen lack

Since PKC ϵ has been implicated in ischemic preconditioning i.e. part of the PKC ϵ protective program is exerted at the mitochondrial level, the possibility existed that mitochondria from PKC ϵ overexpressing mice would be "perpetually preconditioned" and hence resistant to an acute oxygen lack. To test this hypothesis, isolated mitochondria from wildtype and PKC ϵ overexpressing hearts were exposed to an excess ADP-induced anoxic environment within the chamber of the Clarke electrode. Here, transgenic PKC ϵ mice overexpressing constitutively active PKC ϵ displayed increased membrane potential after 45 minutes of ADP-induced anoxia as well as after 45 minutes of ADP-induced anoxia / 7 minutes of reoxygenation. Concomitantly, there was increased recovery of state 3 respiration, retention of cytochrome c, increased ATP

synthesis and ANT functional content compared to those from age-matched wild type littermate controls. In agreement, aPKC ϵ mice showed significantly increased protection in response to an ischemic insult compared to the WT.

To further examine this cardioprotective phenotype expression levels of several cardiac metabolic genes were assessed at baseline. Here, aPKC ϵ mice appear to have a "fetal-like" gene metabolic phenotype, exhibiting elevated mRNA expression for GLUT1 and MHC β compared to WT. Together these data suggest the existence of multiple cardioprotective pathways in the mice overexpressing constitutively active PKC ϵ : 1. An innate ability to maintain optimal intracellular energetics by maintaining mitochondrial ATP synthesis, and 2) fetal-like metabolic gene program at baseline.

5.2 Chronic oxygen lack

Elevated levels of activated PKC ϵ translocated to the particulate fraction were demonstrated as part of the cardioprotective program in hypoxic human infants prior to surgery for cyanotic defects, as well as in an experimental infant rabbit model,[212] engendering resistance to subsequent ischemic insult. Adult humans with a variety of pathological states are also relatively hypoxic: patients with heart failure, cardiomyopathy or chronic obstructive pulmonary disease. An intervention that could improve the outcome of such diseases would have obvious benefit.

Thus the hypothesis for the second part of the study was to investigate if protective mechanisms identified earlier would be engendered in response to chronically reduced oxygen levels.[4,7,184] Since temporal changes were also of interest, overexpressing constitutively active PKC ϵ and littermate wildtype control mice were exposed to either 7 days or 14 days hypobaric hypoxia and endpoints were monitored as previously described.

After 7 days exposure to hypoxia, there was no difference in mitochondrial function between the transgenic PKC ϵ mice and matched wild type littermate controls i.e. state 3, state 4, RCI and rate of ATP synthesis were similar in both groups. Speculatively, this lack of functional difference could be accounted for by mitochondrial biogenesis observed in the wildtype hearts. Electron micrographs of LV tissue from 7-day hypoxic WT mice showed marked mitochondrial biogenesis. In contrast, no biogenesis was evident in the 7-day hypoxic PKC ϵ LV tissue. Moreover, mitochondria from PKC ϵ overexpressing hearts appear normal on comparison to normoxic tissue. This response may have been induced by transcription factors known to be stimulated by hypoxia e.g. HIF-1, PGC-1 α or NRF-1, and to result in mitochondrial biogenesis.

I propose that there may be no requirement for mitochondrial biogenesis in the transgenic PKC ϵ hearts due to the continued activation of innate cardioprotective mechanisms, which permit the heart to function normally within this context.

Despite similar mitochondrial function, there was however a significant difference in terms of the degree of hypertrophy between the two groups i.e. WT hearts exhibited marked hypertrophy compared to PKC ϵ hearts. Hypertrophy is an attempt by the heart to compensate and adapt to the continued pressure stimulus. In a separate set of experiments, hearts were subjected to retrograde perfusion and developed force measured as an assessment of cardiac contractility. Here, we found no difference in cardiac contractility or coronary flow between the PKC ϵ overexpressing and wildtype hearts, indicative of similar cardiac function despite the adaptive hypertrophy in the wild type hearts.

Gene expression analyses showed interesting results. In the first instance, we found that at baseline aPKC ϵ mice had increased GLUT1 and MHC β levels (fetal isoforms), compared to the WT. Although these changes were only observed at the gene level, it raises the interesting possibility that the PKC ϵ overexpressing mice may have increased glucose utilization at baseline, which may account for some protection when exposed to acute or chronic oxygen lack.

After 7 days of hypoxia, GLUT 1 levels markedly decreased in both aPKC ϵ and Wt mice. The reason for this is not entirely clear. One would have predicted increased levels in response to reduced oxygen levels. Since GLUT4 levels were not determined in this study, it is difficult to comment on the GLUT1/GLUT4 ratio at this point. However, PPAR α and CPT1 levels were reduced at this point,

consistent with a shift away from the adult FA-utilization phenotype to a fetal-like phenotype.

After exposure to 14 days hypobaric hypoxia, mitochondria isolated from mice overexpressing constitutively active PKC ϵ exhibited a significant increase in ADP-dependent respiration (state 3) and a higher degree of coupled respiration. The rate of ATP synthesis was also higher in the PKC ϵ overexpressing mice. Furthermore, PKC ϵ mice did not display any mitochondrial biogenesis response, unlike the WT. Interestingly, PKC ϵ mice did not show any ultrastructural changes, compared to WT mitochondria which displayed cristae derangement. However, despite increased mitochondrial numbers in the WT hearts, mice overexpressing constitutively active PKC ϵ still displayed improved bioenergetic respiratory capacity. There was no RV hypertrophic response in the transgenic mice at 14-day point, yet cardiac function was maintained. Furthermore, UCP3 expression was significantly decreased in the overexpressing PKC ϵ mice, suggesting tighter coupling of ADP-dependent respiration. In contrast, the mRNA expression of GLUT 1 decreased significantly in overexpressing constitutively active PKC ϵ at 14 days. No significant changes in GLUT1 were found in WT hearts, suggesting a switch from FAs to a fetal-like gene phenotype in the WT, i.e. utilizing more glucose to maintain cardiac function and cellular energetics. On the other hand, the data suggest overexpressing constitutively active PKC ϵ switch from a mainly fetal gene phenotype to an adult-like gene program. Consistent with the fetal

switch in the WT mice, there is a progressive increase in MHC β levels (fetal isoform re-expression), concomitant with the progression of hypertrophy.

The exact mechanism of the gene switch in the overexpressing constitutively active PKC ϵ is not known. Constitutively active PKC ϵ is known, however, to activate multiple signaling pathways to exert its protective effects on the heart (Fig. 5-1).

5.3 Proposed molecular mechanism for PKC ϵ

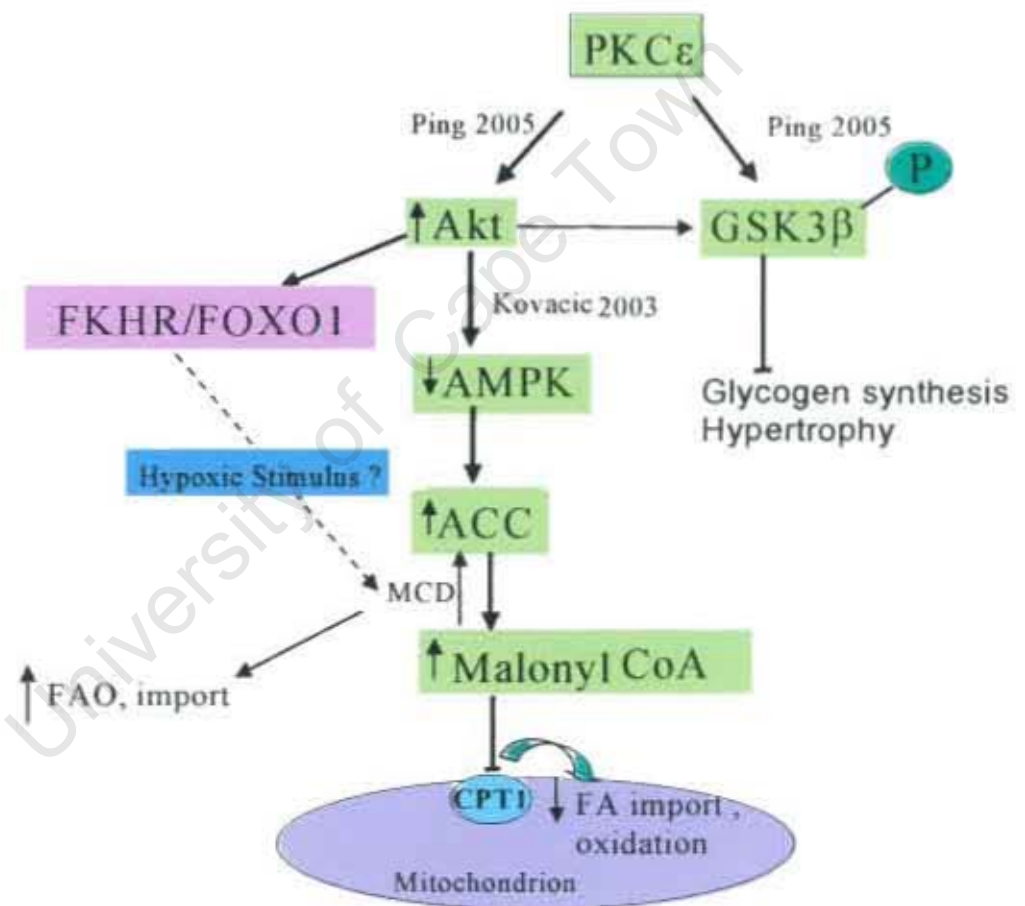


Figure 5-1: Proposed molecular mechanism of PKC ϵ cardioprotection

PKC ϵ is central to a complex network of signaling pathways and my proposals in the above scheme are speculative, with the information acquired thus far. Ping in [66], Kovacic in [239]

FKHR/FOXo1- forkhead transcription factor

As constitutively active PKC ϵ translocates to the nucleus and to the mitochondrion, I speculate that it possibly interacts in the following manner:

- GSK3 β is part of the protein kinase B (PKB/Akt) growth signaling pathway and is known to complex with components of the MPT. When phosphorylated, GSK3 β is inactivated. PKC ϵ has been shown to phosphorylate GSK3 β *in vitro* and *in vivo*, and by their juxtaposition at the MTP, PKC ϵ could directly inactivate GSK3 β , thereby possibly preventing hypertrophy in the aPKC ϵ mice. PKB/Akt, already activated by PKC ϵ , could also directly phosphorylate GSK3 β (Fig 5-1).
- PKC ϵ activates the PKB/Akt directly by phosphorylating Akt at Ser 473 and thus acting as a phosphoinositide dependent kinase 2 (PDK2). PKB/Akt then decreases AMPK activity by phosphorylation, which could account for the “fetal” gene phenotype in the PKC ϵ mice at baseline. AMPK is a fuel sensor switch, altering substrate preference in the heart according to the AMP/ATP ratio. The ratio of AMP to ATP probably does not change in the PKC ϵ overexpressing mice because of their enhanced mitochondrial respiration, so there has to be another hypoxia-inducible factor involved in this gene switch. Likely candidates may include HIF-1, PGC-1 α or NRF-1 (see chapter 1).
- Activated PKC ϵ is present at the nucleus and could therefore influence transcription directly or via others transcription factors induced as a result of its action or by the hypoxic/anoxic insult. Examples of putative target genes may include UCP3, MHC β , and FA genes, resulting in augmented mitochondrial ATP production, thereby preserving RV contractile function.

These mechanisms may therefore account for the F KC ϵ mice displaying a fetal-like or glucose metabolism at baseline. However, the question of how the proposed switch to fatty acid metabolism occurs in response to the chronic hypoxic stimulus still remains.

I speculate as follows:

Akt also activates the transcription factor FOXO-1.[239] Via the recruitment of one of the hypoxia-induced transcription factor (like HIF-1, PGC-1 α or NRF-1) malonyl CoA decarboxylase (MCD) could be induced in response to a chronic hypoxic stress. This might also be mediated directly by the forkhead transcription factor FOXO-1,[240,241] as FOXO-1 has been shown to regulate metabolic genes. MCD would degrade malonyl-CoA, thus relieving the inhibition on CPT-1 and simultaneously decreasing the activity of acetyl CoA carboxylase (ACC). This would increase FA transport into the mitochondria, stimulating FAO enzymes and facilitate the switch from glucose to fatty acid metabolism.

5.4 Future directions

I plan to confirm that the observed changes in mRNA expression observed are in fact paralleled at the translational (protein) and activity level.

Ex vivo substrate metabolism studies will be performed on overexpressing constitutively active PKC ϵ and littermate age- and sex-matched control mice to confirm fuel substrate preferences suggested by the gene data. If these measurements are successful, we will extend them to include the hypoxic animals.

I would like to further explore the proposed mechanism (Fig. 5-1), utilizing adult cardiomyocytes isolated from WT and PKC ϵ overexpressing mice. These cells would be subjected to simulated ischemia, according to a method already established in our laboratory. Metabolism studies (FA uptake and FAO, glucose uptake and oxidation) will be performed on the myocytes using appropriate radiolabelled substrates to confirm fuel preference switches after subjection to a chronic stress. Known inhibitors and activators of the various steps in our proposed scheme could be utilized to confirm putative mechanisms.

To affirm our mRNA expression levels assayed by RT-PCR, hypoxic and normoxic heart tissue from aPKC ϵ mice and wildtype littermate controls will be screened for transcriptional modulation utilizing Affymetrix gene array. This work will form part of a collaborative study with Prof Michael Sack of the National Institute of Health in Washington, USA,. Proteomics studies will also be performed on the tissue to further investigate PKC ϵ interactions in response to the hypoxic stimulus.

5.5 Possible clinical applications

Dr Daria Mochly-Rosen has developed an activated PKC ϵ peptide, which behaves exactly as the full protein – it is induced by PMA (phorbol myristate acetate) and protects against ischemia/reperfusion damage. It is injectable intraperitoneally or intravenously and confers protection, although the molecular mechanisms and signaling pathways are not completely clarified.

PKC isozymes act in concert - a decrease in one isoform triggers a compensatory increase in the others and vice versa. PKC δ antagonizes the action of PKC ϵ , so Dr Mochly-Rosen administered a PKC δ inhibitor together with the PKC ϵ activated peptide and improved the protection. At this point, the protection is of the order of hours, but has obvious clinical implications. If a patient presenting with an acute MI can be injected with a peptide by either route and be protected from the deleterious effects of the reperfusion period, this could be beneficial. Human trials are still a relatively distant prospect, but trials in large animals are underway.

The understanding of the mechanism of PKC ϵ protection is now extended: the activated PKC ϵ peptide prevents oxidant damage by stabilizing the MPTP, maintaining ATP production and thereby preventing apoptosis and hypertrophy, while initiating the switch from FAO to glucose oxidation, known to be protective

during and after ischemia/reperfusion events, via modulation of metabolic gene transcription.

Novel transcriptional targets for PKC ϵ have been identified in this study, GLUT1, MHC β and UCP3. Both GLUT1 and MHC β are part of the fetal gene program known to protect the heart during stress. This could account for the resistance at baseline to anoxic stress. With an hypoxic insult, this fetal-like metabolism is lost and these mice resemble WT and normoxics. However, the reduced UCP3 with hypoxia suggests that constitutively active PKC ϵ , translocated to the nucleus, can regulate transcription of UCP3 in response to an hypoxic stress and confer protection in this manner, by reducing uncoupling of mitochondrial oxidative phosphorylation.

5.6 Limitations of the study

1. Transgenic overexpressing models are not considered physiological as the response is exaggerated in order to examine the molecule or pathway under investigation. The model is extreme and as such, the results obtained have to be regarded with this in mind. A PKC ϵ knock-out mouse is now available and it would be interesting to explore the pathways outlined above utilizing this mouse to delineate PKC ϵ function.

2. Hypobaric hypoxia is only a physiological stress for people and animals living at high altitude or with diseased hearts, so the application and physiological relevance of this data might be considered limited. However, babies

born with cyanotic defects are hypoxic. Perhaps a more clinically relevant model would be an *in vivo* ischemia/reperfusion model. When this study was performed, this technique was not available to us, so we utilized an established model: hypobaric hypoxia model. It should be interesting to repeat the chronic study in a ligated mouse heart model and compare the outcome.

3. It should also be valid to extend the temporal study further to 21 days or even to contractile dysfunction and chart the changes with time to confirm that the indicated shifts in fuel preference do in fact occur. We could also stress the PKC ϵ mice by dietary intervention e.g. high fat diet, and explore the outcome and mechanism.

4. In the first part of the study, excess ADP-induced anoxia was used as an acute stress, which may be criticized as being unphysiological. Investigation of mechanisms in isolated mitochondria may also be similarly criticized. However, the purpose and part-hypothesis of the study was to determine the protective effect of PKC ϵ overexpression on the mitochondria directly, as activated PKC ϵ translocates to the mitochondrion. In addition, we might utilize muscle strips to investigate the PKC ϵ interactions in a more physiological setting for the follow-up studies.

5.7 Publications arising from this work

Papers

McCarthy J, McLeod CJ, Minners JO, Essop MF, Ping P, Sack MN.

PKC ϵ activation augments cardiac mitochondrial respiratory post-anoxic reserve – a putative mechanism in PKC ϵ cardioprotection. J Mol Cell Cardiol, 2005 38(4): 697-700.

McCarthy J, Essop MF, Sack MN, Opie LH.

Moderate overexpression of constitutively active PKC ϵ protects the myocardium by an alteration in metabolism. Manuscript in preparation.

Published Abstracts presented at International Meetings

1. American Heart Association Congress, Florida . November, 2003

McCarthy J, Minners JO, McLeod CJ, Ping P, Sack MN.

PKC ϵ activation augments cardiac mitochondrial respiratory capacity – a putative mechanism in attenuating mitochondrial permeability transition.

Circ 2003; 108 (17): abstract suppl, abstract number 1302.

2. SA Heart Congress , Cape Town, October 2003

McCarthy J, Minners JO, McLeod CJ, Ping P, Sack MN

PKC ϵ activation augments cardiac mitochondrial respiratory capacity – a putative mechanism in attenuating mitochondrial permeability transition.

3. ISHR Satellite meeting: Cellular Injury in Ischemia. August, 2004.

McCarthy J, McLeod CJ, Ping P, Essop MF, Sack MN.

PKC ϵ protects by preserving mitochondrial integrity and preventing MPT

Cardiovasc J of SA: 15(4):suppl 1,s10

4. SA Heart Congress, Durban 2004

McCarthy J, McLeod CJ, Ping P, Essop MF, Sack MN.

Divergent PKC ϵ signaling in response to chronic hypobaric hypoxia preserves mitochondrial integrity and contractile function despite impaired hypertrophic response. SA Heart J, Sept 2004 1(3): p55

5. ISHR European Chapter, Silver Jubilee Meeting, Tromso Norway. June 2005

McCarthy J, Sharma S, Taegtmeyer H, Essop MF.

PKC ϵ protects against chronic hypobaric hypoxia by preserving mitochondrial respiratory capacity and through metabolic gene switching. J Mol Cell Cardiol 2005;38,997.

REFERENCES

1. Dorn, G.W., 2nd, et al., *Sustained in vivo cardiac protection by a rationally designed peptide that causes epsilon protein kinase C translocation*. Proc Natl Acad Sci U S A, 1999. **96**(22): p. 12798-803.
2. Cross, H.R., et al., *Expression of activated PKC epsilon (PKC epsilon) protects the ischemic heart, without attenuating ischemic H(+) production*. J Mol Cell Cardiol, 2002. **34**(3): p. 361-7.
3. Baines, C.P., et al., *Protein kinase Cepsilon interacts with and inhibits the permeability transition pore in cardiac mitochondria*. Circ Res, 2003. **92**(8): p. 873-80.
4. Ping, P., et al., *Ischemic preconditioning induces selective translocation of protein kinase C isoforms epsilon and eta in the heart of conscious rabbits without subcellular redistribution of total protein kinase C activity*. Circ Res, 1997. **81**(3): p. 404-14.
5. Zhang, J., et al., *Cardioprotection involves activation of NF-kappa B via PKC-dependent tyrosine and serine phosphorylation of I kappa B-alpha*. Am J Physiol Heart Circ Physiol, 2003. **285**(4): p. H1753-8.
6. Hu, K., D. Mochly-Rosen, and M. Boutjdir, *Evidence for functional role of epsilonPKC isozyme in the regulation of cardiac Ca(2+) channels*. Am J Physiol Heart Circ Physiol, 2000. **279**(6): p. H2658-64.
7. Ping, P., et al., *Formation of protein kinase C(epsilon)-Lck signaling modules confers cardioprotection*. J Clin Invest, 2002. **109**(4): p. 499-507.
8. Hausenloy, D.J., M.R. Duchon, and D.M. Yellon, *Inhibiting mitochondrial permeability transition pore opening at reperfusion protects against ischaemia-reperfusion injury*. Cardiovasc Res, 2003. **60**(3): p. 617-25.
9. Opie, L.H., *The Heart*. Fourth Edition ed. 2004: Lippincott Williams & Wilkins.
10. Russell, L.K., B.N. Finck, and D.P. Kelly, *Mouse models of mitochondrial dysfunction and heart failure*. J Mol Cell Cardiol, 2005. **38**(1): p. 81-91.

11. Murray CJL, L.A., *The Global Burden of Disease*. Global Burden of Disease and Injury Series, ed. M.C.a.L. AD. 1996, Boston: World Health Organization, Geneva, Switzerland and Harvard Medical School, Boston, USA. 990.
12. Leeder S, R.S., Greenberg H, Liu H, Esson K., *A Race Against Time: The challenge of Cardiovascular Disease in Developing Economies*. 2004: Trustees of Columbia University in the City of New York.
13. Bradshaw, D., *What do we know about the burden of cardiovascular disease in South Africa?* *Cardiovasc J S Afr*, 2005. **16**(3): p. 140-1.
14. Mollentze, W.F., et al., *Coronary heart disease risk factors in a rural and urban Orange Free State black population*. *S Afr Med J*, 1995. **85**(2): p. 90-6.
15. Segal, I., et al., *Glycaemic responses to different carbohydrate foods in healthy and diabetic blacks in Soweto*. *S Afr Med J*, 1991. **80**(11-12): p. 546-9.
16. Dorland, *Dorland's Illustrated Medical dictionary*. 1965: WB Saunders.
17. Maroko, P.R., et al., *Factors influencing infarct size following experimental coronary artery occlusions*. *Circulation*, 1971. **43**(1): p. 67-82.
18. Kloner, R.A., *Lethal "Reperfusion Injury": Is It a Real Entity?* *J Thromb Thrombolysis*, 1997. **4**(1): p. 127-128.
19. Bright, R. and D. Mochly-Rosen, *The role of protein kinase C in cerebral ischemic and reperfusion injury*. *Stroke*, 2005. **36**(12): p. 2781-90.
20. Cross, H.R., et al., *Is a high glycogen content beneficial or detrimental to the ischemic rat heart? A controversy resolved*. *Circ Res*, 1996. **78**(3): p. 482-91.
21. Duchon, M.R., *Roles of mitochondria in health and disease*. *Diabetes*, 2004. **53 Suppl 1**: p. S96-S102.
22. Honda, H.M., P. Korge, and J.N. Weiss, *Mitochondria and ischemia/reperfusion injury*. *Ann N Y Acad Sci*, 2005. **1047**: p. 248-58.

23. Jennings, R.B. and K.A. Reimer, *Factors involved in salvaging ischemic myocardium: effect of reperfusion of arterial blood*. *Circulation*, 1983. **68**(2 Pt 2): p. 125-36.
24. Cain, B.S., D.R. Meldrum, and A.H. Harken, *Protein kinase C in normal and pathologic myocardial states*. *J Surg Res*, 1999. **81**(2): p. 249-59.
25. Meldrum, D.R., et al., *Cardiac surgical implications of calcium dyshomeostasis in the heart*. *Ann Thorac Surg*, 1996. **61**(4): p. 1273-80.
26. Speechly-Dick, M.E., G.J. Grover, and D.M. Yellon, *Does ischemic preconditioning in the human involve protein kinase C and the ATP-dependent K⁺ channel? Studies of contractile function after simulated ischemia in an atrial in vitro model*. *Circ Res*, 1995. **77**(5): p. 1030-5.
27. Murry, C.E., R.B. Jennings, and K.A. Reimer, *Preconditioning with ischemia: a delay of lethal cell injury in ischemic myocardium*. *Circulation*, 1986. **74**(5): p. 1124-36.
28. Jennings, R.B., K.A. Reimer, and C. Steenbergen, *Myocardial ischemia revisited. The osmolar load, membrane damage, and reperfusion*. *J Mol Cell Cardiol*, 1986. **18**(8): p. 769-80.
29. Jennings, R.B., et al., *Myocardial necrosis induced by temporary occlusion of a coronary artery in the dog*. *Arch Pathol*, 1960. **70**: p. 68-78.
30. Jennings, R.B., et al., *Ischemic injury of myocardium*. *Ann N Y Acad Sci*, 1969. **156**(1): p. 61-78.
31. Hearse, D.J., S.M. Humphrey, and E.B. Chain, *Abrupt reoxygenation of the anoxic potassium-arrested perfused rat heart: a study of myocardial enzyme release*. *J Mol Cell Cardiol*, 1973. **5**(4): p. 395-407.
32. Opie, L.H., *Reperfusion injury and its pharmacologic modification*. *Circulation*, 1989. **80**(4): p. 1049-62.
33. Lambiase, P.D., et al., *Exercise-induced ischemia initiates the second window of protection in humans independent of collateral recruitment*. *J Am Coll Cardiol*, 2003. **41**(7): p. 1174-82.

34. Thornton, J.D., et al., *Intravenous pretreatment with A1-selective adenosine analogues protects the heart against infarction*. *Circulation*, 1992. **85**(2): p. 659-65.
35. Verdouw, P.D., B.C. Gho, and D.J. Duncker, *Cardioprotection by organs in stress or distress*. *Basic Res Cardiol*, 1996. **91**(1): p. 44-6.
36. Wolfrum, S., et al., *Remote preconditioning protects the heart by activating myocardial PKCepsilon-isoform*. *Cardiovasc Res*, 2002. **55**(3): p. 583-9.
37. Zhao, Z.Q., et al., *Inhibition of myocardial injury by ischemic postconditioning during reperfusion: comparison with ischemic preconditioning*. *Am J Physiol Heart Circ Physiol*, 2003. **285**(2): p. H579-88.
38. Staat, P., et al., *Postconditioning the human heart*. *Circulation*, 2005. **112**(14): p. 2143-8.
39. Tsang, A., et al., *Postconditioning: a form of "modified reperfusion" protects the myocardium by activating the phosphatidylinositol 3-kinase-Akt pathway*. *Circ Res*, 2004. **95**(3): p. 230-2.
40. Garcia-Dorado, D. and H.M. Piper, *Postconditioning: Reperfusion of "reperfusion injury" after hibernation*. *Cardiovasc Res*, 2006. **69**(1): p. 1-3.
41. Newton, A.C., *Protein kinase C: structure, function, and regulation*. *J Biol Chem*, 1995. **270**(48): p. 28495-8.
42. Hug, H. and T.F. Sarre, *Protein kinase C isoenzymes: divergence in signal transduction?* *Biochem J*, 1993. **291** (Pt 2): p. 329-43.
43. Sugden, P.H. and M.A. Bogoyevitch, *Intracellular signalling through protein kinases in the heart*. *Cardiovasc Res*, 1995. **30**(4): p. 478-92.
44. Steinberg, S.F., M. Goldberg, and V.O. Rybin, *Protein kinase C isoform diversity in the heart*. *J Mol Cell Cardiol*, 1995. **27**(1): p. 141-53.
45. Simkhovich, B.Z., K. Przyklenk, and R.A. Kloner, *Role of protein kinase C as a cellular mediator of ischemic preconditioning: a critical review*. *Cardiovasc Res*, 1998. **40**(1): p. 9-22.
46. Jideama, N.M., et al., *Phosphorylation specificities of protein kinase C isozymes for bovine cardiac troponin I and troponin T and sites within*

- these proteins and regulation of myofilament properties.* J Biol Chem, 1996. **271**(38): p. 23277-83.
47. Chen, L., et al., *Opposing cardioprotective actions and parallel hypertrophic effects of delta PKC and epsilon PKC.* Proc Natl Acad Sci U S A, 2001. **98**(20): p. 11114-9.
 48. Budnikhov YY, P.A., Doroshchuk, A.G. AD, Postnov YV., and K. 47-50, *Method for rate of ATP synthesis.* Kardiologiya, 2002. **42**(12): p. 47-50.
 49. Murphy, S. and W.H. Frishman, *Protein kinase C in cardiac disease and as a potential therapeutic target.* Cardiol Rev, 2005. **13**(1): p. 3-12.
 50. Kishimoto, A., et al., *Activation of calcium and phospholipid-dependent protein kinase by diacylglycerol, its possible relation to phosphatidylinositol turnover.* J Biol Chem, 1980. **255**(6): p. 2273-6.
 51. Nishizuka, Y., *Protein kinase C and lipid signaling for sustained cellular responses.* Faseb J, 1995. **9**(7): p. 484-96.
 52. Rouet-Benzineb, P., et al., *Protein kinase C isoform expression in normal and failing rabbit hearts.* Circ Res, 1996. **79**(2): p. 153-61.
 53. MacLeod, K.T. and S.E. Harding, *Effects of phorbol ester on contraction, intracellular pH and intracellular Ca²⁺ in isolated mammalian ventricular myocytes.* J Physiol, 1991. **444**: p. 481-98.
 54. Capogrossi, M.C., et al., *Phorbol ester and dioctanoylglycerol stimulate membrane association of protein kinase C and have a negative inotropic effect mediated by changes in cytosolic Ca²⁺ in adult rat cardiac myocytes.* Circ Res, 1990. **66**(4): p. 1143-55.
 55. Armstrong, S.C., *Protein kinase activation and myocardial ischemia/reperfusion injury.* Cardiovasc Res, 2004. **61**(3): p. 427-36.
 56. Yoshida, K., et al., *Translocation of protein kinase C-alpha, delta and epsilon isoforms in ischemic rat heart.* Biochim Biophys Acta, 1996. **1317**(1): p. 36-44.
 57. Albert, C.J. and D.A. Ford, *Protein kinase C translocation and PKC-dependent protein phosphorylation during myocardial ischemia.* Am J Physiol, 1999. **276**(2 Pt 2): p. H642-50.

58. Inagaki, K., et al., *Additive protection of the ischemic heart ex vivo by combined treatment with delta-protein kinase C inhibitor and epsilon-protein kinase C activator*. *Circulation*, 2003. **108**(7): p. 869-75.
59. Downey, J.M. and M.V. Cohen, *Signal transduction in ischemic preconditioning*. *Z Kardiol*, 1995. **84 Suppl 4**: p. 77-86.
60. Ytrehus, K., et al., *Rat and rabbit heart infarction: effects of anesthesia, perfusate, risk zone, and method of infarct sizing*. *Am J Physiol*, 1994. **267**(6 Pt 2): p. H2383-90.
61. Liu, Y., K. Ytrehus, and J.M. Downey, *Evidence that translocation of protein kinase C is a key event during ischemic preconditioning of rabbit myocardium*. *J Mol Cell Cardiol*, 1994. **26**(5): p. 661-8.
62. Saurin, A.T., et al., *Targeted disruption of the protein kinase C epsilon gene abolishes the infarct size reduction that follows ischaemic preconditioning of isolated buffer-perfused mouse hearts*. *Cardiovasc Res*, 2002. **55**(3): p. 672-80.
63. Goto, M., et al., *Role of bradykinin in protection of ischemic preconditioning in rabbit hearts*. *Circ Res*, 1995. **77**(3): p. 611-21.
64. Yellon, D.M. and J.M. Downey, *Preconditioning the myocardium: from cellular physiology to clinical cardiology*. *Physiol Rev*, 2003. **83**(4): p. 1113-51.
65. Hausenloy, D.J., A. Tsang, and D.M. Yellon, *The reperfusion injury salvage kinase pathway: a common target for both ischemic preconditioning and postconditioning*. *Trends Cardiovasc Med*, 2005. **15**(2): p. 69-75.
66. Zhang, J., et al., *Functional proteomic analysis of a three-tier PKCepsilon-Akt-eNOS signaling module in cardiac protection*. *Am J Physiol Heart Circ Physiol*, 2005. **288**(2): p. H954-61.
67. Gray, M.O., J.S. Karliner, and D. Mochly-Rosen, *A selective epsilon-protein kinase C antagonist inhibits protection of cardiac myocytes from hypoxia-induced cell death*. *J Biol Chem*, 1997. **272**(49): p. 30945-51.

68. Liu, G.S., et al., *Protein kinase C-epsilon is responsible for the protection of preconditioning in rabbit cardiomyocytes*. J Mol Cell Cardiol, 1999. **31**(10): p. 1937-48.
69. Ping, P., et al., *Functional proteomic analysis of protein kinase C epsilon signaling complexes in the normal heart and during cardioprotection*. Circ Res, 2001. **88**(1): p. 59-62.
70. Edmondson, R.D., et al., *Protein kinase C epsilon signaling complexes include metabolism- and transcription/translation-related proteins: complimentary separation techniques with LC/MS/MS*. Mol Cell Proteomics, 2002. **1**(6): p. 421-33.
71. Kim, L.H., LeMasters JJ, *MPT - a common pathway to necrosis and apoptosis*. BBRC, 2003. **304**: p. 463-470.
72. Gores, G.J., et al., *Intracellular pH during "chemical hypoxia" in cultured rat hepatocytes. Protection by intracellular acidosis against the onset of cell death*. J Clin Invest, 1989. **83**(2): p. 386-96.
73. Bronk, S.F. and G.J. Gores, *Efflux of protons from acidic vesicles contributes to cytosolic acidification of hepatocytes during ATP depletion*. Hepatology, 1991. **14**(4 Pt 1): p. 626-33.
74. Qian, T., et al., *Mitochondrial permeability transition in pH-dependent reperfusion injury to rat hepatocytes*. Am J Physiol, 1997. **273**(6 Pt 1): p. C1783-92.
75. Halestrap, A.P. and A.M. Davidson, *Inhibition of Ca²⁺-induced large-amplitude swelling of liver and heart mitochondria by cyclosporin is probably caused by the inhibitor binding to mitochondrial-matrix peptidyl-prolyl cis-trans isomerase and preventing it interacting with the adenine nucleotide translocase*. Biochem J, 1990. **268**(1): p. 153-60.
76. Kloner, R.A., et al., *Protection Conferred by Preinfarct Angina is Manifest in the Aged Heart: Evidence from the TIMI 4 Trial*. J Thromb Thrombolysis, 1998. **6**(2): p. 89-92.

77. Baines, C.P. and J.D. Molkentin, *STRESS signaling pathways that modulate cardiac myocyte apoptosis*. J Mol Cell Cardiol, 2005. **38**(1): p. 47-62.
78. Inagaki, K., et al., *Cardioprotection by epsilon-protein kinase C activation from ischemia: continuous delivery and antiarrhythmic effect of an epsilon-protein kinase C-activating peptide*. Circulation, 2005. **111**(1): p. 44-50.
79. Bing, R.J., et al., *Metabolic studies on the human heart in vivo. I. Studies on carbohydrate metabolism of the human heart*. Am J Med, 1953. **15**(3): p. 284-96.
80. Essop, M.F. and L.H. Opie, *Metabolic therapy for heart failure*. Eur Heart J, 2004. **25**(20): p. 1765-8.
81. Jacobson J, D.M.R., *Interplay between mitochondria and cellular calcium signalling*. Molecular and cellular Biochemistry, 2004. **256/257**: p. 209-218.
82. Opie, L.H., *Metabolism of the heart in health and disease. I*. Am Heart J, 1968. **76**(5): p. 685-98.
83. Kroemer, G., *Mitochondrial control of apoptosis: an introduction*. Biochem Biophys Res Commun, 2003. **304**(3): p. 433-5.
84. Regula, K.M. and L.A. Kirshenbaum, *Apoptosis of ventricular myocytes: a means to an end*. J Mol Cell Cardiol, 2005. **38**(1): p. 3-13.
85. Petronilli V, P.D., Scorrano L, Bernardi P, di Lisa F, *The Mitochondrial Permeability Transition, Release of cytochrome C and Cell Death*. Journal of Biological Chemistry, 2000. **276**(15): p. 12030-12034.
86. Stryer, L., *Biochemistry*. 3rd ed. 1988: WH Freeman and Company , NY. 1089.
87. Anderson, S., et al., *Sequence and organization of the human mitochondrial genome*. Nature, 1981. **290**(5806): p. 457-65.
88. Lehninger, A.L., *Biochemistry The Molecular Basis of Cell Structure and Function*. 1972: Worth Publishers Inc. 833.

89. Paradies, G., et al., *Decrease in mitochondrial complex I activity in ischemic/reperfused rat heart: involvement of reactive oxygen species and cardiolipin*. *Circ Res*, 2004. **94**(1): p. 53-9.
90. Halestrap, A.P., G.P. McStay, and S.J. Clarke, *The permeability transition pore complex: another view*. *Biochimie*, 2002. **84**(2-3): p. 153-66.
91. Brown, N.F., et al., *Mitochondrial carnitine palmitoyltransferase I isoform switching in the developing rat heart*. *J Biol Chem*, 1995. **270**(15): p. 8952-7.
92. McFalls, E.O., et al., *Mitochondrial function: the heart of myocardial preservation*. *J Lab Clin Med*, 2003. **142**(3): p. 141-8.
93. Mitchell, P., *Keilin's respiratory chain concept and its chemiosmotic consequences*. *Science*, 1979. **206**(4423): p. 1148-59.
94. Klingenberg, M. and D.R. Nelson, *Structure-function relationships of the ADP/ATP carrier*. *Biochim Biophys Acta*, 1994. **1187**(2): p. 241-4.
95. Rousset, S., et al., *The biology of mitochondrial uncoupling proteins*. *Diabetes*, 2004. **53** Suppl 1: p. S130-5.
96. Krauss, S., C.Y. Zhang, and B.B. Lowell, *The mitochondrial uncoupling-protein homologues*. *Nat Rev Mol Cell Biol*, 2005. **6**(3): p. 248-61.
97. Lindqvist, A., et al., *Decreased UCP2 mRNA expression in rat stomach following vagotomy: novel role for UCP2 as free radical scavenger in the stomach?* *Nutr Neurosci*, 2004. **7**(4): p. 217-22.
98. Pawade, T., et al., *Uncoupling proteins: targets of endocrine disruptors?* *Mol Cell Endocrinol*, 2005. **244**(1-2): p. 79-86.
99. Andrews, Z.B., S. Diano, and T.L. Horvath, *Mitochondrial uncoupling proteins in the CNS: in support of function and survival*. *Nat Rev Neurosci*, 2005. **6**(11): p. 829-40.
100. Sokolova, I.M. and E.P. Sokolov, *Evolution of mitochondrial uncoupling proteins: novel invertebrate UCP homologues suggest early evolutionary divergence of the UCP family*. *FEBS Lett*, 2005. **579**(2): p. 313-7.

101. Saleh, M.C., M.B. Wheeler, and C.B. Chan, *Uncoupling protein-2: evidence for its function as a metabolic regulator*. *Diabetologia*, 2002. **45**(2): p. 174-87.
102. Zhang, C.Y., et al., *Uncoupling protein-2 negatively regulates insulin secretion and is a major link between obesity, beta cell dysfunction, and type 2 diabetes*. *Cell*, 2001. **105**(6): p. 745-55.
103. Arsenijevic, D., et al., *Disruption of the uncoupling protein-2 gene in mice reveals a role in immunity and reactive oxygen species production*. *Nat Genet*, 2000. **26**(4): p. 435-9.
104. Teshima, Y., et al., *Uncoupling protein-2 overexpression inhibits mitochondrial death pathway in cardiomyocytes*. *Circ Res*, 2003. **93**(3): p. 192-200.
105. Boss, O., T. Hagen, and B.B. Lowell, *Uncoupling proteins 2 and 3: potential regulators of mitochondrial energy metabolism*. *Diabetes*, 2000. **49**(2): p. 143-56.
106. Garlid, K.D., M. Jaburek, and P. Jezek, *The mechanism of proton transport mediated by mitochondrial uncoupling proteins*. *FEBS Lett*, 1998. **438**(1-2): p. 10-4.
107. Talbot, D.A., A.J. Lambert, and M.D. Brand, *Production of endogenous matrix superoxide from mitochondrial complex I leads to activation of uncoupling protein 3*. *FEBS Lett*, 2004. **556**(1-3): p. 111-5.
108. Clapham, J.C., et al., *Mice overexpressing human uncoupling protein-3 in skeletal muscle are hyperphagic and lean*. *Nature*, 2000. **406**(6794): p. 415-8.
109. Harper, M.E., et al., *Decreased mitochondrial proton leak and reduced expression of uncoupling protein 3 in skeletal muscle of obese diet-resistant women*. *Diabetes*, 2002. **51**(8): p. 2459-66.
110. Lanouette, C.M., et al., *Association between uncoupling protein 3 gene and obesity-related phenotypes in the Quebec Family Study*. *Mol Med*, 2001. **7**(7): p. 433-41.

111. Skarka, L., et al., *Expression of mitochondrial uncoupling protein 3 and adenine nucleotide translocase 1 genes in developing rat heart: putative involvement in control of mitochondrial membrane potential*. J Mol Cell Cardiol, 2003. **35**(3): p. 321-30.
112. Ingwall, J.S., *Transgenesis and cardiac energetics: new insights into cardiac metabolism*. J Mol Cell Cardiol, 2004. **37**(3): p. 613-23.
113. Ingwall, J., *ATP and the Heart*, ed. B. Swynghedauw. 2002: Kluwer Academic Publishers.
114. Kaasik, A., et al., *Energetic crosstalk between organelles: architectural integration of energy production and utilization*. Circ Res, 2001. **89**(2): p. 153-9.
115. Bessman, S.P. and C.L. Carpenter, *The creatine-creatine phosphate energy shuttle*. Annu Rev Biochem, 1985. **54**: p. 831-62.
116. Janssen, E., et al., *Adenylate kinase 1 gene deletion disrupts muscle energetic economy despite metabolic rearrangement*. Embo J, 2000. **19**(23): p. 6371-81.
117. Kaasik, A., et al., *A novel mechanism of regulation of cardiac contractility by mitochondrial functional state*. Faseb J, 2004. **18**(11): p. 1219-27.
118. Garnier, A., et al., *Depressed mitochondrial transcription factors and oxidative capacity in rat failing cardiac and skeletal muscles*. J Physiol, 2003. **551**(Pt 2): p. 491-501.
119. Ventura-Clapier, R., A. Garnier, and V. Veksler, *Energy metabolism in heart failure*. J Physiol, 2004. **555**(Pt 1): p. 1-13.
120. Finck, B.N., et al., *Regulatory networks controlling mitochondrial energy production in the developing, hypertrophied, and diabetic heart*. Cold Spring Harb Symp Quant Biol, 2002. **67**: p. 371-82.
121. Nishio, Y., et al., *Regulation and role of the mitochondrial transcription factor in the diabetic rat heart*. Ann N Y Acad Sci, 2004. **1011**: p. 78-85.
122. Shen, X., et al., *Cardiac mitochondrial damage and biogenesis in a chronic model of type 1 diabetes*. Am J Physiol Endocrinol Metab, 2004. **287**(5): p. E896-905.

123. Sparks, L.M., et al., *A high-fat diet coordinately downregulates genes required for mitochondrial oxidative phosphorylation in skeletal muscle*. *Diabetes*, 2005. **54**(7): p. 1926-33.
124. Razeghi, P., et al., *Hypoxia-induced switches of myosin heavy chain iso-gene expression in rat heart*. *Biochem Biophys Res Commun*, 2003. **303**(4): p. 1024-7.
125. Ray, J., et al., *Long-chain fatty acids increase basal metabolism and depolarize mitochondria in cardiac muscle cells*. *Am J Physiol Heart Circ Physiol*, 2002. **282**(4): p. H1495-501.
126. Schonfeld, P., M.R. Wieckowski, and L. Wojtczak, *Long-chain fatty acid-promoted swelling of mitochondria: further evidence for the protonophoric effect of fatty acids in the inner mitochondrial membrane*. *FEBS Lett*, 2000. **471**(1): p. 108-12.
127. Skulachev, V.P., *Uncoupling: new approaches to an old problem of bioenergetics*. *Biochim Biophys Acta*, 1998. **1363**(2): p. 100-24.
128. Martin, G., et al., *Coordinate regulation of the expression of the fatty acid transport protein and acyl-CoA synthetase genes by PPARalpha and PPARgamma activators*. *J Biol Chem*, 1997. **272**(45): p. 28210-7.
129. Schoonjans, K., et al., *PPARalpha and PPARgamma activators direct a distinct tissue-specific transcriptional response via a PPRE in the lipoprotein lipase gene*. *Embo J*, 1996. **15**(19): p. 5336-48.
130. McCarthy, J., et al., *PKCepsilon activation augments cardiac mitochondrial respiratory post-anoxic reserve—a putative mechanism in PKCepsilon cardioprotection*. *J Mol Cell Cardiol*, 2005. **38**(4): p. 697-700.
131. Gleyzer, N., K. Vercauteren, and R.C. Scarpulla, *Control of mitochondrial transcription specificity factors (TFB1M and TFB2M) by nuclear respiratory factors (NRF-1 and NRF-2) and PGC-1 family coactivators*. *Mol Cell Biol*, 2005. **25**(4): p. 1354-66.
132. Young, M.E., et al., *Intrinsic diurnal variations in cardiac metabolism and contractile function*. *Circ Res*, 2001. **89**(12): p. 1199-208.

133. Sharma, S., et al., *Dynamic changes of gene expression in hypoxia-induced right ventricular hypertrophy*. *Am J Physiol Heart Circ Physiol*, 2004. **286**(3): p. H1185-92.
134. Garland, J.M. and A. Halestrap, *Energy metabolism during apoptosis. Bcl-2 promotes survival in hematopoietic cells induced to apoptose by growth factor withdrawal by stabilizing a form of metabolic arrest*. *J Biol Chem*, 1997. **272**(8): p. 4680-8.
135. Rego, A.C., S. Vesce, and D.G. Nicholls, *The mechanism of mitochondrial membrane potential retention following release of cytochrome c in apoptotic GT1-7 neural cells*. *Cell Death Differ*, 2001. **8**(10): p. 995-1003.
136. Marzo, I., et al., *The permeability transition pore complex: a target for apoptosis regulation by caspases and bcl-2-related proteins*. *J Exp Med*, 1998. **187**(8): p. 1261-71.
137. Beutner, G., et al., *Complexes between porin, hexokinase, mitochondrial creatine kinase and adenylate translocator display properties of the permeability transition pore. Implication for regulation of permeability transition by the kinases*. *Biochim Biophys Acta*, 1998. **1368**(1): p. 7-18.
138. Bernardi, P., et al., *The mitochondrial permeability transition*. *Biofactors*, 1998. **8**(3-4): p. 273-81.
139. Zoratti, M., I. Szabo, and U. De Marchi, *Mitochondrial permeability transitions: how many doors to the house?* *Biochim Biophys Acta*, 2005. **1706**(1-2): p. 40-52.
140. Reed, J.C., *Bcl-2 family proteins*. *Oncogene*, 1998. **17**(25): p. 3225-36.
141. Kowaltowski, A.J., *Alternative mitochondrial functions in cell physiopathology: beyond ATP production*. *Braz J Med Biol Res*, 2000. **33**(2): p. 241-50.
142. Danial, N.N. and S.J. Korsmeyer, *Cell death: critical control points*. *Cell*, 2004. **116**(2): p. 205-19.
143. Green, D.R. and G. Kroemer, *The pathophysiology of mitochondrial cell death*. *Science*, 2004. **305**(5684): p. 626-9.

144. Dejean, L.M., et al., *Regulation of the mitochondrial apoptosis-induced channel, MAC, by BCL-2 family proteins*. *Biochim Biophys Acta*, 2006. **1762**(2): p. 191-201.
145. Doran E, H.A., *Cytochrome C release from isolate rat liver mitochondria can occur independently of outer-membrane rupture: possible role of contact sites*. *Biochemical Journal*, 2000. **348**: p. 343-350.
146. Halestrap, A.P., *The mitochondrial permeability transition pore in reperfusion injury and cardioprotection*. *Cardiovasc J S Afr*, 2004. **15**(4 Suppl 1): p. S5.
147. Halestrap, A., *Biochemistry: a pore way to die*. *Nature*, 2005. **434**(7033): p. 578-9.
148. Kokoszka, J.E., et al., *The ADP/ATP translocator is not essential for the mitochondrial permeability transition pore*. *Nature*, 2004. **427**(6973): p. 461-5.
149. Halestrap, A.P., *Mitochondrial permeability: dual role for the ADP/ATP translocator?* *Nature*, 2004. **430**(7003): p. 1 p following 983.
150. Liu, X., et al., *Induction of apoptotic program in cell-free extracts: requirement for dATP and cytochrome c*. *Cell*, 1996. **86**(1): p. 147-57.
151. Wei, M.C., et al., *Proapoptotic BAX and BAK: a requisite gateway to mitochondrial dysfunction and death*. *Science*, 2001. **292**(5517): p. 727-30.
152. De Giorgi, F., et al., *The permeability transition pore signals apoptosis by directing Bax translocation and multimerization*. *Faseb J*, 2002. **16**(6): p. 607-9.
153. Pavlov, E.V., et al., *A novel, high conductance channel of mitochondria linked to apoptosis in mammalian cells and Bax expression in yeast*. *J Cell Biol*, 2001. **155**(5): p. 725-31.
154. Scorrano, L. and S.J. Korsmeyer, *Mechanisms of cytochrome c release by proapoptotic BCL-2 family members*. *Biochem Biophys Res Commun*, 2003. **304**(3): p. 437-44.

155. Wieckowski, M.R., D. Brdiczka, and L. Wojtczak, *Long-chain fatty acids promote opening of the reconstituted mitochondrial permeability transition pore*. FEBS Lett, 2000. **484**(2): p. 61-4.
156. Carafoli, E., *Historical review: mitochondria and calcium: ups and downs of an unusual relationship*. Trends Biochem Sci, 2003. **28**(4): p. 175-81.
157. Rizzuto, R., M.R. Duchen, and T. Pozzan, *Flirting in little space: the ER/mitochondria Ca²⁺ liaison*. Sci STKE, 2004. **2004**(215): p. re1.
158. Cain, K., S.B. Bratton, and G.M. Cohen, *The Apaf-1 apoptosome: a large caspase-activating complex*. Biochimie, 2002. **84**(2-3): p. 203-14.
159. Cao, W., et al., *TNF-alpha promotes Doxorubicin-induced cell apoptosis and anti-cancer effect through downregulation of p21 in p53-deficient tumor cells*. Biochem Biophys Res Commun, 2005. **330**(4): p. 1034-40.
160. Kumamoto, H. and K. Ooya, *Expression of tumor necrosis factor alpha, TNF-related apoptosis-inducing ligand, and their associated molecules in ameloblastomas*. J Oral Pathol Med, 2005. **34**(5): p. 287-94.
161. Takeishi, Y., et al., *Transgenic overexpression of constitutively active protein kinase C epsilon causes concentric cardiac hypertrophy*. Circ Res, 2000. **86**(12): p. 1218-23.
162. Pass, J.M., Gao J, Jones KW, Wead W et al, *Enhanced PKCbeta II translocation and PKCbeta II-RACK1 interactions in PKCe-induced heart failure : a role for RACK1*. Am J Physiol Heart Circ Physiol, 2001. **281**: p. H2500-2510.
163. Smith, R.M., et al., *Classic ischemic but not pharmacologic preconditioning is abrogated following genetic ablation of the TNFalpha gene*. Cardiovasc Res, 2002. **55**(3): p. 553-60.
164. Sumeray, M.S., D.D. Rees, and D.M. Yellon, *Infarct size and nitric oxide synthase in murine myocardium*. J Mol Cell Cardiol, 2000. **32**(1): p. 35-42.
165. Sordahl, L.A., et al., *Enzymatic aspects of the cardiac muscle cell: mitochondria, sarcoplasmic reticulum and nonvalent cation active transport system*. Methods Achiev Exp Pathol, 1971. **5**: p. 287-346.

166. Peterson, G.L., *A simplification of the protein assay method of Lowry et al. which is more generally applicable.* Anal Biochem, 1977. **83**(2): p. 346-56.
167. Henke, W., et al., *Ischemia-induced alterations of rat kidney mitochondria.* Transplantation, 1990. **49**(5): p. 997-9.
168. Ken-ichi Yabe, Y.N., Mamoru Sato, Rie Iijima, Satoshi Takeo, *Preconditioning preserves mitochondrial function and glycolytic flux during an early period of reperfusion in perfused rat hearts.* Cardiovascular Research, 1997. **33**: p. 677-685.
169. Dzeja, P.P., et al., *Targeting nucleotide-requiring enzymes: implications for diazoxide-induced cardioprotection.* Am J Physiol Heart Circ Physiol, 2003. **284**(4): p. H1048-56.
170. Plasek J, S.K., *Slow Fluorescent indicators of membrane potential: a survey of different approaches to probe response analysis.* J Photochem Photobiol B, 1996. **33**(2): p. 101-24.
171. Cossarizza, A., et al., *A new method for the cytofluorimetric analysis of mitochondrial membrane potential using the J-aggregate forming lipophilic cation 5,5',6,6'-tetrachloro-1,1',3,3'-tetraethylbenzimidazolcarbocyanine iodide (JC-1).* Biochem Biophys Res Commun, 1993. **197**(1): p. 40-5.
172. Yabe, K., et al., *Preconditioning preserves mitochondrial function and glycolytic flux during an early period of reperfusion in perfused rat hearts.* Cardiovasc Res, 1997. **33**(3): p. 677-85.
173. Smith, R.M., J. McCarthy, and M.N. Sack, *TNF alpha is required for hypoxia-mediated right ventricular hypertrophy.* Mol Cell Biochem, 2001. **219**(1-2): p. 139-43.
174. Depre, C., et al., *Unloaded heart in vivo replicates fetal gene expression of cardiac hypertrophy.* Nat Med, 1998. **4**(11): p. 1269-75.
175. Staat P, R.G., Piot C, et al, *Postconditioning the human heart.* Circulation (in press), 2005.
176. Esposito, L.A., et al., *Mitochondrial disease in mouse results in increased oxidative stress.* Proc Natl Acad Sci U S A, 1999. **96**(9): p. 4820-5.

177. Baxter, G.F., F.M. Goma, and D.M. Yellon, *Characterisation of the infarct-limiting effect of delayed preconditioning: timecourse and dose-dependency studies in rabbit myocardium*. Basic Res Cardiol, 1997. **92**(3): p. 159-67.
178. Strehler, B.L., *Bioluminescence assay: principles and practice*. Methods Biochem Anal, 1968. **16**: p. 99-181.
179. Xu, Y., V. Menon, and B.I. Jugdutt, *Cardioprotection after angiotensin II type 1 blockade involves angiotensin II type 2 receptor expression and activation of protein kinase C-epsilon in acutely reperfused myocardial infarction in the dog. Effect of UP269-6 and losartan on AT1 and AT2-receptor expression and IP3 receptor and PKCepsilon proteins*. J Renin Angiotensin Aldosterone Syst, 2000. **1**(2): p. 184-95.
180. Xu, Y., A.S. Clanachan, and B.I. Jugdutt, *Enhanced expression of angiotensin II type 2 receptor, inositol 1,4, 5-trisphosphate receptor, and protein kinase cepsilon during cardioprotection induced by angiotensin II type 2 receptor blockade*. Hypertension, 2000. **36**(4): p. 506-10.
181. Mitchell, P., *Vectorial chemistry and the molecular mechanics of chemiosmotic coupling: power transmission by proticity*. Biochem Soc Trans, 1976. **4**(3): p. 399-430.
182. Costa, A.D., et al., *Protein kinase G transmits the cardioprotective signal from cytosol to mitochondria*. Circ Res, 2005. **97**(4): p. 329-36.
183. Ping, P., et al., *Cardiac toxic effects of trans-2-hexenal are mediated by induction of cardiomyocyte apoptotic pathways*. Cardiovasc Toxicol, 2003. **3**(4): p. 341-51.
184. Abdel-Aleem, S., et al., *Metabolic changes in the normal and hypoxic neonatal myocardium*. Ann N Y Acad Sci, 1999. **874**: p. 254-61.
185. Ostadal, B., I. Ostadalova, and N.S. Dhalla, *Development of cardiac sensitivity to oxygen deficiency: comparative and ontogenetic aspects*. Physiol Rev, 1999. **79**(3): p. 635-59.
186. Acker, H., *Oxygen sensing in the carotid body: ideas and models*. Adv Exp Med Biol, 1994. **360**: p. 21-7.

187. Youngson, C., et al., *Oxygen sensing in airway chemoreceptors*. Nature, 1993. **365**(6442): p. 153-5.
188. Forsythe, J.A., et al., *Activation of vascular endothelial growth factor gene transcription by hypoxia-inducible factor 1*. Mol Cell Biol, 1996. **16**(9): p. 4604-13.
189. Detmar, M., *Molecular regulation of angiogenesis in the skin*. J Invest Dermatol, 1996. **106**(2): p. 207-8.
190. Ogita, F. and S. Taniguchi, *The comparison of peak oxygen uptake between swim-bench exercise and arm stroke*. Eur J Appl Physiol Occup Physiol, 1995. **71**(4): p. 295-300.
191. Goldberg, M.A., S.P. Dunning, and H.F. Bunn, *Regulation of the erythropoietin gene: evidence that the oxygen sensor is a heme protein*. Science, 1988. **242**(4884): p. 1412-5.
192. Maxwell, P.H., C.W. Pugh, and P.J. Ratcliffe, *Inducible operation of the erythropoietin 3' enhancer in multiple cell lines: evidence for a widespread oxygen-sensing mechanism*. Proc Natl Acad Sci U S A, 1993. **90**(6): p. 2423-7.
193. Wang, G.L., et al., *Hypoxia-inducible factor 1 is a basic-helix-loop-helix-PAS heterodimer regulated by cellular O₂ tension*. Proc Natl Acad Sci U S A, 1995. **92**(12): p. 5510-4.
194. Hochachka, P.W., et al., *Metabolic and work efficiencies during exercise in Andean natives*. J Appl Physiol, 1991. **70**(4): p. 1720-30.
195. Hochachka, P.W., et al., *Unifying theory of hypoxia tolerance: molecular/metabolic defense and rescue mechanisms for surviving oxygen lack*. Proc Natl Acad Sci U S A, 1996. **93**(18): p. 9493-8.
196. Bunn, H.F. and R.O. Poyton, *Oxygen sensing and molecular adaptation to hypoxia*. Physiol Rev, 1996. **76**(3): p. 839-85.
197. Heath D, W.D., *Man at High Altitude*. 1991, London: Churchill Livingstone. 3-23.

198. Harik, N., et al., *Time-course and reversibility of the hypoxia-induced alterations in cerebral vascularity and cerebral capillary glucose transporter density*. Brain Res, 1996. **737**(1-2): p. 335-8.
199. Winslow RM, M.C., *Hypoxia, polycythemia and chronic mountain sickness*. 1987, Baltimore: Johns Hopkins University Press.
200. Rumsey, W.L., et al., *Adaptation to hypoxia alters energy metabolism in rat heart*. Am J Physiol, 1999. **276**(1 Pt 2): p. H71-80.
201. Meirhaeghe, A., et al., *Characterization of the human, mouse and rat PGC1 beta (peroxisome-proliferator-activated receptor-gamma co-activator 1 beta) gene in vitro and in vivo*. Biochem J, 2003. **373**(Pt 1): p. 155-65.
202. Puigserver, P., *Tissue-specific regulation of metabolic pathways through the transcriptional coactivator PGC1-alpha*. Int J Obes (Lond), 2005. **29 Suppl 1**: p. S5-9.
203. Sack, M.N., et al., *Fatty acid oxidation enzyme gene expression is downregulated in the failing heart*. Circulation, 1996. **94**(11): p. 2837-42.
204. Taegtmeyer, H., P. McNulty, and M.E. Young, *Adaptation and maladaptation of the heart in diabetes: Part I: general concepts*. Circulation, 2002. **105**(14): p. 1727-33.
205. Young, M.E., et al., *Reactivation of peroxisome proliferator-activated receptor alpha is associated with contractile dysfunction in hypertrophied rat heart*. J Biol Chem, 2001. **276**(48): p. 44390-5.
206. Golubeva, L., et al., *[Adaptation to hypoxia, as opposed to adaptation to stress, does not protect the isolated heart from reperfusion after total ischemia. A nuclear magnetic resonance study]*. Biull Eksp Biol Med, 1995. **120**(11): p. 481-4.
207. Meerson, F.Z., O.A. Gomzakov, and M.V. Shimkovich, *Adaptation to high altitude hypoxia as a factor preventing development of myocardial ischemic necrosis*. Am J Cardiol, 1973. **31**(1): p. 30-4.
208. Hasenfuss, G. and B. Pieske, *Calcium cycling in congestive heart failure*. J Mol Cell Cardiol, 2002. **34**(8): p. 951-69.

209. Schwarz, K.O., *Species and age difference in the collagen types of the arterial wall - a possible explanation for differences in susceptibility to atherosclerosis*. *Med Hypotheses*, 1982. **8**(6): p. 619-20.
210. Meerson, F., *The Failing Heart : Adaptation and Deadaptation*. 1983: Raven Press.
211. Lowes, B.D., et al., *Changes in gene expression in the intact human heart. Downregulation of alpha-myosin heavy chain in hypertrophied, failing ventricular myocardium*. *J Clin Invest*, 1997. **100**(9): p. 2315-24.
212. Rafiee, P., et al., *Activation of protein kinases in chronically hypoxic infant human and rabbit hearts: role in cardioprotection*. *Circulation*, 2002. **106**(2): p. 239-45.
213. Postic, C., et al., *Development and regulation of glucose transporter and hexokinase expression in rat*. *Am J Physiol*, 1994. **266**(4 Pt 1): p. E548-59.
214. van Bilsen, M., G.J. van der Vusse, and R.S. Reneman, *Transcriptional regulation of metabolic processes: implications for cardiac metabolism*. *Pflugers Arch*, 1998. **437**(1): p. 2-14.
215. Yu, X.X., et al., *Characterization of novel UCP5/BMCP1 isoforms and differential regulation of UCP4 and UCP5 expression through dietary or temperature manipulation*. *Faseb J*, 2000. **14**(11): p. 1611-8.
216. Echtay, K.S., et al., *Uncoupling proteins 2 and 3 are highly active H(+) transporters and highly nucleotide sensitive when activated by coenzyme Q (ubiquinone)*. *Proc Natl Acad Sci U S A*, 2001. **98**(4): p. 1416-21.
217. Garcia-Martinez, C., et al., *Overexpression of UCP3 in cultured human muscle lowers mitochondrial membrane potential, raises ATP/ADP ratio, and favors fatty acid vs. glucose oxidation*. *Faseb J*, 2001. **15**(11): p. 2033-5.
218. Himms-Hagen, J. and M.E. Harper, *Physiological role of UCP3 may be export of fatty acids from mitochondria when fatty acid oxidation predominates: an hypothesis*. *Exp Biol Med (Maywood)*, 2001. **226**(2): p. 78-84.

219. Harper, M.E. and J. Himms-Hagen, *Mitochondrial efficiency: lessons learned from transgenic mice*. *Biochim Biophys Acta*, 2001. **1504**(1): p. 159-72.
220. Aasum, E., et al., *Effect of BM 17.0744, a PPARalpha ligand, on the metabolism of perfused hearts from control and diabetic mice*. *Can J Physiol Pharmacol*, 2005. **83**(2): p. 183-90.
221. Kelly, D.P., et al., *The tissue-specific expression and developmental regulation of two nuclear genes encoding rat mitochondrial proteins. Medium chain acyl-CoA dehydrogenase and mitochondrial malate dehydrogenase*. *J Biol Chem*, 1989. **264**(32): p. 18921-5.
222. Barger, P.M., et al., *Deactivation of peroxisome proliferator-activated receptor-alpha during cardiac hypertrophic growth*. *J Clin Invest*, 2000. **105**(12): p. 1723-30.
223. Kliewer, S.A., et al., *Differential expression and activation of a family of murine peroxisome proliferator-activated receptors*. *Proc Natl Acad Sci U S A*, 1994. **91**(15): p. 7355-9.
224. Lionetti, V., et al., *Carnitine palmitoyl transferase-I inhibition prevents ventricular remodeling and delays decompensation in pacing-induced heart failure*. *Cardiovasc Res*, 2005. **66**(3): p. 454-61.
225. Wu, G., et al., *Epsilon protein kinase C in pathological myocardial hypertrophy. Analysis by combined transgenic expression of translocation modifiers and Galphaq*. *J Biol Chem*, 2000. **275**(39): p. 29927-30.
226. Steinberg, S.F. and M.A. Sussman, *Cardiac hypertrophy served with protein kinase Cepsilon: delta isoform substitution available at additional cost*. *Circ Res*, 2005. **96**(7): p. 711-3.
227. Klein, G., et al., *Increased collagen deposition and diastolic dysfunction but preserved myocardial hypertrophy after pressure overload in mice lacking PKCepsilon*. *Circ Res*, 2005. **96**(7): p. 748-55.
228. McLeod CJ, P.I., Sack MN, *The mitochondrial biogenesis regulatory program in cardiac adaptation to ischemia - a putative target for therapeutic intervention*. *TCM*, 2005.

229. Nisoli, E., et al., *Mitochondrial biogenesis by NO yields functionally active mitochondria in mammals*. Proc Natl Acad Sci U S A, 2004. **101**(47): p. 16507-12.
230. St-Pierre, J., et al., *Bioenergetic analysis of peroxisome proliferator-activated receptor gamma coactivators 1alpha and 1beta (PGC-1alpha and PGC-1beta) in muscle cells*. J Biol Chem, 2003. **278**(29): p. 26597-603.
231. Boudina, S., et al., *Reduced mitochondrial oxidative capacity and increased mitochondrial uncoupling impair myocardial energetics in obesity*. Circulation, 2005. **112**(17): p. 2686-95.
232. McLeod, C.J., et al., *Delayed ischemic preconditioning activates nuclear-encoded electron-transfer-chain gene expression in parallel with enhanced postanoxic mitochondrial respiratory recovery*. Circulation, 2004. **110**(5): p. 534-9.
233. Sack, M.N., et al., *Coordinate regulation of metabolic enzyme encoding genes during cardiac development and following carvedilol therapy in spontaneously hypertensive rats*. Cardiovasc Drugs Ther, 2000. **14**(1): p. 31-9.
234. Hashimoto, T., S. Yamasaki, and S. Taguchi, *Alterations in the expression of myosin heavy chain isoforms in hypoxia-induced hypertrophied ventricles in rats*. Comp Biochem Physiol B Biochem Mol Biol, 2003. **136**(1): p. 139-45.
235. Adrogué, J.V., et al., *Acclimatization to chronic hypobaric hypoxia is associated with a differential transcriptional profile between the right and left ventricle*. Mol Cell Biochem, 2005. **278**(1-2): p. 71-8.
236. Mochly-Rosen, D., et al., *Cardiotrophic effects of protein kinase C epsilon: analysis by in vivo modulation of PKCepsilon translocation*. Circ Res, 2000. **86**(11): p. 1173-9.
237. Goldspink, P.H., et al., *Protein kinase Cepsilon overexpression alters myofilament properties and composition during the progression of heart failure*. Circ Res, 2004. **95**(4): p. 424-32.

238. Strait, J.B., 3rd, et al., *Role of protein kinase C-epsilon in hypertrophy of cultured neonatal rat ventricular myocytes*. Am J Physiol Heart Circ Physiol, 2001. **280**(2): p. H756-66.
239. Kovacic, S., et al., *Akt activity negatively regulates phosphorylation of AMP-activated protein kinase in the heart*. J Biol Chem, 2003. **278**(41): p. 39422-7.
240. Burgering, B.M. and G.J. Kops, *Cell cycle and death control: long live Forkheads*. Trends Biochem Sci, 2002. **27**(7): p. 352-60.
241. Arden, N. and M.J. Betenbaugh, *Life and death in mammalian cell culture: strategies for apoptosis inhibition*. Trends Biotechnol, 2004. **22**(4): p. 174-80.
242. Tran, H., et al., *The many forks in FOXO's road*. Sci STKE, 2003. **2003**(172): p. RE5.